

2

CR-103038



ANWA-PEP13-W395

To AEC-NASA Space Nuclear Propulsion Office

FINAL REPORT
PROPULSION/ELECTRICAL POWER GENERATION

December 1970

Contract SNP-1

N71-18049	
(ACCESSION NUMBER) <u>143</u>	(THRU) <u>63</u>
(PAGES) <u>CR-103038</u>	(CODE) <u>28</u>
(NASA CR OR TMX OR AD NUMBER)	



AEROJET NUCLEAR SYSTEMS COMPANY

A DIVISION OF AEROJET-GENERAL

Reproduced by
**NATIONAL TECHNICAL
 INFORMATION SERVICE**
 Springfield, Va. 22151



ANWA-PEP13-W395

To AEC-NASA Space Nuclear Propulsion Office

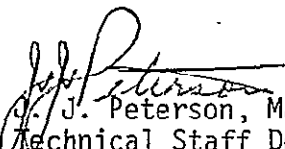
FINAL REPORT
PROPULSION/ELECTRICAL POWER GENERATION

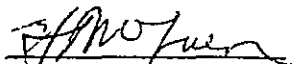
NERVA Program



Contract SNP-1

December 1970


J. J. Peterson, Manager
Technical Staff Department
Aerojet Nuclear Systems Company

Classification Category
UNCLASSIFIED
 12/15/70
Classifying Officer Date
e

FOREWORD

The work reported herein is in fulfillment of Project 395 of Contract SNP-1. The period of performance extended from July 1969 through November 1970.

The Technical Director is William T. White of the Astrionics Laboratory of the Marshall Space Flight Center, Huntsville, Alabama.

Westinghouse Astronuclear Laboratory Project 495 of Subcontract NP-I and North American Rockwell Space Division Contract NAS 8-26346 were supporting studies, portions of which are reported herein.

ABSTRACT

A study was made concerning the feasibility of using the NERVA rocket engine as a heat source for generating 25 kw of electrical power. An organic Rankine power-conversion system, with a hydrogen-filled primary loop and heat-rejection system, was selected in the study. The heat-rejection system utilizes the stage meteoroid shield as the radiating surface.

The dual-mode feature provides a means to greatly increase the utilization of the NERVA engine as an energy source and permits increased operating flexibility. For planetary missions the capability of generating electrical power permits increased payloads. For short-duration missions (e.g., earth orbit to lunar orbit) the reduced duration of cooldown thrusting and the reduction of fluid requirements during cooldown are significant.

CONTENTS

	<u>Page</u>
I. Summary	1
II. Introduction	2
III. Ground Rules and Major Problems	5
A. Ground Rules	5
B. Major Problems	5
IV. Applications of the Dual-Mode System	7
A. Prepressurized Tank	7
B. Preconditioned Turbopump Assembly	7
C. Destratification	8
D. Actuator Size	8
E. Independent Source of Power	8
F. Redundant Energy System	9
G. Utilization of NERVA	9
H. Weight Comparison	10
I. Cooldown Propellant Requirement	10
J. Thrust Termination	12
K. Electrical Power Demand	12
L. Heat	13
M. End Use of NERVA	13
V. Engine Definition	14
VI. System Description	15
A. Primary Loop	15
B. Power-Conversion System	15
C. Heat-Rejection Loop	21
D. System Operation	24
E. Control System	35
F. Location of Components	37
G. System Weights	38
H. Off-Design Operation	41
I. Life of System	44
J. Radiation Effects	46

CONTENTS (cont.)

	<u>Page</u>
VII. Subsystem Description	49
A. Primary Loop	49
B. Power Comparison System	59
C. Heat-Rejection Subsystem	66
D. Control System	71
VIII. Description of Major Components	79
A. Primary Heat Exchanger	79
B. Boiler	107
C. Turbine-Alternator Pump Assembly	108
D. Condenser	115
E. Radiator	119
IX. Recommendations For Future Work	132
A. 25 kw Electrical System	132
B. Impact of 25 kw Electrical System	134

TABLES

<u>No.</u>		<u>Page</u>
1	Summary-Power Conversion Systems For 25 kw(e)	20
2	Cooldown Propellant Savings Using NERVA Electrical System For Eight-Burn Lunar Mission, ALM	27
3	Comparison of Cooldown Mode Options-Four Burn Lunar Mission	33
4	Summary-Payload Increments For Three Missions Utilizing Dual Mode Vs Reference NERVA	36
5	Hardware Weight Breakdown (Preliminary) Dual-Mode System 25 kw(e)	40
6	Summary of Burnup Analysis For Dual-Mode Reactor	99
7	Calculation of Cold-to-Hot Reactivity in Electrical Mode	101
8	Reactivity Requirement For Electrical-Mode Operations	103
9	Initial Reactor Reliability Estimate For the Dual-Mode System	105
10	Typical Operating Performance	113

FIGURES

<u>No.</u>		<u>Page</u>
1	Reusable Nuclear Shuttle with Dual-Mode NERVA	4
2	Domains for Space Electrical Power Systems	11
3	Propulsion-Electrical Power Generation System	16
4	Thermodynamic Cycle Efficiency as a Function of Temperature Ratio	18
5	Variation of Cycle Efficiency with Condenser Temperature	23
6	Cooldown Propellant Consumption and Duration Vs Burn Time for 0, 200, 500 kw(t) Decay-Heat Removal Systems	25
7	Flight Profile for Eight-Burn Lunar Mission	26
8	Time from Scram and Decay Power Level for Initiation of NERVA Electrical Operation	29
9	Nominal Load Profile, Eight-Burn ALM Mission, Total Integrated Power of 34 kw-Hr	30
10	Flight Profile for Four-Burn Lunar Mission	32
11	Effect of Radiator on Reusable Nuclear Shuttle Payload Capability	34
12	Average Specific Impulse Vs Burn Time	43
13	Effect of Maximum Temperature Upon Life of Power Conversion Systems	45
14	Dual-Mode System Primary Coolant Lines	54
15	Specific Speed and Efficiency for Primary Coolant Loop Fan	56
16	Effect of Primary Coolant Loop Pressure Upon Efficiency of Fan	57
17	Effect of Primary Coolant Loop Temperature Difference Upon Efficiency of Fan	58
18	Temperature Vs Power for Power Conversion Systems	60
19	Variation of Cycle Efficiency as a Function of Maximum Cycle Temperature	63
20	Dual-Mode Electrical Power Generating System	65
21	Specific Speed and Efficiency for Heat-Rejection Loop Fans	68
22	Effect of Temperature Difference in Heat-Rejection Loop Upon Fan Efficiency	69

FIGURES (cont.)

<u>No.</u>		<u>Page</u>
23	Effect of Pressure in the Heat-Rejection Loop Upon Fan Efficiency	70
24	Control System Block Diagram	72
25	Estimated Core Centerline Temperature with NERVA R-1 Dual-Mode Heat Removal at Aluminum Cylinder ID	81
26	Estimated Core Thermal-Power Removal by Aluminum Cylinder Coolant Flow Only, NERVA R-1	82
27	Flow Schematic, Aluminum Barrel Heat-Removal Concept, Separated Flow System	84
28	Pump Power Vs Channel Diameter	88
29	Pump Power Vs Flow Area	89
30	Stem Temperature Vs Unfueled Element Temperature for Radiation Cooling	91
31	Control Drum Temperature Vs Reflector Temperature for Radiation Cooling	92
32	Radiation Changes in Beryllium	96
33	Boiler, Dual-Mode System, 25 kw(e)	109
34	Turbine-Alternator-Pump Assembly	110
35	Wick Condenser	116
36	Tubing Layout, No Interposition	122
37	Total Weight of Tubes and Additional Meteoroid Shield Vs Tube Diameter	123
38	Extended Surface Effectiveness Vs Fin Length	125
39	Meteoroid Shield Thickness Vs Area Exposed	127
40	Hydrogen Radiator Inlet to Exit Temperature Difference Vs Tube Diameter	128
41	Gas-to-Wall Film Delta Temperature Vs Tube Diameter	129
42	Tubing Layout, With Interposition	131

I. SUMMARY

The feasibility of utilizing the NERVA engine as a heat source for a 25-kw(e) electrical power system was investigated. A minimum number of additions to the NERVA engine to perform the dual function was an important ground rule. Several concepts for removing heat from the engine were evaluated. A closed loop, independent of the normal NERVA flow path, was identified as a practical solution to the engine portion of the primary coolant loop. Warm hydrogen circulating in the primary loop carries heat from the engine to the forward end of the stage where it supplies heat to a boiler. An organic working fluid, thiophene, was selected as the most desirable fluid for the Rankine-cycle power-conversion system. A wick-type condenser was conceived for operation in a zero-gravity environment. The heat-rejection system utilizes gaseous hydrogen to conduct heat from the condenser to the exterior surface of the stage. Multiple loops in the radiator provide a large number of parallel independent loops to enhance reliability and reduce the potential effects of meteoroid damage.

The operating characteristics of the NERVA electrical system enhance the operation of the nuclear rocket engine by providing a radiative means of dissipation of decay thermal energy. Thus, cooldown impulse may be reduced by 30%, cooldown propellants reduced by 50%, and the cooldown thrusting period reduced by 90%. This increased operating flexibility is especially important for short-duration missions from a guidance, navigation, and docking standpoint.

For interplanetary missions, the electrical power could be used to re-liquefy boiloff hydrogen. From a weight tradeoff standpoint, this is desirable because the propellant recovery is expected to be an order of magnitude greater than the hardware weight of the NERVA electrical system.

II. INTRODUCTION

Use of the 75,000-lb-thrust nuclear rocket engine as a propulsion device may be made more attractive by incorporating it into an energy system for space flight. This greatly enlarged concept includes the use of the NERVA engine as a low-temperature, low-power heat source for generating electrical power, as well as for other applications (e.g., the thermal source for the operation of propellant-management, environmental-control, and waste-management systems).

In this report, the utilization of the NERVA engine as an energy source for a 25-kw electrical power system is described. The purpose of these initial studies was to show the feasibility, potential practicability, and desirability of the dual-mode concept.

Larger systems, such as a 50 kw(e), were also considered. Problems with the higher power systems, however, occur in the reactor portion of the primary loop and with the surface area required for the radiator.

It should be recognized that during the normal propulsion mode, the nuclear fuel contained within the reactor of the NERVA engine is utilized to only a fraction of 1% of its ultimate capability as an energy source. As a consequence, the dual-mode, or electrical-power-generation concept makes it possible to more effectively utilize the inherent energy potential of the NERVA engine. While the normal rocket mode of operation lasts only minutes, the electrical-power mode can be operable during the normal coast periods which may be for periods of weeks or years. As a result, significant reactor utilization can be achieved though the power level is small compared with the normal propulsion mode. For example, operation of 25-kw electrical power system for one year represents approximately the same thermal energy requirement as a 1-hr full-power burn in the rocket mode. In this study, the dual-mode operation for a period of eight years (i.e., a mission to the outer planets) is the operational life goal.

The major component of the electrical system from a size and weight standpoint is the space radiator. NASA/MSFC contracted with North American Rockwell to provide a concurrent feasibility study of an integrated space radiator-meteoroid shield for the reusable nuclear shuttle. The complete stage is shown in Figure 1.

III. GROUND RULES AND MAJOR PROBLEMS

A. GROUND RULES

A basic ground rule for the dual-mode study is that the NERVA engine will be utilized as the energy source in "as is" condition or design. It is recognized that major changes in the design of the engine for the purposes of enhancing the electrical-power mode are undesirable. The results of the feasibility studies suggest that relatively insignificant additions to the current engine design are required to provide for the removal of heat from the engine for the low-temperature, low-power mode of operation required for electrical power generation.

The second ground rule utilized was that checkout and operational constraints would not be incurred as a result of the dual-mode system. As a consequence, primary-coolant-loop fluids which would contaminate the engine (e.g., sodium or NaK) were not considered though they would potentially reduce parasitic power requirements.

A third ground rule was that the dual-mode electrical system would be appropriate only to a nuclear-rocket-propelled stage. Hence, integration of dual-mode and NERVA components (e.g., the radiator with the meteoroid shield) on the nuclear stage was a potential option. The fact that the NERVA electrical system is unique to a nuclear-rocket-propelled stage has a significant effect upon weight studies. Hence, engine and shield weights which are inherent to the nuclear stage are not assessed against the dual-mode system.

B. MAJOR PROBLEMS

The results of the study show that no major research problems exist to prevent achievement of a reasonable system design. The problems are

of an engineering nature and, therefore, are capable of being solved through normal engineering development. For example, a major problem of the primary coolant loop was identified as leakage of the gaseous-hydrogen coolant through seals in the reactor assembly. The long-duration requirements for the NERVA electrical mode of operation put much greater emphasis upon adequate sealing, as compared with the normal rocket mode of operation, wherein minor internal leakages do not have significant effects upon engine performance, operation, or life.

To accommodate the dual-mode system in the NERVA stage, it is necessary to make provision for the NERVA electrical systems. Insofar as the engine is concerned, the hardware provisions are relatively minor. Of greater significance are the changes in the engine operating mode and changes in stage design which will be desirable to achieve the best overall vehicle. To best utilize the resources allotted to the development of the nuclear stage, an early decision to incorporate the dual-mode system is necessary.

IV. APPLICATIONS OF THE DUAL-MODE SYSTEM

Applications of the dual-mode system illustrate the potential of the NERVA engine, as a space energy system. Benefits for short-duration missions (e.g., synchronous orbit or lunar missions) are considerably different from those benefits which accrue from long-duration or planetary missions. Some benefits arise in the form of improved engine performance or reduced propellant requirements, while others result from increased engine-vehicle operating flexibility.

A. PREPRESSURIZED TANK

The bootstrap startup of the NERVA engine is a simple and inherently reliable method of initiating propellant flow. However, engine bootstrap characteristics are a function of tank pressure and net positive suction pressure. To prepressurize the tank, significant amounts of warm vapor may be required, especially when the tank is only partially full of liquid. The dual-mode system may be used to provide thermal energy for vaporizing propellants and electrical power for pumping liquid propellant through the vaporizer to prepressurize the propellant tank. This is a desirable feature both from an operational and performance standpoint. And hydrogen that is vaporized for tank pressurization gas is not lost from the system but may be used for cooldown flow.

B. PRECONDITIONED TURBOPUMP ASSEMBLY

Consistent bootstrap startup pressure-flow rate schedules and mechanical integrity of the shaft thrust-balance piston and hydrogen-lubricated bearings in the NERVA turbopump assembly (TPA) require preconditioning of the TPA. The dual-mode system can provide electrical power for a recirculating liquid hydrogen preconditioning circuit. This type of preconditioning system has been successfully used on Centaur flights and

represents a significant propellant savings in comparison with preconditioning concepts which involve flowing propellant from the tank through the rocket engine prior to startup.

C. DESTRATIFICATION

During coast periods in a zero-gravity environment, heat leakage through the tank wall heats the hydrogen adjacent to the wall to a temperature significantly above that of the core liquid. Under prolonged conditions the vapor pressure of the warm fluid can increase to a pressure which exceeds tank pressure limits, thus requiring tank venting with resultant loss of propellant. The dual-mode electrical system provides sufficient electrical power so tank fluids can be stirred to destratify the tank fluid and thereby reduce tank pressure and prevent tank venting. It is conceivable that the tank destratification system can be integrated with the TPA cooldown circuit with resultant weight savings.

D. ACTUATOR SIZE

Overall reliability of the NERVA vehicle may be enhanced by the relatively large power capability of the dual-mode electrical system. Actuator motors can be oversized without placing undue electrical demands upon the electrical power system. Thus, the design philosophy for the entire vehicle is potentially affected.

E. INDEPENDENT SOURCE OF POWER

The dual-mode electrical system also offers the promise of providing relatively large quantities of electrical power to the NERVA stage during its lifetime with the exception of the few hours during which the engine is burning. This is in marked contrast to the current design approach for the reusable nuclear shuttle which utilizes fuel cells for electrical

power and requires an electrical umbilical connection to a space station during approximately half of its useable lifetime in space.* This independence will result in a large increase in flexibility of operation of the nuclear stage in comparison with the chemical shuttle or fuel-cell nuclear shuttle and should improve overall system reliability because the vehicle does not have to depend upon other systems for electrical power.

F. REDUNDANT ENERGY SYSTEM

Redundancy in the Apollo vehicle electrical power system was obtained by multiple fuel cells. In the future, redundancy requirements for some systems may require independent methods of providing electrical power. If this philosophy becomes a design requirement for space vehicles, the dual-mode electrical system will be a very attractive candidate for one of the electrical power systems. Use of the system, however, does not preclude use of fuel cells. In fact, the abundant power furnished by the dual-mode system could be used to electrolyze water and thereby manufacture hydrogen and oxygen to replenish fuel cell reactant tanks (fuel cell tanks have high boiloff rates).

G. UTILIZATION OF NERVA

If the dual-mode electrical system is utilized as one or the only space energy system, the inherent energy potential of the NERVA is better utilized. Or, in another sense, the nuclear stage becomes much more cost-effective. If the NERVA engine is utilized for thermal energy, it may eliminate the need for other reactors or radioisotopes on board the vehicle, resulting not only in a reduction of hazard potentials, but also a reduction in cost. It is anticipated that the cost of development associated with the dual-mode system will be a small fraction of the cost of other nuclear systems because of its low temperature cycle, and because the cost of the major

*See Nuclear Shuttle System Definition Study, Phase III, First Interim Review, North American Rockwell-Space Division Report PDS70-242, 2 September 1970.

portions of the system (e.g., reactor and radiator-meteoroid bumper) are already amortized.

H. WEIGHT COMPARISON

Studies of the 25-kw(e) electrical system have shown the additional weight to the NERVA stage, in the form of hardware associated with the system, to be approximately 6,000 lb. This weight is an order of magnitude less than weight estimates for comparable reactor-powered space electrical power systems which would be required for planetary missions. For near-earth missions (e.g., the lunar shuttle) the average electrical power demand has been estimated to be an average of only 3 kw. Fuel cells and reactants for the 3-kw system have been estimated to be in the range of 3,000 lb for each lunar trip. This weight provides power for the flight portion of each lunar trip, which is approximately half of the total cycle time. The weight of the dual-mode electrical system could be reduced substantially if it were designed to operate in the range of 3 to 6 kw(e). Thus, a direct comparison of electrical system hardware weights may not prove valid for the shuttle mission. On a basis of specific weight (i.e. weight per kilowatt) the dual-mode system is very attractive. Figure 2 shows the power level-life domains of several space power systems.

I. COOLDOWN PROPELLANT REQUIREMENT

From the preceding discussion of weights, it is apparent that for short-duration, multiple-burn missions (e.g., the lunar shuttle) conventional electrical systems of low power (i.e., 3 kw(e)) have less hardware weight than the 25-kw(e) dual-mode system. In the case of a NERVA stage this tells only a part of the story. The dual-mode system provides a means of removing decay heat from the NERVA engine by means of a closed primary loop. The heat removed can be radiated into space, thus reducing the cooldown propellant requirement for the engine. The reduction of cooldown propellant flow for a

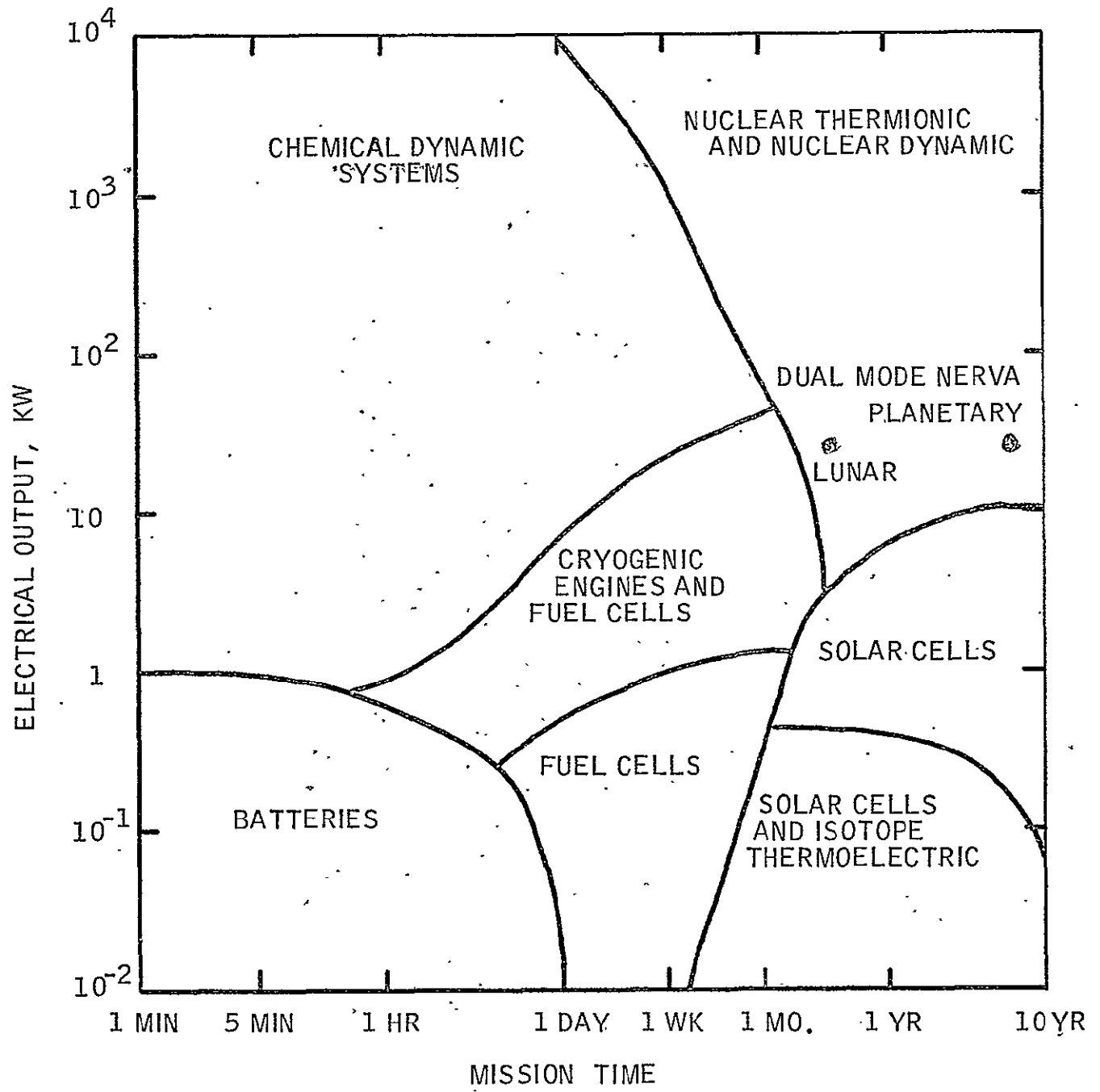


Figure 2 - Domains for Space Electrical Power Systems

single lunar trip is in the range of 10,000 lb. This reduction more than compensates for the entire hardware weight associated with the system.

J. THRUST TERMINATION

Current NERVA engine design requires a cooldown flow through the engine with resulting thrust during the entire flight to, and return from, the moon. In addition to being wasteful of propellant, this long period of low-level thrusting makes trajectory calculations extremely difficult to compute. The dual-mode system with its radiative heat rejection provides a means of reducing the thrusting period by 90% or more: e.g., cooldown flow periods are reduced from 60 to 6 hr for the 1500 sec depart-earth-orbit burn.

In addition to the early termination of cooldown flow, the dual-mode system would make it practical to greatly extend "no-thrust" periods during the early portion of cooldown. Early thrust nulling is required for docking maneuvers for such short-duration flights as NERVA-powered stages traveling from low-altitude orbit to synchronous orbit and return.

K. ELECTRICAL POWER DEMAND

The applications of electrical power on space vehicles depend heavily upon the availability of electrical power. If the power is available in relatively large amounts for a small weight addition, there will be a greatly increased demand. For example, on a Mars mission the boiloff of propellants for an optimum nuclear vehicle without the dual-mode electrical system is in the range of 50,000 lb of propellant. With an abundance of electrical power, which the dual-mode system can provide, it may be desirable to re-liquefy a major portion of this propellant.

An abundance of power will make it practical to have greatly improved communications systems between earth and distant space vehicles. For example, real-time television from Jupiter will require power at the tens-of-kilowatts level.

L. HEAT

The primary loop and radiator loop of the dual-mode system can provide significant amounts of thermal energy at temperatures of 300° and 80°F, respectively. This heat may be utilized for a variety of purposes. For example, heat which would normally be dissipated by the radiator system may be utilized to provide environmental warmth for the payload, the instrumentation section, and for localized heating adjacent to cryogenic circuits.

The higher-temperature thermal energy from the primary loop may be used in a waste management system for dehydrating solids and re-distilling liquids. There is a potential need for heat to provide energy for monopropellant (i.e., hydrogen) reaction control and attitude control systems. If electrical power is available, the temperature of the working fluid of these auxiliary thruster systems may be increased to 1000° to 1500°R. This is desirable because the specific impulse of warmed hydrogen is equal to that of hydrogen-oxygen auxiliary rocket systems.

M. END USE FOR NERVA

Current plans for spent NERVA stages involve the injection of the stage into a flight path far removed from earth orbit. The dual-mode system provides an alternative for a NERVA stage no longer serviceable for normal rocket operation. This concept involves the conversion, in effect, of the NERVA stage to a space-energy stage. While the radiation environment of the vehicle will make it necessary to have the NERVA space-energy stage removed from inhabited space stations, it may be practical to transmit

electric power from the stage to the space station by means of a transmission line. Also, it may be practical to transfer some of the functions from the space station to the space-energy stage and thereby increase the utilization of space-energy systems. In this way it may prove practical to not have a reactor or radioisotope power source in the manned space station.

V. ENGINE DEFINITION

During the period of this study, significant advances occurred in the design goals for the 75,000-lb-thrust NERVA engine. For example, the design operating life was extended from 1 to 10 hr. To achieve this longer life, a slight lowering of nozzle-inlet gas temperature was deemed desirable to enhance core life. The flow cycle was changed from a hot bleed to a full-flow to offset the effect of the reduction in nozzle-inlet temperature upon specific impulse. Engine control actuators also were changed from pneumatic to electrical.

These modifications had a beneficial effect upon the possibility of dual-mode operation of the engine. The decision to eliminate a thrust-nulling system from the engine design enhanced the opportunities of the dual-mode electrical system because the system provides a means of disposing of low-level decay heat without producing thrust.

VI. SYSTEM DESCRIPTION

The dual-mode electrical system (shown schematically in Figure 3) includes a NERVA engine, a system for converting heat to electricity, and a circuit for rejecting waste heat from the power-conversion system. Only small additions to the engine are necessary to provide a means of transporting low-temperature, low-power thermal energy from the engine to the power-conversion system. The basic reason for the relatively modest additions is that the thermal power level of the engine in the rocket mode is approximately 10,000 times the thermal power level required for electrical operation.

A. PRIMARY LOOP

The technique of heat removal from the engine for the electrical-power mode is to circulate gaseous hydrogen through the metal parts of the reactor (i.e., within the pressure vessel) and duct the warmed hydrogen to the forward end of the stage where the heat is used to boil the working fluid of the power-conversion system (see Figure 3). The cooled hydrogen is then compressed slightly to cause it to return to the heat source. The primary-loop lines are shown running the length of the propellant tank in Figure 1. Rechargeable batteries will provide electrical power to the engine during the rocket mode and for the transition to electrical operation. After the transition, the electrical power system will be used to recharge the batteries.

B. POWER-CONVERSION SYSTEM

In the initial phase of the study, the space nuclear auxiliary power (SNAP) systems were evaluated for their potential application to the NERVA electrical system. It soon became apparent that all SNAP power-conversion systems currently in development are designed for relatively high-temperature heat sources (i.e., 1100°F and up) and, thus, were unsuited for NERVA electrical application. The thermal-electric generator and the Brayton cycle

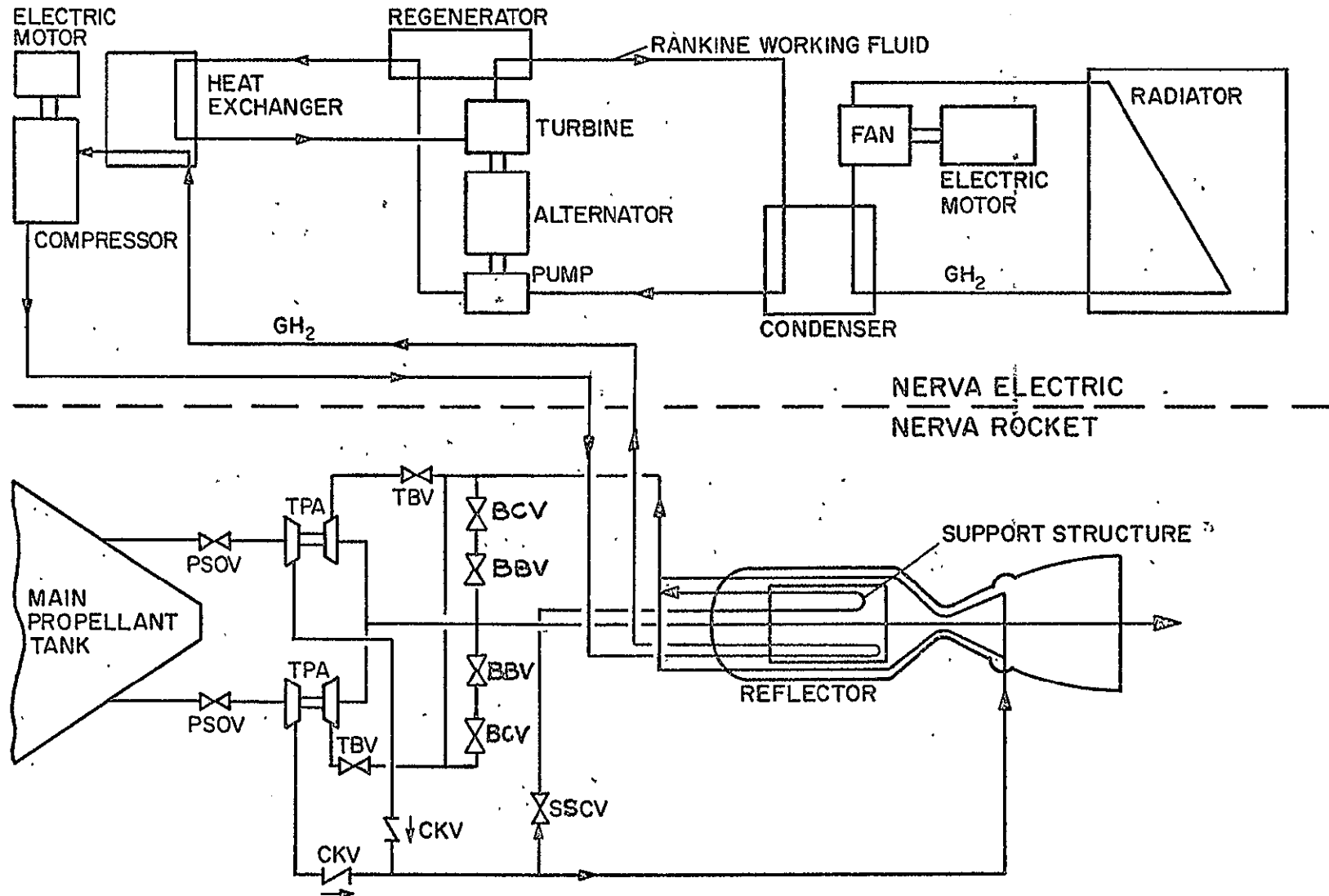


Figure 3 - Propulsion-Electrical Power Generation System

(i.e., a closed-cycle gas turbine) were determined also to be unsuitable for the temperatures which could be considered. For example, a Brayton cycle requires a sink-to-source temperature ratio of less than 0.5. Since the dual-mode electrical system was limited to approximately a minimum temperature of 550°R and a maximum temperature of 775°R, the temperature ratio of approximately 0.7 is far from feasible for application with a Brayton cycle. Thermodynamic analyses of Rankine cycles showed that useful cycle efficiencies were feasible with the source and sink temperature available to the dual-mode system. Figure 4 shows the efficiency of various heat engines as a function of temperature ratio. The dual-mode system, it should be noted, has a uniquely high ratio.

A number of potential Rankine-cycle fluids were evaluated. From these evaluations it was determined that maximum cycle performance would be obtained with working fluids which had relatively low boiling pressures at the maximum cycle temperature. The reason is that the power consumption of the boiler feed pump is minimized when boiler pressure is low. For example, at the maximum cycle temperature, ammonia with a vapor pressure of approximately 1700 psia has approximately 50 times the boiler feed pump work as water which has a vapor pressure of approximately 50 psia. A wide variety of organic fluids which have vapor pressures similar to that of water were also evaluated. In general, organic fluids have ideal thermodynamic-cycle-performance capabilities similar to that of water: however, some have definite advantages over water for small, low-power (i.e., 25 to 50 kw(e)) power-conversion systems. One advantage is a higher molecular weight in comparison with that of water. The higher molecular weight makes it possible to assume the entire enthalpy drop across a single rotor as compared with the 15 stages which may be required in the steam turbine.

Such organic fluids as benzene, pyridine, furan, and thiophene have an additional advantage over water in that the adiabatic expansion of the vapor from the turbine-inlet to the turbine-exit condition is parallel

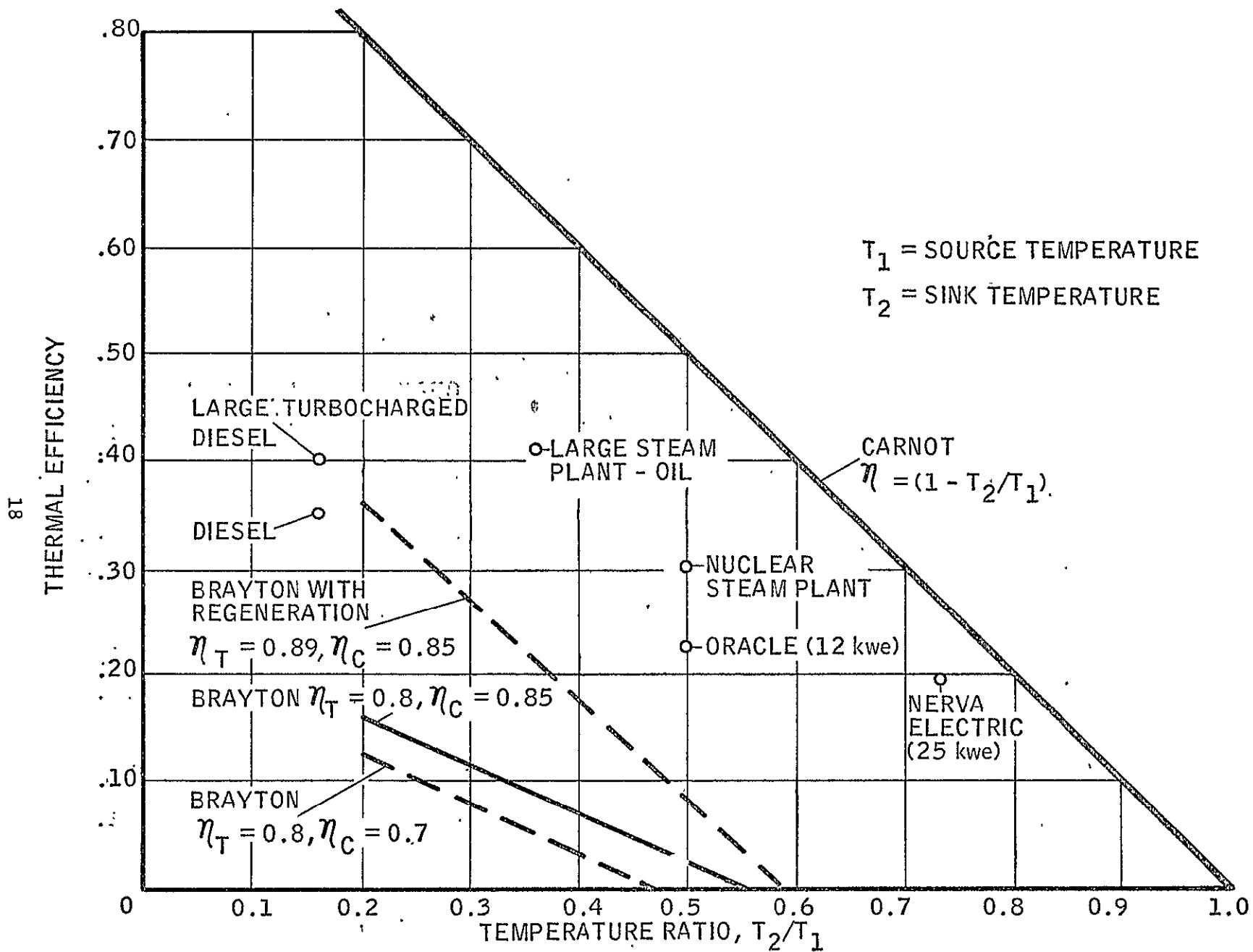


Figure 4 - Thermodynamic Cycle Efficiency as a Function of Temperature Ratio

to the saturated-vapor line on the temperature-entropy diagram. As a consequence, the expansion process does not produce wet vapors as it does in a steam turbine. In fact, it is sometimes desirable with organic fluids to provide a small recuperator or regenerator between the turbine outlet and the condenser inlet because the turbine-outlet temperature is normally slightly higher than the condenser temperature (superheat), hence some thermal energy may be transferred by the regenerator to the boiler feed pump effluent.

Thiophene (C_4H_4S) was selected over other similar candidates (e.g., benzene and pyridine) primarily on the basis of its slightly greater vapor pressure at the condensing temperature. This greater pressure reduces the size of the turbine, regenerator, and condenser and eases the potential problem of boiler feed pump suction conditions in a zero-gravity environment. The thermodynamic performance of benzene, pyridine, steam, and thiophene is essentially the same. Table 1 provides comparative data. Although thiophene is a combustible hydrocarbon in air, this should not present a problem for space application.

In a zero-gravity environment, the static head of liquid cannot be used to provide a head for moving condensed liquid from the condensing surface into the suction of the boiler-feed pump. Several types of condensers are currently utilized in zero-gravity Rankine cycle power systems. For such liquid metals as potassium and mercury, the condensing liquid may be swept to the condenser outlet by means of the flow of uncondensed vapors. Subcooling of the condensate can provide sufficient net positive suction pressure (NPSP) to permit the fluid to be forced into the boiler feed pump suction as a liquid. In the case of fluids with poor thermal conductivity, which includes all of the organic working fluids, a jet condenser is normally used. In the jet condenser, the incoming vapors are condensed in high-velocity, subcooled liquid streams that converge in the jet-condenser throat and are then diffused to recover velocity head and, thereby, provide the pressure necessary

TABLE 1

SUMMARY ~ POWER CONVERSION SYSTEMS FOR 25 kw(e)

	Thiophene	Pyridin	Benzene	Ammonia	Water
Chemical Formula	C_4H_4S	C_5H_5N	C_6H_6	NH_3	H_2O
Molecular Weight	84	79	78	17	18
Freezing Temperature °R	420	418	415	352	492
Maximum Vapor Temperature, °R	750	750	750	740	760
Condensing Temperature, °R	550	550	550	550	550
Pressure Levels in Boiler, psia	44.7	20.2	62.5	1580	40
	34.7	15.0	52.5	--	32
	28.4	12.5	44.5	--	25
	--	--	37.5	--	19.3
Condensing Pressure, psia	2.4	0.6	1.5	180	0.7
Turbine Efficiency (Aerodynamic only)	0.90	0.90	0.90	0.85	0.85
Rankine Cycle Efficiency with Regeneration, %	0.19	0.19	0.19	0.18	0.18
Total Turbine Weight Flow, $\frac{lb}{sec}$	0.9	--	--	--	--
Turbine Weight Flows, % at the Three Pressure Levels in % of Total Weight Flow	50	50	25	100	25
	30	30	25	--	25
	20	20	25	--	25
	--	--	25	--	25

to cause the liquid (i.e., jet streams plus condensate) to circulate through the radiator and provide NPSP for the recirculating pump operation.

The relatively large parasitic-pumping power and subcooling requirements for the jet-condenser streams established a significant burden on the modest temperature conditions of the electrical system. To avoid the undesirable characteristics of the jet condenser and to take maximum advantage of the characteristics of thiophene, a wick-type condenser was designed. Although the new condenser does not have the experimental-testing background of the jet condenser, the various facets of its operation are subject to analytical evaluation, and it is believed to be the best solution at present.

C.. HEAT-REJECTION LOOP

The function of the heat-rejection loop is to transport the waste thermal energy of the power-conversion-system condensing fluid to the outer skin of the vehicle which then radiates the thermal energy to space. The type of system studied was a closed-loop, gaseous-hydrogen circulating system, similar in concept to the primary loop. The magnitude of thermal energy to be rejected is approximately 80% of the thermal power of the primary loop. It is desirable to maintain a relatively small temperature difference in the hydrogen flowing through the condenser. Therefore, it is necessary to flow at a much greater rate through the radiator as compared with the primary loop. The larger flow rate necessitates an increased flow area to maintain the parasitic pumping power (required for the circulating fan) at a reasonable level. It is relatively simple to provide redundancy in the condenser-radiator system by having many individual circulating loops, each with its own section in the condenser and circulating fan.

As a result of the relatively low maximum cycle temperature inherent with the dual-mode system, the radiator temperature selected is of

a relatively low value (i.e., approximately 540°R). This rather nominal temperature makes it relatively easy to integrate the radiator heat-distribution tubes with the meteoroid skin which forms the exterior surface of the vehicle. The concept of using the entire exterior surface of the stage as the radiating surface means that the only additional weight to the meteoroid skin is that of the tubing of the thermal-distribution system and its additional, meteoroid protective shield. Preliminary studies show that the thermal energy dissipation required for a 25-kw(e) system can be accomplished by use of the exterior surface of the vehicle in a near-earth environment. As the space vehicle departs from a near-planet orbit, the radiating capability increases: thus a lowering of condenser temperature is possible.

The most severe environmental operating condition identified was the low-altitude-orbit, full-sun situation at the moon. Methods for circumventing this worst case are described in North American Rockwell Reports SD 70-591 and SD 70-621.

The power-conversion system cycle operation is not affected provided the radiator can maintain condenser temperature at or less than the design value. Figure 5 shows the change in cycle performance as a function of condenser temperature for a nonfixed system. A given set of hardware would react less favorably to a changing condenser temperature.

For long-duration operation of the dual-mode system on a stage with liquid hydrogen in the tank, it will be necessary to use high-performance insulation to minimize heat leakage from the warm radiator to the hydrogen in the tank. The effect of this additional leakage can be eliminated by using some of the electrical power for re-liquefaction of the hydrogen. Another possible solution is to operate radiators on stages which have had their hydrogen expended.

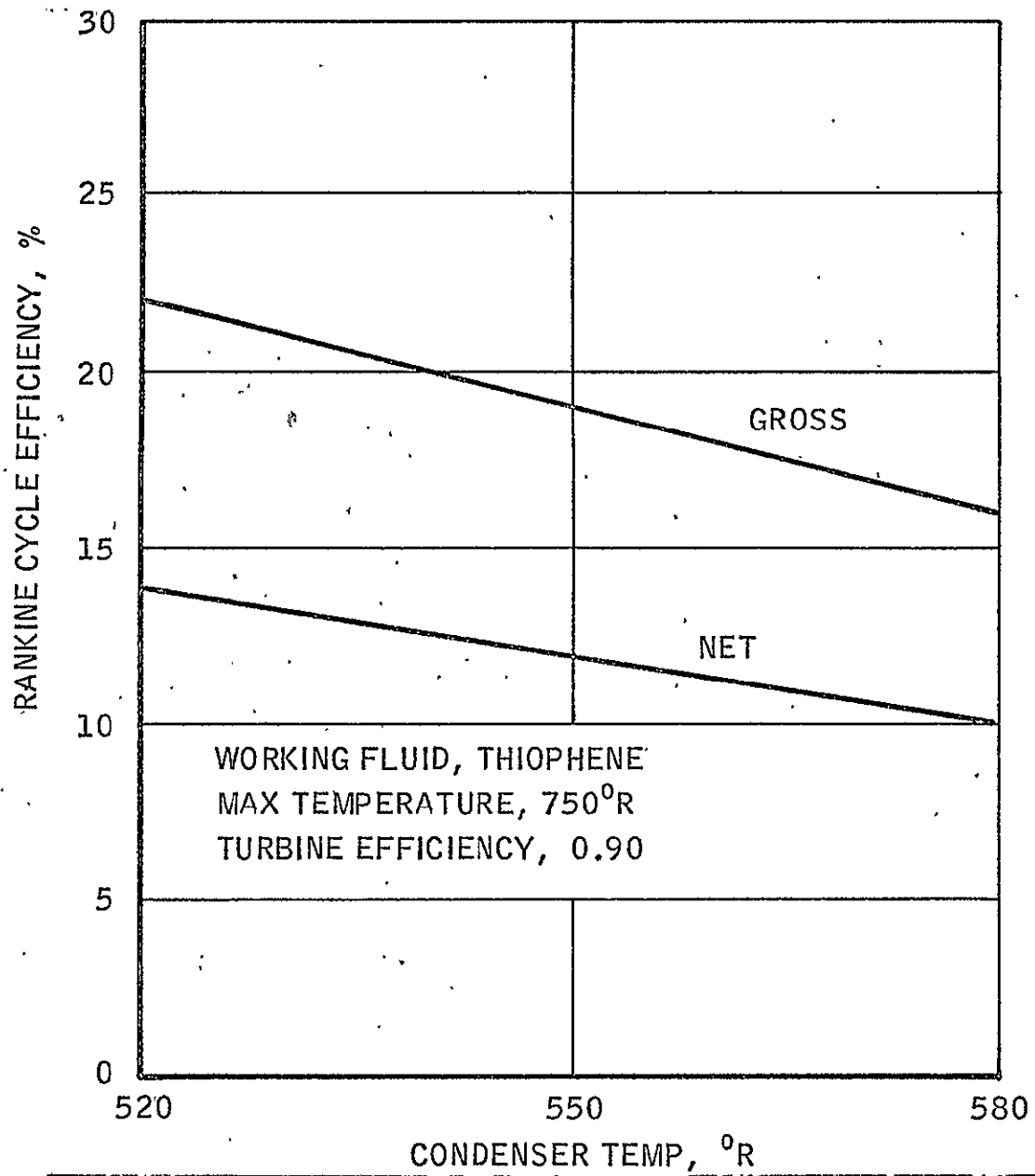


Figure 5 - Variation of Cycle Efficiency with Condenser Temperature !

D. SYSTEM OPERATION

The goal of the dual-mode system design is to provide a NERVA electrical capability without placing significant restraints upon the normal rocket mode of operation of the engine. It is highly desirable to be able to operate in the electrical mode both before and after rocket-mode operation. In fact, for all flight applications, the earlier the electrical mode is initiated after the rocket mode, the greater the cooldown propellant savings achieved. An approximate 50% additional saving of cooldown propellant is achieved by starting the electrical power system at the end of the engine shutdown period as compared with waiting until the decay power is at the level required for electrical system operation. Figure 6 shows the cooldown fluid requirements for a single burn as a function of burn duration for nominal (i.e., 200 kw(t) and 500 kw(t)) nuclear rocket dual-mode systems. The 200 kw(t) system corresponds to 25 kw(e). The difference in the curves represents potential cooldown-fluid savings.

For unmanned NERVA rocket applications requiring only one burn (e.g., some deep-space probes), a relatively long burn is used, and the amount of cooldown fluid consumed is a relatively small percentage of the total. For such missions, the requirement for electrical power may be comparatively large and of long duration.

For missions of short duration (i.e., one month or less) where replenishment of consumables is practical, low-weight power systems such as fuel cells are normally advantageous. Dual-mode system weights are competitive with these systems: however, significant savings of cooldown fluid with the electrical mode enhance the competitive position of the nuclear-powered stage. For an eight-burn lunar shuttle mission, pictured in Figure 7, cooldown propellant savings are listed in Table 2. The corresponding cooldown flow

COMPUTER RUN C-317 14A (1/28/70)

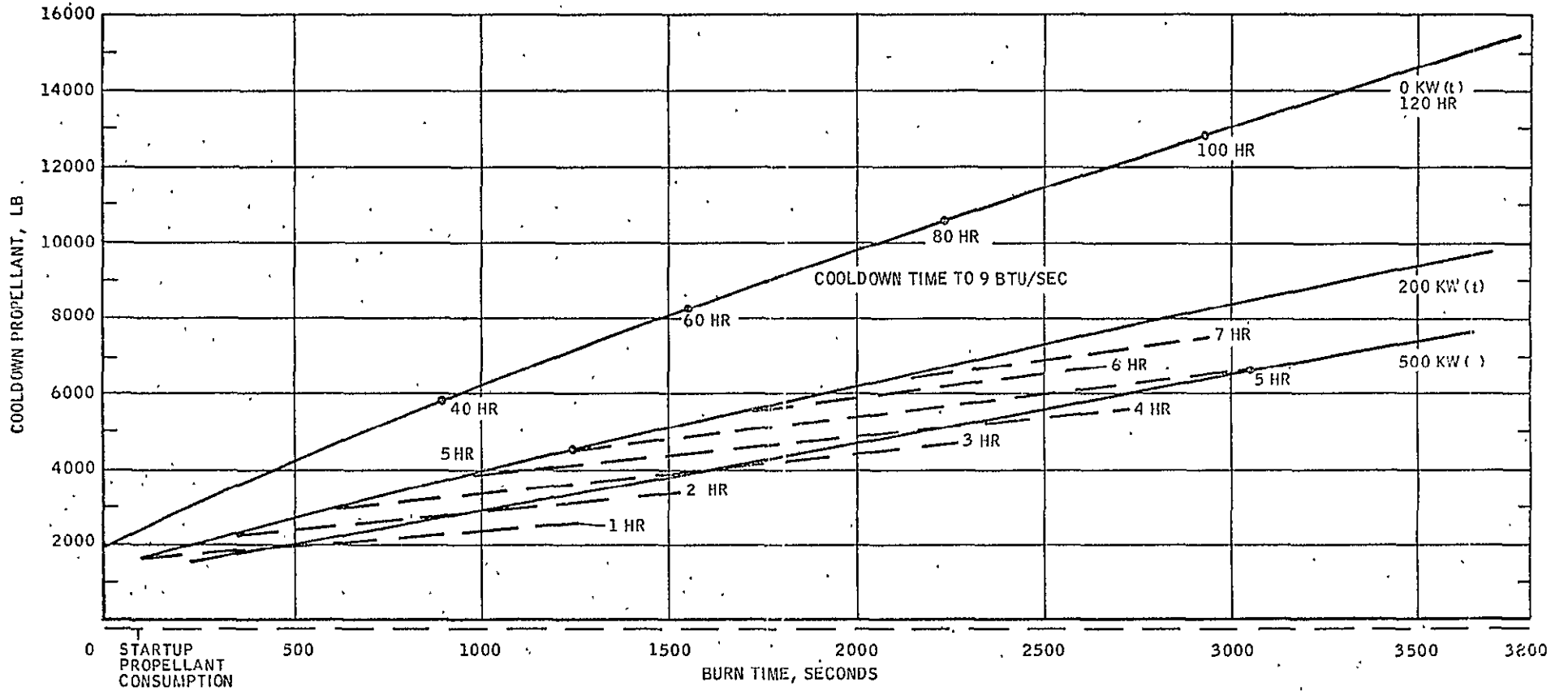
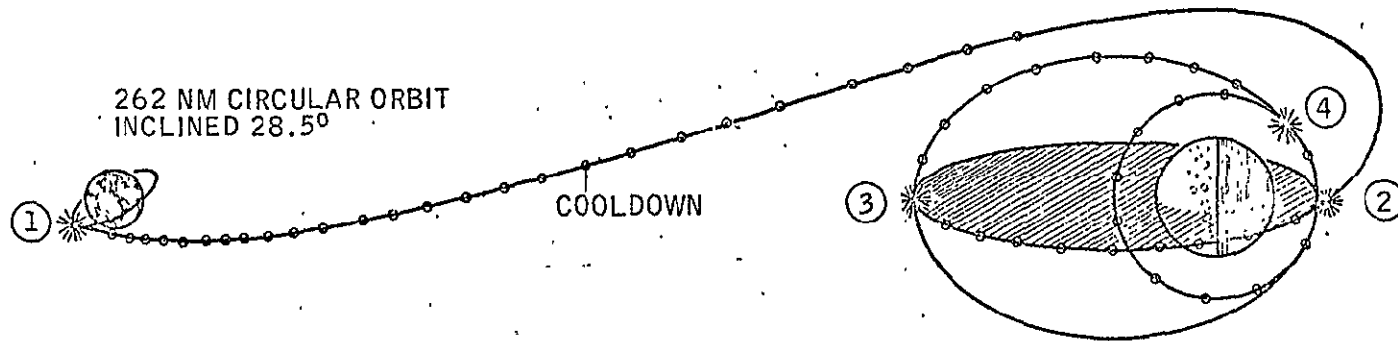


Figure 6 - Cooldown Propellant Consumption and Duration Vs Burn Time for 0, 200, 500 kw(t) Decay-Heat Removal Systems



BURN NUMBER →	1	2	3	4	5	6	7	8
FULL POWER DURATION (MIN)	24.9	2.0	1.3	2.2	1.9	0.8	1.2	10.0
COOLDOWN DURATION (HRS)	63.3	7.5	7.5	21.0	7.5	7.5	22.0	31.0
VELOCITY INCREMENT (FPS)	10500	1460	1135	1790	1790	1135	1460	10200

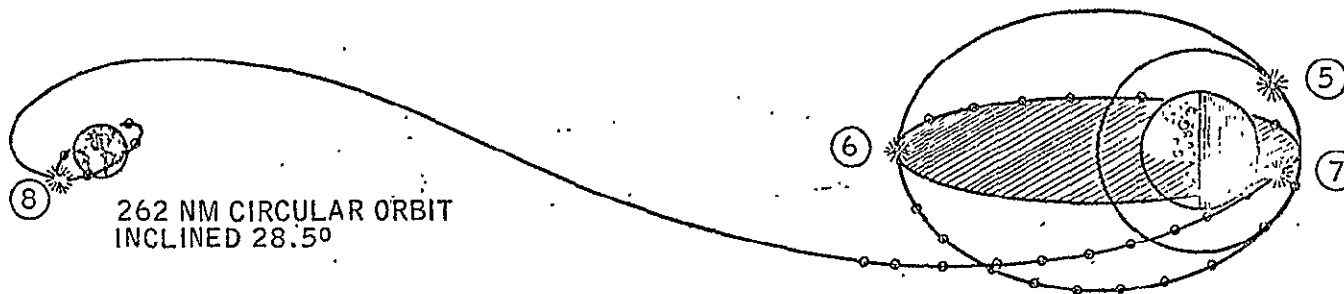


Figure 7 - Flight Profile for Eight-Burn Lunar Mission

TABLE 2

COOLDOWN PROPELLANT SAVINGS USING NERVA ELECTRICAL
SYSTEM FOR EIGHT-BURN LUNAR MISSION, ALM

500 kw(t) Reactor Power Output							200 kw(t) Reactor Power Output						
Burn No. and Burn Time Min	Cooldown to 500 kw(e)	Hours Time	From 500 kw(t) Down	Time	Total lb	Hours Time	Cooldown to 200 kw(e)	Hours Time	From 200 kw(t) Down	Time	Total lb	Hours Time	
1	24.9	1,335	3.1	3,148	57.3	4,483	60.4	1,274	6.4	2,094	54.0	3,368	60.4
2	2.0	246	0.40	550	6.1	796	6.5	220	0.9	345	5.6	565	6.5
3	1.3	195	0.10	499	6.8	694	6.9	173	0.75	359	6.15	532	6.9
4	2.2	272	0.24	1,211	32.56	1,483	32.8	219	1.10	1,031	31.7	1,250	32.8
5	1.9	241	0.28	542	6.72	783	7.0	208	0.95	374	6.05	582	7.0
6	0.8	180	0.05	410	6.75	590	6.8	148	0.70	310	6.1	458	6.8
7	1.2	164	0.23	913	23.67	1,077	23.9	165	0.8	793	23.1	958	23.9
8	10.0	781	1.5	1,795	37.4	2,576	38.9	375	3.6	1,179	35.3	1,554	38.9
TOTAL		3,414 lb	5.9	9,068 lb	177.3	12,482	183.2	2,782 lb	15.2	6,485 lb	168.0	9,267	183.2

Conventional Cooldown Consumption = 20,720 lb.

Total Time - 9 Btu/sec

27.

durations for 500 kw(t) and 200 kw(t) systems are also shown in Table 2. As indicated by the summation values, approximately 10,000 lb of cooldown flow can be saved, and the duration of cooldown can be reduced to approximately 5 to 10% of the conventional nuclear rocket system (cooldown thrust durations for single, independent burns are shown in Figure 7).

The time from reactor scram to initiation of dual-mode operation as a function of engine-burn duration is shown in Figure 8. For a short burn time (e.g., two minutes) the corresponding delay to initiation of dual-mode operation is approximately two minutes. For burns of longer durations (e.g., 25 minutes), the corresponding delay to initiation of dual-mode operation is only six minutes. Delay times are based upon the normal engine shutdown periods used for the eight-burn lunar mission, ALM. These values may be used with the data presented in Figure 7.

The corresponding decay power levels at initiation of dual-mode operation as a function of engine burn time are also shown in Figure 8. The decay power level at initiation of dual-mode operation is many times greater than the 200 kw(t) power level required for steady-state 25 kw(e) electrical system operation for all practical engine burn durations. Initially, the major portion of the decay power is removed from the engine by the hydrogen cooldown flow. To permit concurrent dual-mode operation, it is essential that the cooldown flow be proportioned through the nozzle-reflector and core regions to remove decay power without overcooling the aluminum reflector cylinder.

The electrical-power demand profile of the NERVA engine is shown in Figure 9 for an eight-burn lunar shuttle mission. The peak demands of approximately 5 kw(e) occur during engine firing, but the integrated power is maximum during the long cooldown transients. Since the electrical mode would normally be operative during the cooldown phase, it would be desirable to supply power to the engine during this period with the electrical system.

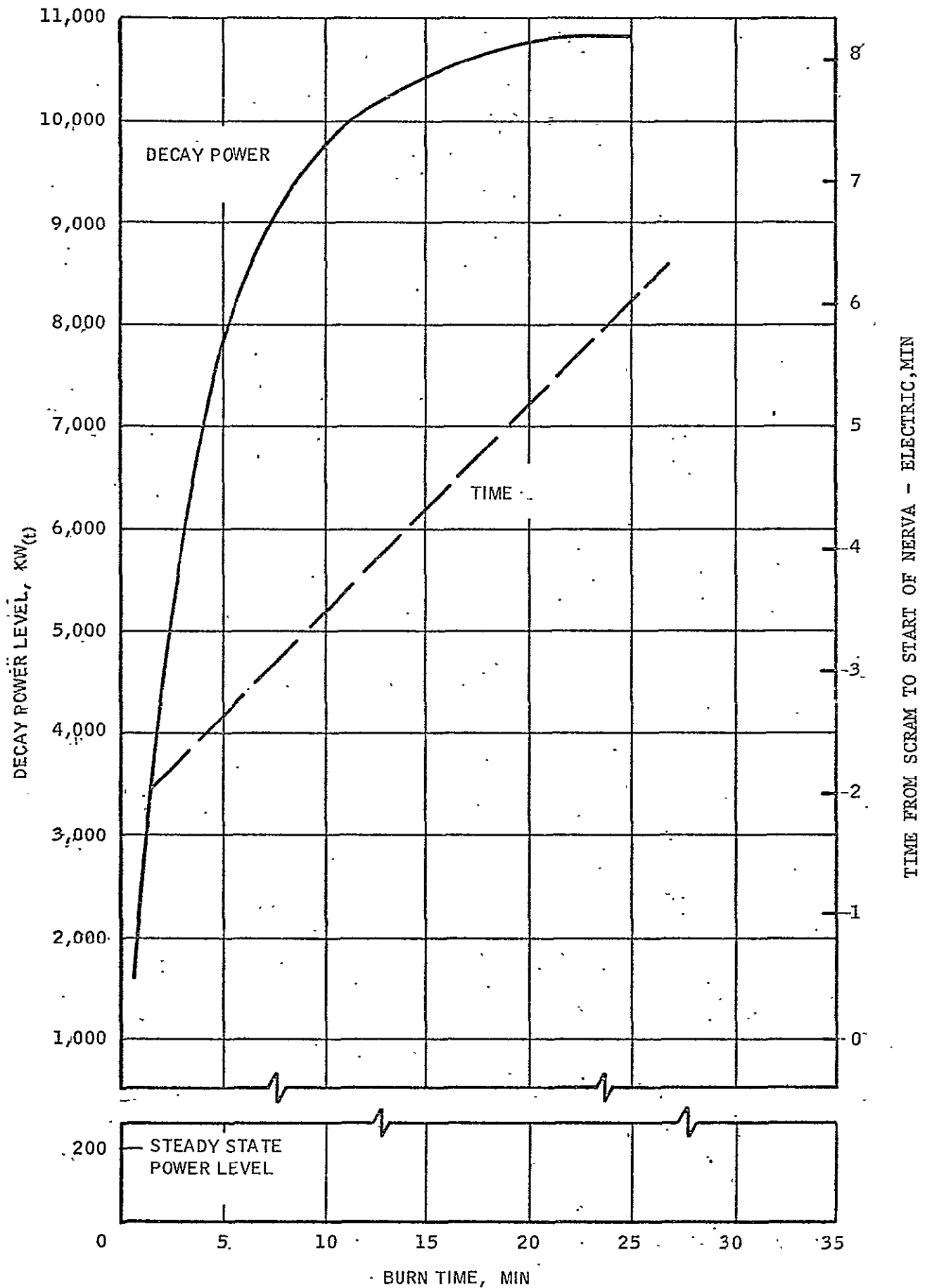


Figure 8 - Time from Scram and Decay Power Level for Initiation of NERVA Electrical Operation

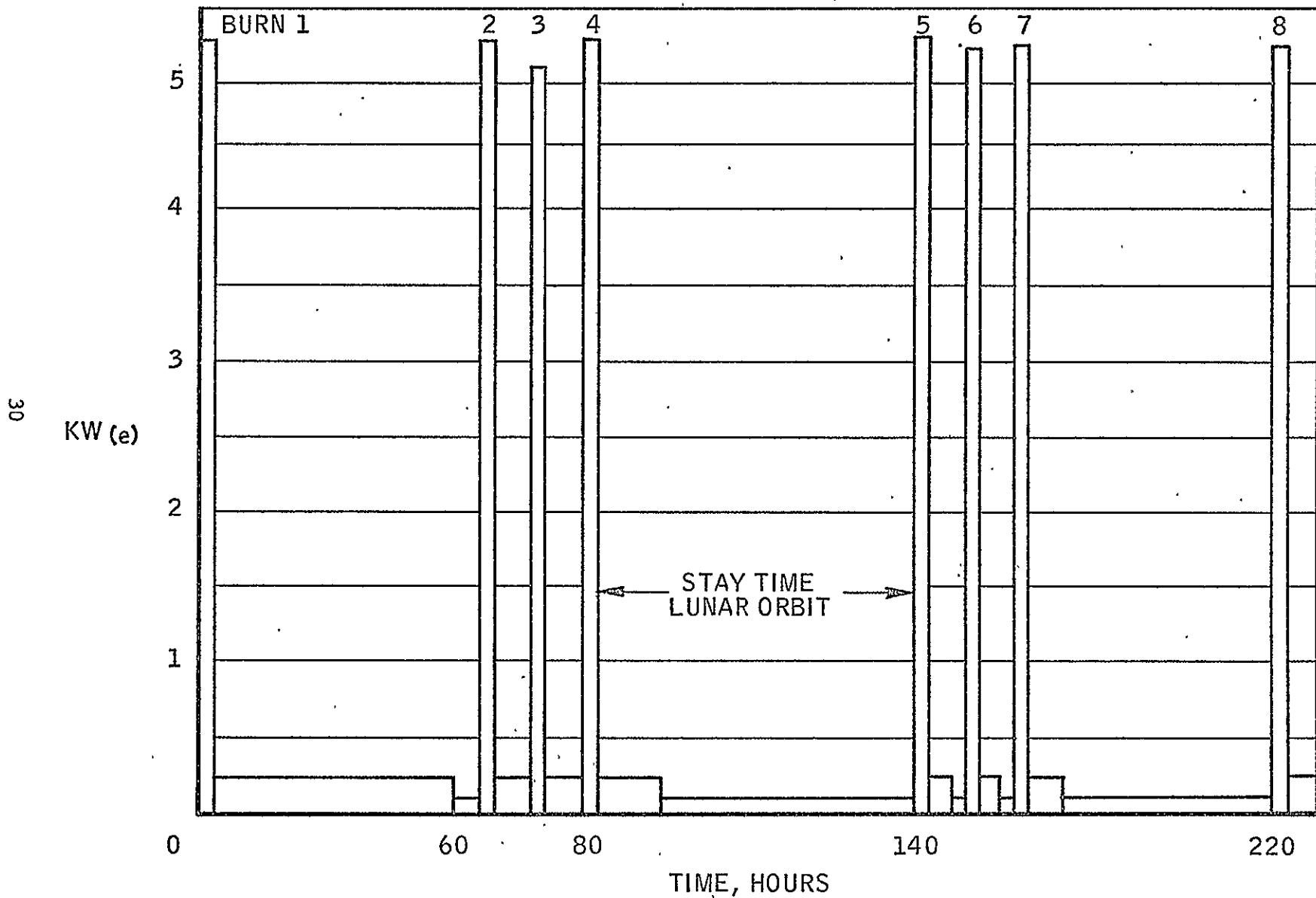


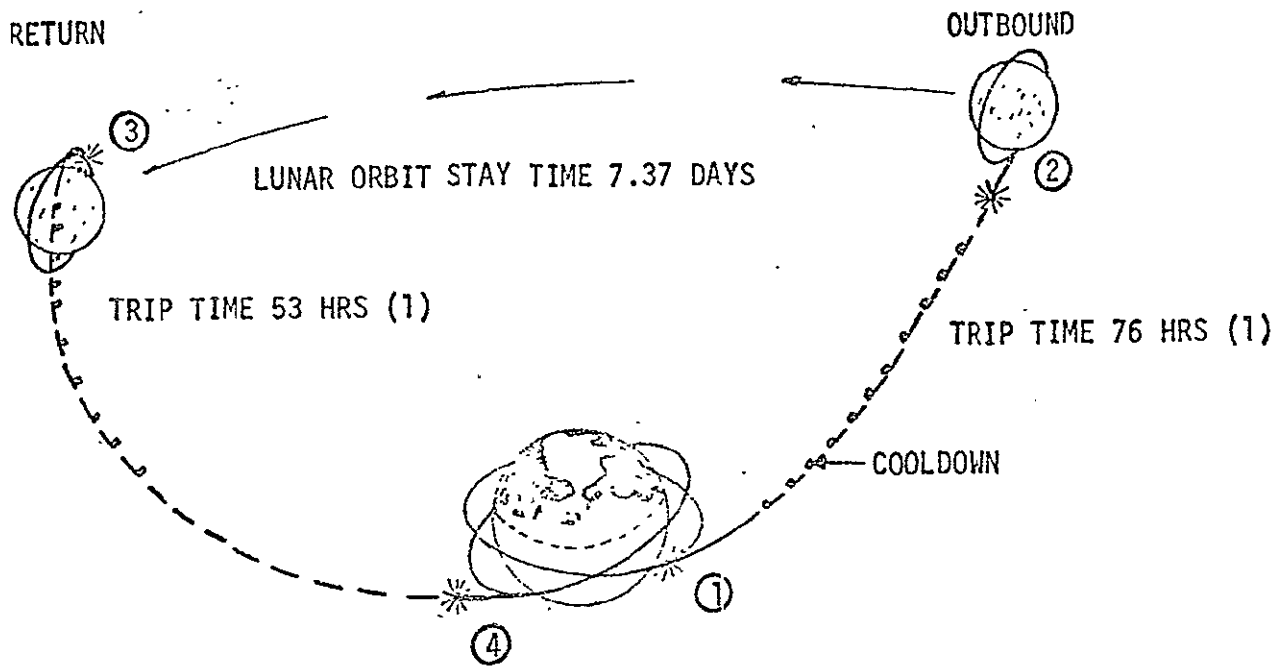
Figure 9 - Nominal Load Profile, Eight-Burn ALM Mission,
Total Integrated Power of 34 kw-Hr

Engine power requirements for the normal rocket mode can be supplied by storage batteries which are then recharged by the electrical power system during the cooldown phase. The weight of the storage batteries has been estimated to be only 80 to 100 lb.

A four-burn lunar mission was also investigated. In this flight plan, the additional variable of vapor cooldown was introduced. ANSC and North American Rockwell studies have shown that use of all-liquid cooldown for the reference NERVA engine and reference reusable nuclear shuttle results in the need to vent the tank after the second and third burns. The flight plan is pictured in Figure 10. When liquid and vapor are used for cooldown, tank pressure does not reach limits and tank venting can be avoided. This is desirable because a significantly increased payload results. Comparison of the reference liquid cooldown mode (Case 1) with three possible vapor cooldown modes is shown in Table 3.

Use of vapor in the cooldown mode is even more important for dual-mode operation. The radiator-meteoroid bumper slightly increases heat leakage into the propellant. As a consequence, when all-liquid cooldown is used, additional tank venting is required and the payload is reduced significantly. Use of liquid and vapor in cooldown provides a means for self-refrigerating the remaining tank liquid, thus overcoming the need to vent the tank. This flight mode is shown as Case 5 in Table 3 where a total of 7614 lb of cooldown fluids are required as compared with 14,433 lb of cooldown fluids for other nonventing operating modes. In Case 1 of Table 3, an additional 5150 lb of propellant are vented. The total payload advantage of the dual-mode system with vapor cooldown is 30,667 lb relative to the reference system, Case 1. This is a 20% increase for the lunar orbit mission.

Case 5 of Table 3 shows a significantly greater payload advantage in comparison with that shown by North American Rockwell Space Division in Figure 11. This difference results from initiating dual-mode operation at decay power levels shown in Figure 6, as against waiting until the decay



BURN NUMBER →	1	2	3	4
FULL POWER DURATION (MIN)	29.75	5.28	2.76	7.24
COOLDOWN DURATION (HRS)	76.26	90.24*	36.89	72.59*

* DOCKING OCCURS AFTER 10 HRS, REMAINDER OF COOLDOWN IS NULLED

(1) DURATION FROM FIRST FLOW INTERRUPT (END OF SHUTDOWN) TO NEXT STARTUP

- ① BURN NO. 1 DEPART 262 N.M. CIRCULAR EARTH ORBIT - TRANSLUNAR INJECTION
- ② BURN NO. 2 RETRO INTO LUNAR ORBIT
- ③ BURN NO. 3 DEPART 60 N.M. CIRCULAR LUNAR ORBIT - TRANSEARTH INJECTION
- ④ BURN NO. 4 RETRO INTO EARTH ORBIT

ORBIT PARAMETERS	EARTH ORBIT	LUNAR ORBIT
ALTITUDE (NM)	262 CIRCULAR	60 CIRCULAR
INCLINATION (DEG)	28.5	90
PERIOD (MIN)	94.2	119
RATE OF PRECESSION (°/ DAY)	-6.77	-
MOON'S ANGULAR MOTION (°/DAY)	-	13.2

NOTE: TOTAL ELAPSED TIME EARTH ORBIT IGNITION TO EARTH ORBIT DOCKING IS 13.62 DAYS

Figure 10 - Flight Profile for Four-Burn Lunar Mission

TABLE 3
COMPARISON OF COOLDOWN MODE OPTIONS - FOUR-BURN LUNAR MISSION

	<u>All Liquid Cooldown</u>	<u>Vapor Cooldown Following Last Burn</u>	<u>Vapor Cooldown After All Burns</u>	<u>Vapor Cooldown After All Burns</u>	<u>NERVA Electric, Vapor Cooldown</u>
Vapor Pressure, Start (psia)	15.0	15.0	15.0	23.0	27.0
1st Cooldown					
LH ₂ (lbm)	7,381	7,381	5,600	1,600	1,958
GH ₂ (lbm)	0	0	2,781**	5,781*	2,302
Vent (lbm)	0	0	0	0	0
Vapor Pressure, End (psia)	19.6	19.6	16.3	16.9	17.7
2nd Cooldown					
LH ₂ (lbm)	2,467	2,467	1,500	500	807
GH ₂ (lbm)	0	0	1,967*	1,967*	291
Vent (lbm)	2,000	2,000	0	0	0
Vapor Pressure End (psia)	26.0	26.0	23.9	24.1	--
3rd Cooldown					
LH ₂ (lbm)	1,510	1,510	350	350	567
GH ₂ (lbm)	0	0	1,160*	1,160*	189
Vent (lbm)	3,150	3,150	0	0	0
Vapor Pressure, End (psia)	22.0	22.0	24.4	24.5	--
4th Cooldown					
LH ₂ (lbm)	3,085	500	500	500	567
GH ₂ (lbm)	0	2,585*	2,585*	2,585*	933
Vent (lbm)	0	0	0	0	0
Ullage Pressure, End (psia)	27.0	17.0	16.1	16.2	16.2
Residual Vapor (lbm)	10,250	7,000	6,100	6,200	6,200
ΔFL _{outbound} ***	0	+12,000	+27,000	+26,600	30,667

*Switch from liquid to vapor cooldown at reactor decay power of 2900 Btu/sec

**Switch from liquid to vapor cooldown at reactor decay power of 400 Btu/sec

***Reference Case Total payload = 150,000 lbm (approximate)

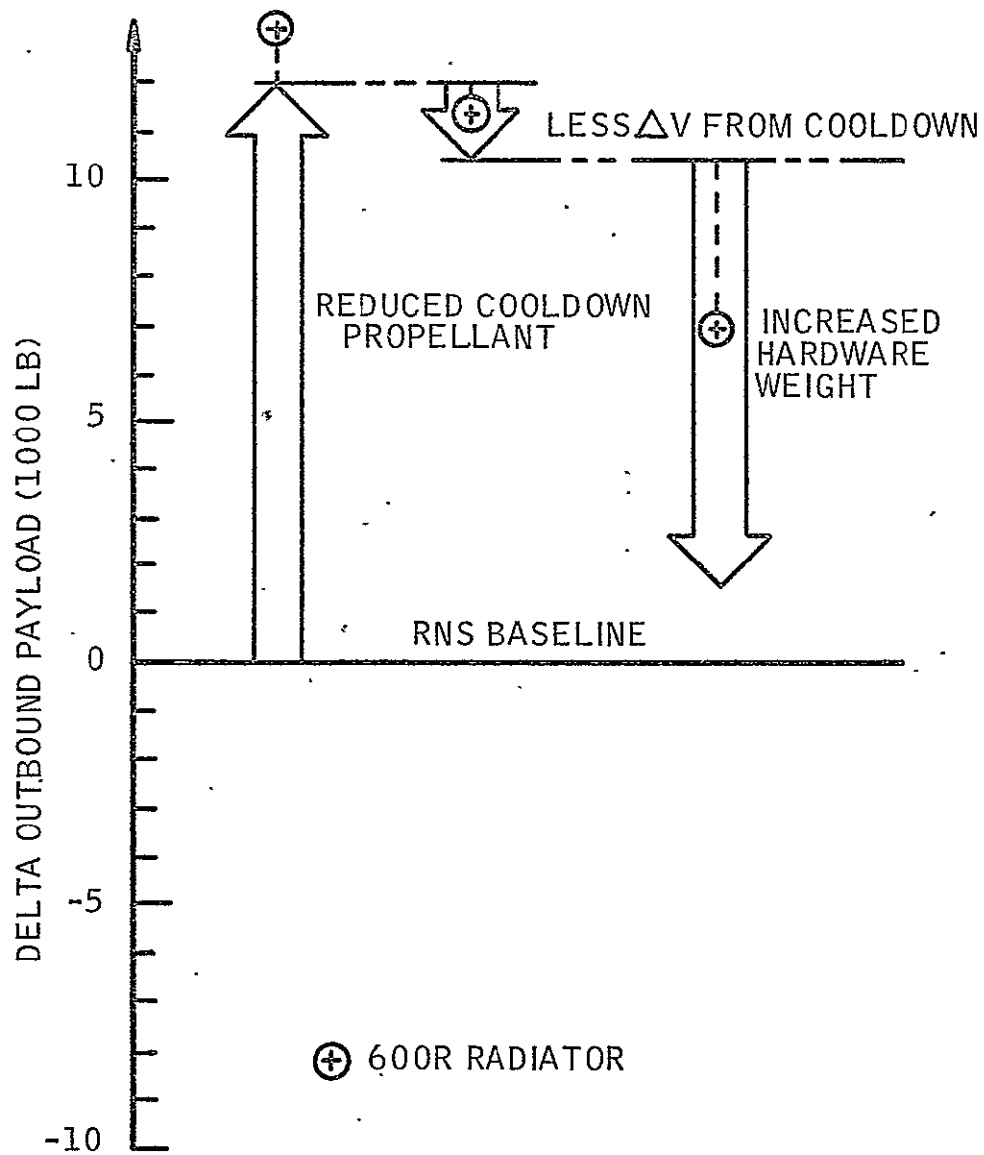


Figure 11 - Effect of Radiator on Reusable Nuclear Shuttle Payload Capability

power was 200 kw(t) as assumed in the North American Rockwell calculation, and utilizing liquid and vapor cooldown fluid, eliminating the boiloff and insulation weight penalty. Though the increased hardware weight penalty is real, it should be noted that 25 kw(e) is available for the dual-mode system as opposed to 3 kw(e) for the fuel-cell system. Figure 11 also shows a correction in payload for the reduced amount of cooldown fluid used. This correction is labeled ΔV cooldown. The greater the amount of cooldown fluid conserved, the greater the loss in ΔV . It is still desirable to conserve cooldown fluids because the cooldown fluid is exhausted at low velocity as compared with the exhaust velocity during normal engine operation.

A summary of the payload increment for the dual-mode system relative to the conventional reusable nuclear shuttle is shown in Table 4. The payload increment is increased for each mission because of cooldown fluid savings, decreased by the ΔV because of lesser cooldown, and decreased by the greater hardware weight of the 25 kw(e) system. In the cases of the eight-burn lunar mission and the four-burn deep space injection mission, the payload increases are 3618 and 6432 lb as compared with normal payloads of 135,000 and 90,000 lb, respectively. For these missions, the nature of the cooldown fluid (i.e., all-liquid or liquid and vapor) is not important because tank venting does not occur. The four-burn lunar mission with the reference vehicle system (i.e., a NERVA engine with liquid cooldown) requires tank venting for the 30-day lunar orbit. Comparison of the reference system with the dual-mode system with liquid-and-vapor cooldown favors the latter system by 30,667 lb for a nominal payload of 150,000 lb. If the reference vehicle were to use liquid-and-vapor cooldown, the payload advantage of the dual-mode system would be reduced to 4067 lb.

E. CONTROL SYSTEM

The type of control system most appropriate is the one which has the least impact upon reactor operation. Thus, a parasitic load control

TABLE 4

SUMMARY-PAYLOAD INCREMENTS FOR THREE MISSIONS
UTILIZING DUAL MODE VS REFERENCE NERVA

	<u>Total Hydrogen Savings lb</u>	<u>Payload Increase Due to Hydrogen- Savings lb</u>	<u>Payload Decrease Because of ΔV lb</u>	<u>Payload Decrease Because of Added Weight lb</u>	<u>Effective Payload Increase</u>
Eight Burn Lunar Mission - ALM	9,267	21,080	-9,200	-8,262	+3,618
Four Burns Lunar Mission	6,833	16,385	-4,462	-7,856	+4,067* +30,667**
Four Burn Deep Space Injection	5,196	17,068	-2,064	-8,572	+6,432

*Relative to reference engine with vapor cooldown.

**Relative to reference engine with all liquid cooldown.

system was selected. The thermal power from the NERVA engine is maintained at a constant level insofar as practical. This primary-loop thermal power is converted into electrical energy and waste heat. Electrical power is supplied to the load and excess electrical power is dissipated by means of the parasitic load resistor in the control system. Thus, the power-conversion system also operates at essentially a constant output. This design approach is desirable from the standpoint of overall simplicity and reliability because it greatly simplifies the system design by eliminating control valves.

F. LOCATION OF COMPONENTS

As shown in Figure 1, dual-mode electrical system components are located in the engine compartment, on the outer skin of the stage, and in the compartment immediately above the tank. The primary loop includes a flow circuit within the engine pressure vessel, lines across the gimbal system that run forward on the outer surface of the stage to the payload end of the vehicle, and a heat exchanger in the payload compartment. These insulated lines are the upcomer and downcomer for the primary-loop coolant, which has a maximum pressure of approximately 600-1000 psia and a maximum temperature of 775°R. At the forward end of the stage, the primary-loop coolant passes through a heat-exchanger boiler where the heat is transferred from the hydrogen in the primary loop to the working fluid in the power-conversion system. The primary-loop coolant-makeup-fluid subsystem and the compressor-motor unit for circulating the gaseous hydrogen are located at the forward end of the stage.

All of the power-conversion system components are located at the forward end of the stage. The major components include a boiler, turbo alternator-pump assembly (TAPA), regenerator, condenser, and working-fluid injection start system. The forward location for these components is desirable because it separates them from the radiation source as far

as practical. Thus, less shielding is required, and limited maintenance can be provided. The working fluid for the power-conversion system will not experience degradation from either nuclear or thermal radiation in the environment at the forward end of the stage.

The heat-rejection system is comprised of a number of parallel, independent, coolant flow circuits that transport heat from the condenser to the outer surface of the meteoroid shield. Each of these 600-1000 psia hydrogen-filled flow circuits is provided with a completely enclosed electric-motor-driven fan which circulates the hydrogen. The compressor-motor units are also mounted in the payload end of the vehicle for radiation protection and ease of maintenance. Each of the radiator loops is provided with a means for charging the system with gaseous hydrogen. Should a major leak develop in any loop, it would be undesirable to continue charging. Therefore, a means for rejecting nonoperating loops would be provided.

The stage battery-inverter system, also located in the payload compartment, will provide the energy source to enable the primary loop and/or the heat-rejection loop to operate independently from the operation of the power-conversion system. This is necessary for stage checkout and startup provisions. It may also be necessary to utilize these circuits to temperature condition the power-conversion-unit compartment. The temperature range for the gaseous hydrogen in the primary and heat-rejection loops is sufficiently ample so that it is not necessary to be concerned about their operating temperature limits caused by the space environment.

G. SYSTEM WEIGHTS

The weight estimate of the dual-mode system presents unusual problems because the system must be integrated with other systems on the stage to be competitive. It is assumed that these other systems are essential to the stage and are present even if the dual-mode electrical system is not.

Therefore, only those additional weights related to the system are considered in the weight analysis. The additional weight necessary for the application of the system may be compared with conventional electrical power systems for weight-comparison purposes.

The hardware weights listed in Table 5 for the 25-kw(e) system show that the heat-rejection system estimated weight of 3600 lb is the major portion of the total system weight of 6000 lb. The major item is the aluminum tubing that comprises the header-manifold system for distribution of thermal energy to the skin of the meteoroid shield. This concept was studied by North American Rockwell and the results are discussed in detail in this report. The controlling parameter which can be varied is the system's internal hydrogen pressure. Significant weight savings can be realized by increasing pressure. The pressure level initially selected was 600 psia which results in the weight figures of Table 5. Pressure in the range of 1000 to 3000 psia are very attractive from a weight standpoint. The weight advantage of the higher-pressure system arises from a stress-limited header-manifold system which requires less manifolding and less meteoroid protection because of a smaller tube-profile area. Less pumping power also is required.

The total weight estimate of 1500 lb for the power conversion system reflects a conservative design needed for long-duration operation. The low maximum cycle temperature permits the extensive use of aluminum alloys, which also helps reduce system weight. The specific weight of the power conversion system is approximately 60 lb/kw(e) net.

Comparison of the above weight estimate with the SNAP-8 mercury-Rankine and the lower-temperature Aerojet ORACLE systems proved interesting. The 50-kw(e) SNAP-8 power conversion system weight per kilowatt for an unmanned, deep-space application is 100 lb-kw(e). The corresponding ORACLE power conversion system specific weight is also in range of 100 lb/kw(e).

TABLE 5

HARDWARE WEIGHT BREAKDOWN (PRELIMINARY)
DUAL-MODE SYSTEM 25 kw(e)

<u>Primary Loop (600 psia)</u>		<u>lb</u>	
1.	Engine - Additional Weight		
	(1) Reactor Subsystem	290	
	(2) Pressure Vessel	120	
2.	Lines and Joints	380	
3.	Insulation	10	
4.	Charging System	40	
5.	Compressor and Motor and Inverter	35	
6.	Control	<u>25</u>	
	Subtotal		900
<u>Power-Conversion System</u>			
1.	Boiler	200	
2.	Turbine-Alternator-Pump Assy	200	
3.	Regenerator	70	
4.	Condenser	200	
5.	Charging System	20	
6.	Inventory	80	
7.	Speed Control	60	
8.	Piping and Valves	220	
9.	Structure, Cable, Boxes, etc.	<u>450</u>	
	Subtotal		1500
<u>Heat Rejection (600 psia)</u>			
1.	Radiator Loops	3000	
2.	Fan-Motor and Inverter	200	
3.	Control	100	
4.	Charging Subsystem	<u>300</u>	
	Subtotal		3600
	Total Weight		6000
	Specific Weight		
	6000/25 =		240 lb/kw(e)

The primary loop weight estimate of 900 lb includes those components that must be added to the engine and stage to duct heat from the engine to the booster at the forward end of the stage. This weight is for a 600-psia internal pressure of the hydrogen which was the maximum allowable pressure for one of the circuits in the reactor under consideration for the heat exchanger. Because the circuit selected for the dual-mode electrical system is separate from the normal engine flow circuit, the original limitation is not appropriate. Increasing the pressure should be evaluated because it will permit reduced channel flow area and reduction in weight. The reduction of channel flow area in the reactor portion of the engine may be a very important consideration because it tends to minimize the impact of the dual-mode system upon the design of the engine.

In addition to the savings in cooldown flow, the NERVA electrical system offers early termination of the thrusting period associated with cooldown. Cooldown thrust-duration curves are also shown in Figure 6. A single 1500-sec full-thrust burn requires more than 60 hr of cooldown flow. This period of thrusting is reduced to approximately 6 and 3 hr for 200- and 500-kw(t) systems, respectively.

The reduction of cooldown-propellant requirement and the reduced period of cooldown thrusting represent potential weight savings for the nuclear stage in comparison with a nuclear stage with other forms of electrical power systems.

H. OFF-DESIGN OPERATION

In the preceding discussion of cooldown flow and duration requirements, it was noted that the greater the thermal-power capability of the NERVA electrical system, the greater the cooldown-flow savings and the shorter the duration of the cooldown thrusting period (see Figure 6). It is anticipated that it will be desirable to operate any particular NERVA electrical

system at a greater-than-normal power rating for the duration of the cooldown flow cycle. This off-design operation may decrease the net-output electrical-power capability during the cooldown period because of the additional electrical power needs of the primary-loop compressor motor and the heat-rejector-loop fan motors. Since the duration of off-design, high-power operation is anticipated to be only a few hours, it would not be significant in the overall electrical power production of the NERVA electrical system.

To accurately assess the maximum thermal capability of a 25-kw(e) system, more component detail is required than is currently available. An increase in thermal rating from 200 to 500 kw(t) is probably a reasonable limit for the maximum off-design condition. The incremental propellant saving for 500 versus 200 kw(t) for a 1500-sec burn is 1000 lb of cooldown flow: reducing the duration of cooldown thrust from approximately 6 to 3 hr for a 16-minute burn may be an improvement worth seeking.

Figure 6 shows the amount of the cooldown propellant required as a function of full-power burn time for three dual-mode cases: (1) 0 kw(t); (2) a 200-kw(t) system; and (3) a 500-kw(t) system. The 0-kw(t) system is representative of a conventional nuclear-rocket system without a dual-mode system. The 200-kw(t) thermal system is representative of a 25-kw(e) system, and the 500-kw(t) system could be a 50-kw(e) system or a modified 25-kw(e) system. The startup flow requirement of 275 lb is shown in Figure 6 for comparison.

From the sum of the startup and cooldown propellant curves, it is apparent that multiple short burns will consume more startup-cooldown propellant than a single burn of equal duration. This is reflected as an average specific-impulse degradation in comparison with the normal-burn specific impulse (see Figure 12). An increase of approximately 15 sec of average specific impulse may be obtained for long-duration burns and even greater increase is obtained on short-duration burns.

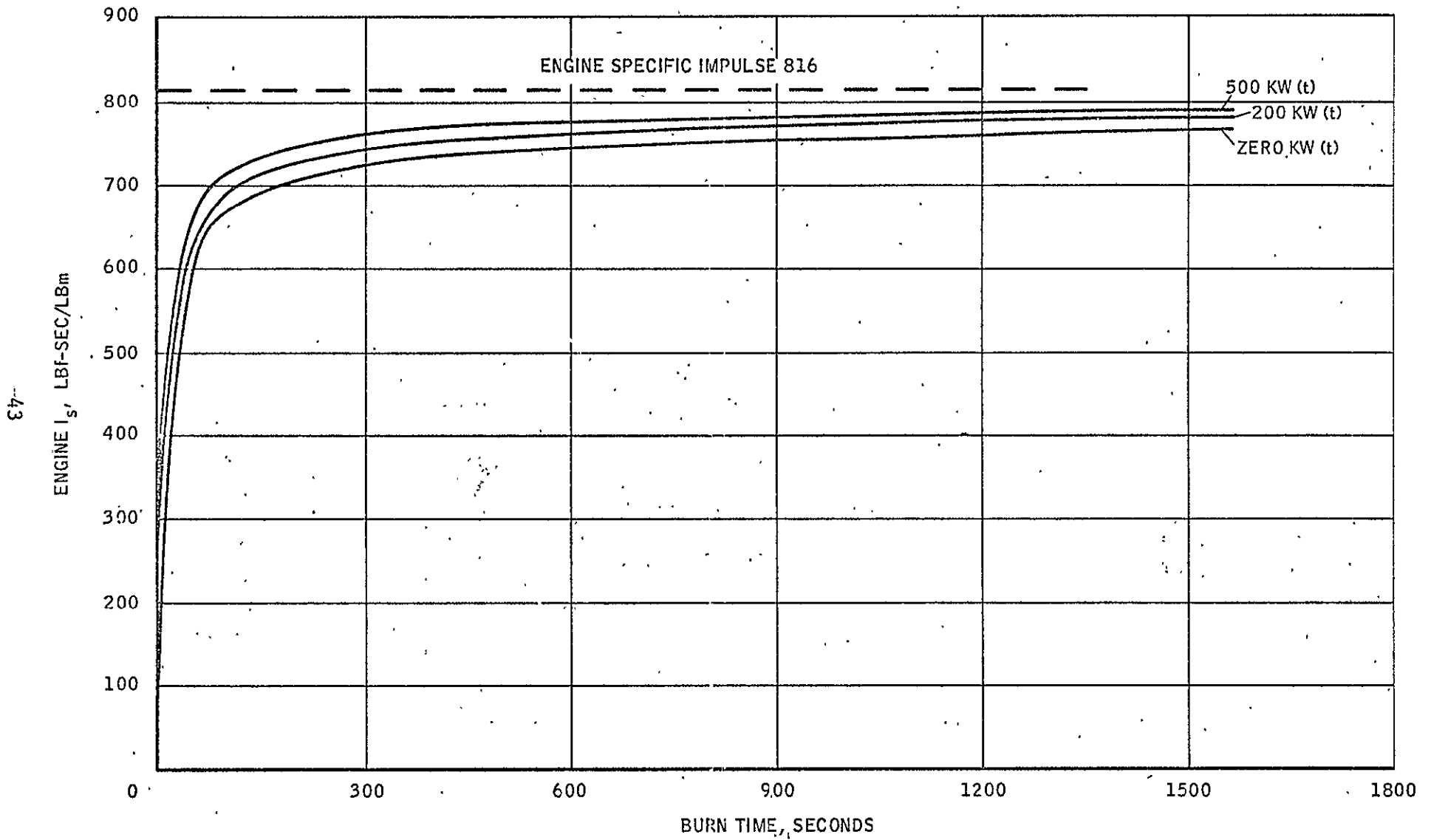


Figure 12 - Average Specific Impulse Vs Burn Time

I. LIFE OF SYSTEM

The major parameter that determines the operating life of heat engines is the maximum cycle temperature. Figure 13 shows the operating life that has been achieved with various types of heat-generating engines as a function of their maximum cycle temperature (the higher the maximum cycle temperature, the shorter the normal operating life). However, the maximum cycle temperature of 775°R, which is characteristic of the dual-mode electrical system, should permit very-long-life systems. At this modest temperature, organic working fluids and lubricating oils thermally decompose at such low rates that other factors will control engine life. Because the power-conversion system is located at the forward end of the stage, the radiation emanating from the reactor will be greatly attenuated by the shielding and reduced in intensity by the relatively large spacing between the reactor and the power-conversion system working fluid.

The major factor concerning the operating life of the NEP^{VA} electrical system is leakage. The working fluid of the power conversion system will be a relatively heavy, large-molecule fluid, and the system can be completely sealed. With the exception of the charging system, valves are not required: no packing or rotating-shaft seals vent to space. As a result, the working-fluid retention should not be a problem. However, the primary loop and the radiator loops are filled with high-pressure gaseous hydrogen. Leakage from these loops could be the major factor limiting life. The condenser-radiator loops can be made redundant and can be completely sealed by brazed or welded joints, except for the recharging valve. This feature is especially important in the radiator because of the large areas exposed to meteoroid damage. The primary loop has much smaller area and can be well protected for a small weight penalty. For applications such as a lunar shuttle, where resupply will occur at one- to two-month intervals, nominal leakage rates are acceptable: however, for deep-space missions lasting years, only very small leakage rates can be tolerated.

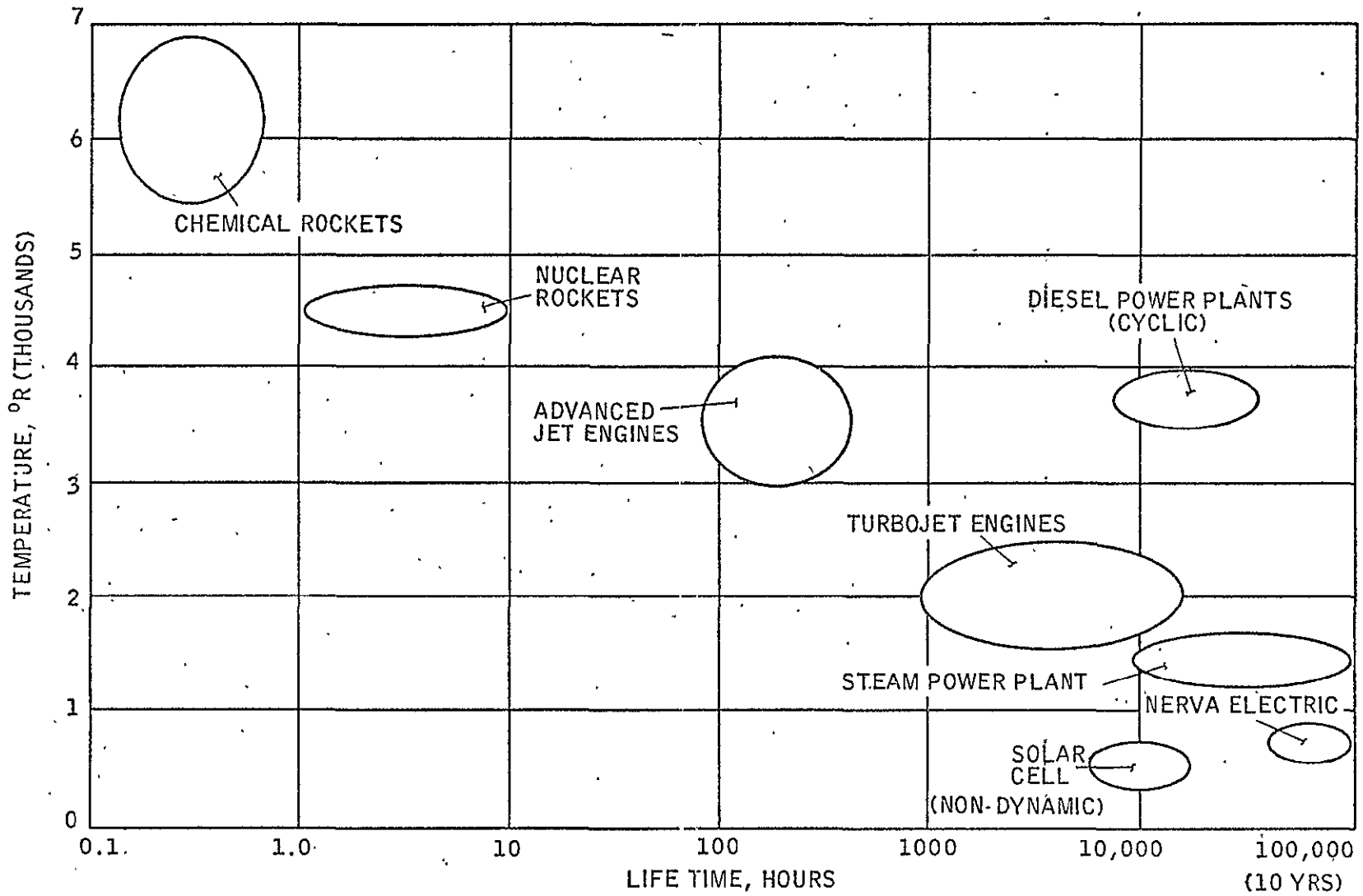


Figure 13 - Effect of Maximum Temperature Upon Life of Power Conversion Systems

While primary-loop designs to prevent leakage were given prime consideration, it should be recognized that a NERVA-powered stage has a large quantity of hydrogen on-board in the "empty" propellant tank, which could be used as make-up fluid for the primary and heat-rejection loops.

The multiple-loop redundancy concept for the radiator is described in Section VIII. This design feature is also important from the environmental standpoint where sections of the radiator exposed to high thermal inputs would be shut down because they would actually cause heat input to the condenser rather than heat rejection. To shut down a loop, the circulating fan would be turned off. In case of meteoroid puncture of a particular loop its hydrogen would be lost (including that in its recharging bottle) and the loop would become ineffective. By inter-positioning loop distribution tubes, adjacent loops would more efficiently utilize the fin area of the inactive loop. In this manner partial recovery of radiating capability is realized.

J. RADIATION EFFECTS

The radiation dose to a payload is affected by the engine design, the shielding, and the stage design. A minimum-weight system requires attention to design in all three major units.

The radiation inside the NERVA engine during normal rocket-mode operation is extremely intense. To protect engine and stage components, an internal shield is provided within the pressure vessel. Provision has also been made for a second shield to be located directly above the pressure vessel if manned missions required it. These two shields weight approximately 3500 and 10,000 lb, respectively. Stage optimization studies conducted by a vehicle contractor have shown that the secondary shield should have a weight of only 1500 lb to reduce the tank-top dose to 10 rem*.

*Nuclear Shuttle System Definition Study, North American Rockwell Space Division Report PDS70-242, 25 September 1970.

The engine shielding is also effective during the electrical mode of operation. Because the rate of power generation is only one part in 10,000 compared with NERVA rocket modes, thermal heating of engine components other than the core does not present a problem. The total dose per year is approximately the same as that for a 1-hr full-power burn. If the propellant tank is not filled with liquid hydrogen, the attenuation of the tankage propellant is significantly reduced.

A shielding calculation was made for a lunar mission with the dual-mode system in operation during cooldown. A shielding weight increase of 80 lb resulted. This value is well within the estimated error of calculation and is not significant.

During the period of this study, stage contractors have made significant changes in the design of the nuclear shuttle to reduce the radiation dose to the payload. They have greatly reduced the aft cone angle of the tank and the radius of the aft closure to eliminate the scatter radiation resulting from engine radiation outside the shadow shields. These modifications also increase the separation distance and increase the effectiveness of hydrogen as a shielding medium in the tank.

From the standpoint of the dual-mode electrical system, the new tank designs are a very important improvement. In the "fat-bottom" configurations, liquid hydrogen provided the attenuation for the scatter radiation resulting from the tank overhanging the shadow-shield envelope. The new designs do not overhang the shadow-shield envelope and do not cause scattering. In some applications the electrical system will operate with a partially filled or empty tank: thus, hydrogen is not always available for shielding. Figure 1 shows the design of a reusable nuclear shuttle with a narrow-cone section.

For long-duration manned space flights, significant additional shielding is provided the astronauts by the spacecraft. The spacecraft

shielding is expected to reduce radiation to the crew by a factor of 100 over that incident on the forward end of the stage. If this is the situation, the radiation dose to the crew, as a result of the dual-mode electrical system, is within the tolerance limits of the crew with the additional engine disk shield in place.

For deep-space flights of more than one-year duration, radiation-hardened components will be used in the payload. For these components, disk shielding is not anticipated to be necessary. Radiation-hardened components are anticipated to have a threshold damage of 10^6 rads as compared with an anticipated dose of 10^5 rads for a ten-year flight.

Docking maneuvers for propellant transfer will require maintaining the orientation of the NERVA stage relative to the propellant unit so that the engine shadow shields are effective. It makes little difference if NERVA is operating in the electrical mode, provided that the shield orientation is maintained and that there is a significant amount of propellant in the tank.

VII. SUBSYSTEM DESCRIPTION

A. PRIMARY LOOP

The primary loop extracts heat from the reactor core by flowing gaseous hydrogen through passages that run the length of the inner-reflector cylinder. This coolant is circulated by an electrically powered blower. The hydrogen gives up its heat to a series of heat exchangers that consist of superheaters, boilers, and preheaters for the power-conversion loop.

The primary-loop major design influences identified are: (1) heat extraction rate; (2) maximum allowable reactor core temperature; (3) coolant circuit flow resistance; and (4) pressure level of the coolant circuit.

The heat-extraction rate is directly proportional to the net delivered electric power required of the system (25 kw(e)). The variable influence on the amount of reactor power needed depends upon the achievable thermal efficiency. A thermal efficiency of 12.5% results from not only the design limits of the primary loop but also those of the power-conversion loop and the condenser-radiator loop. The heat-extraction rate is, therefore, directly dependent upon the net electrical power desired and influenced by: (1) the sink temperature achievable in the radiator; (2) the component efficiencies; and (3) the "delta" temperatures required to drive the heat across the various heat-transfer surfaces. A heat power extraction rate from the reactor core of 200 kw(t) resulted from the study design limits.

To maximize thermal efficiency and minimize the flow rates of heat-transfer fluids and thus physical size, the source heat temperature should be as high as possible. However, the goal of minimizing the system's impact upon the NERVA engine requires that configuration and materials currently being used be unchanged. With this ground rule, the maximum reactor-core temperature of 800°R (775°R maximum coolant temperature) was assumed to be

compatible with the aluminum structure. These same parts function safely at much higher reactor-core temperatures during the thrusting mode because the use of liquid hydrogen maintains them at temperatures thousands of degrees cooler than the core. Without this advantage of an external coolant, many engine parts must operate within a few hundred degrees of core temperature. This situation is the primary influence that limits the maximum cycle temperature to 775°R.

A third design consideration is flow resistance in the primary loop. The major resistance is the heat-transfer surfaces of the reactor, the heat exchangers. A smaller but not significant one is the interconnecting lines between the reactor and heat exchanger.

The selection of hydrogen as the primary-loop heat-transfer medium was influenced by considerations of reactivity, radiation, and availability. As a result, the transport properties, thermal conductivity, specific heat, and viscosity of hydrogen must be accepted. However, this is not a penalty, because hydrogen is a good heat-transfer medium. To identify the variables available to the designer, the parameters that influence the film driving temperature and the power expended in pumping may be expressed as

$$\Delta T_f \frac{\dot{H}_p}{\dot{H}_t} = \frac{\mu^{0.65}}{9100 k^{0.6} c_p^{0.4} \rho^2} \cdot \left(\frac{\dot{w}}{n} \right)^{1.95} \frac{1}{d^{3.95}}$$

where:

- c_p = Specific heat at constant pressure $\frac{\text{Btu}}{\text{lb}^\circ\text{F}}$
- d = Diameter of passage ft
- \dot{H}_p = Pumping power $\frac{\text{Btu}}{\text{sec}}$
- \dot{H}_t = Heat transfer rate $\frac{\text{Btu}}{\text{sec}}$

k	= Thermal conductivity	$\frac{\text{Btu}}{\text{sec-ft-}^\circ\text{F}}$
n	= Number of passages	---
ΔT_f	= Differential film temperature	$\Delta^\circ\text{F}$
\dot{W}	= Mass flow rate	lb/sec
ρ	= Specific weight	lb/ft ³
μ	= Viscosity	lb/sec-ft

For turbulent flow through circular passages, this may be approximated by

$$\Delta T_f \frac{\dot{H}_p}{\dot{H}_t} = \frac{0.65}{9100 k^{0.6} c_p^{0.4}} \left(\frac{\dot{W}}{\rho n d^2} \right)^2$$

and as

$$\dot{W} = \rho A V = \rho \frac{n \pi d^2}{4} V, \text{ where } V \text{ is average velocity.}$$

Substituting and combining the transport properties:

$$\Delta T_f \frac{\dot{H}_p}{\dot{H}_t} (f) \text{ const. } V^2.$$

The single parameter of velocity squared is the primary variable that can be altered by the designer to minimize the film driving temperature, ΔT_f , and the pumping power for a given heat transferred, \dot{H}_p / \dot{H}_t . But, the velocity for a given design depends upon: (1) the weight flow rate, \dot{W} , which is, in turn, dependent upon the temperature change across the heat exchanger; (2) the frontal area, $\frac{n \pi d^2}{4}$, normal to through-flow; and (3) the specific weight, ρ , of the heat-transport fluid. These temperature change across the heat exchangers, frontal area, and specific weight are the specific influences upon heat-exchanger design. The density is, in turn, a function

of the pressure selected for the loop (the higher the pressure, the smaller the film driving temperatures and pumping powers). Practical limits must be considered, however, since high pressures can mean higher stresses or weights of the piping and containers (higher pressures also mean higher pressure supply or refill sources).

Pumping power is reduced as the pressure and thus specific weight of the hydrogen is raised for a given weight flow rate and heat-exchanger frontal area. Heat-transfer coefficients remain the same (velocity would be inversely proportional to specific weight) and thus Reynolds Numbers remain constant. Reducing the frontal area of the heat exchanger reduces the number of tubes and/or the tube diameter. In fact, reducing the frontal area in proportion to an increase of specific weight of the hydrogen can yield a design requiring the same film "delta" temperature and pumping power to heat-transfer power ratio,

$$\Delta T_f \frac{\dot{H}_p}{\dot{H}_t}$$

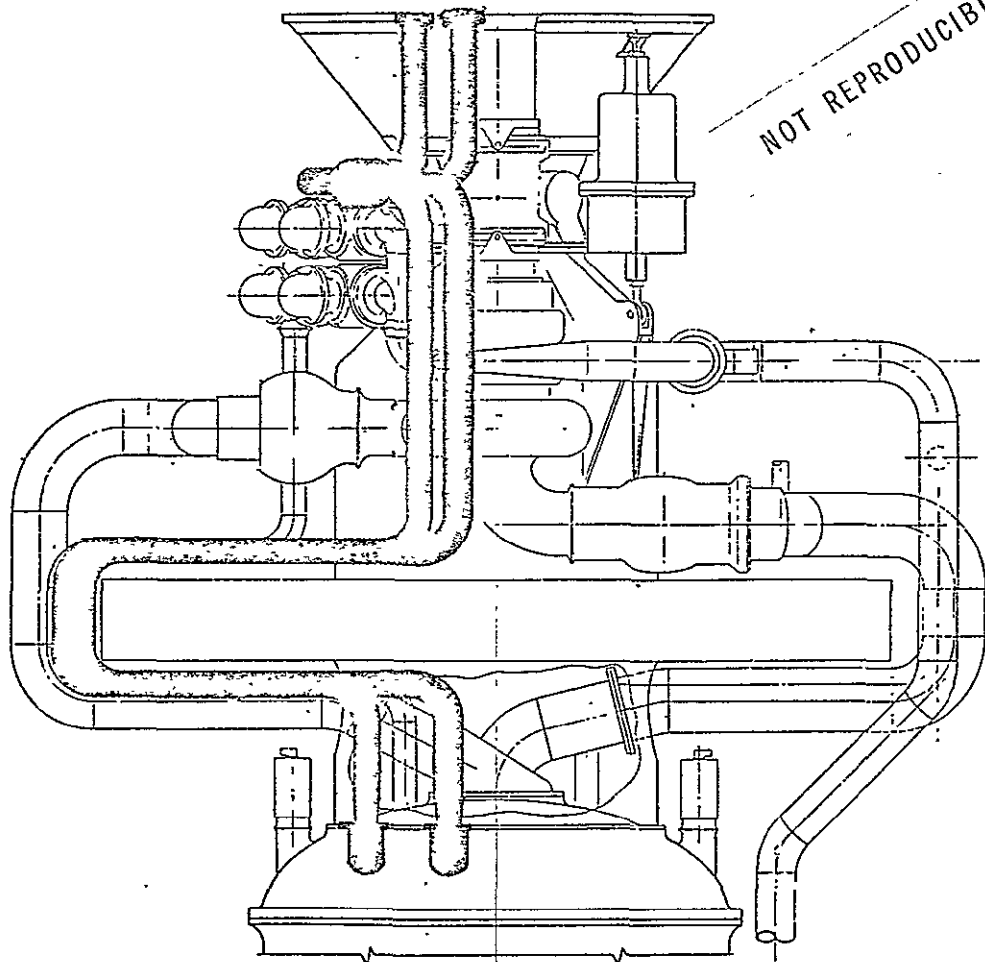
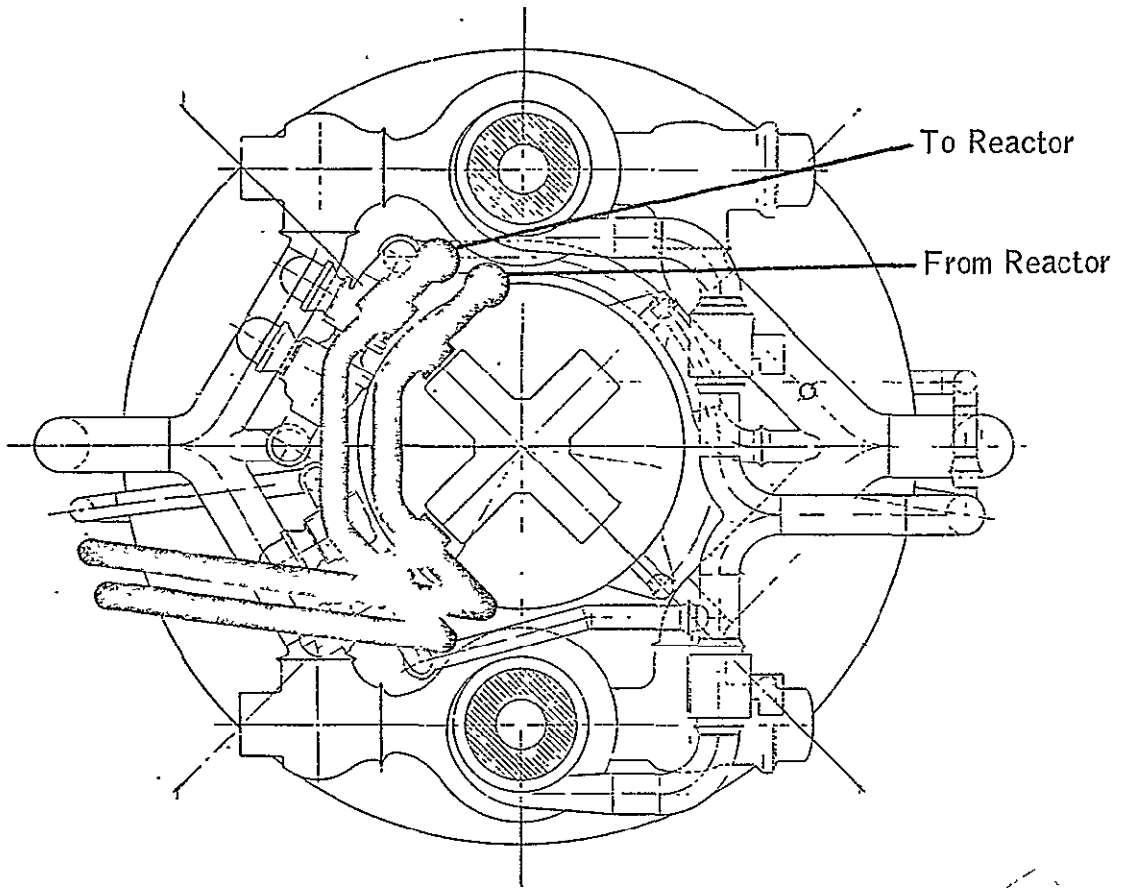
The heat exchanger is also shorter, however, in addition to having a smaller frontal area. Thus, a higher pressure in the heat exchanger is offset by smaller-diameter tubing, which results in no change in stress. But the shorter passage length required permits a lighter, smaller-volume heat exchanger. The selection of operating loop pressures should be optimized on the basis of: (1) combined weights of the loops and hydrogen supply systems; and (2) maximum volume allotted to the system.

To transport heat from the engine assembly to the forward end of the stage, a closed-loop circulating system is provided. The coolant is gaseous hydrogen at approximately 600 to 1000 psia. Hydrogen enters the reactor at approximately 775°R. The warm fluid flows through approximately 4-in. diameter insulated aluminum tubes which pass along the side of the hydrogen

tank between the outer layers of insulation and the meteorid shield. These lines can be supported by the same structure used to support the meteoroid shield. Because of the relatively low weight of this portion of the primary coolant loop, it may be practical to provide two loops for redundancy. At the forward end of the vehicle, an electric-motor-driven compressor, with a rotor supported by gas bearings, is provided for circulating the hydrogen gas. The high-pressure gas for charging the loop may be gaseous hydrogen, which has been compressed to the required pressure, or a high-pressure liquid may be vaporized to provide a source of hydrogen gas. Gaseous hydrogen has been selected for the primary loop because it does not contaminate the reactor nor does it become radioactive: therefore, it cannot cause secondary radiation problems in the payload compartment. Since the primary-loop operating pressure is greater than its environmental ambient pressures and since it is comprised of an all-metal system, it is nearly impossible to transport radioactive material from the engine to the payload end of the vehicle.

In the region where the primary-loop lines cross the gimbal plane, it will be necessary to provide flexible piping sections. Figure 14 shows the approximate routing of the lines from the 34.8-in.-pitch-diameter connections on the pressure-vessel dome, around the gimbal plane, and up to the remote-coupling engine-vehicle interface. The 600-psi lines are 4-in. in diameter and made of aluminum except for the flexible sections which are made of Inconel. The lines contract to 3-in.-diameter connections at the pressure-vessel connectors.

The primary loop requires a compressor or fan to circulate high-pressure gaseous hydrogen through the heat exchangers within the reactor ducting and boiler. Since this fluid pumping power is a parasitic load on the overall system, it is essential to select system design parameters that will insure that the pumping power is reasonable.



NOT REPRODUCIBLE

Figure-14 - Dual-Mode System Primary Coolant Lines

An additional consideration is that the efficiency of the fan be reasonable (e.g., above 50%). The fan efficiency also depends upon the system parameters which define the pumping load and the selection of the fan rotative speed. These parameters define the specific speed, N_s , which is related to fan efficiency.

To minimize the size and weight of the fan and drive motor, it is desirable to operate the fan at the highest speed consistent with the power supply. In the case of 400-cycle, three-phase power assumed to be generated by the electrical system, a two-pole electric induction motor can have a maximum speed of 24,000 rpm. Full-load speed will be approximately 2% less because of slippage.

The range of specific speed for a single-stage, 24,000-rpm fan for the primary loop, as shown in Figure 15, is from 100 to 425 and the corresponding efficiency range is from 0.85 to 0.77. The fan efficiency is only slightly affected by system pressure levels in the range from 600 to 1000 psia and changes from the nominal flow rate of 0.7 lb/sec and 75° ΔT. This figure is based upon a primary-loop coolant fluid pumping power requirement of 1.5 kw. These same efficiency data are cross-plotted in Figures 16 and 17 as functions of system pressure level and coolant ΔT. It is reasonable to plot the fan efficiency for a constant pumping power because the design of the heat exchangers and ducting would be adjusted to provide the reasonable pumping power required. For a given set of hardware, pumping power decreases rapidly with increasing system pressure and/or increasing coolant ΔT (i.e., decreasing weight flow rate). As primary-loop design studies continue, consideration of ducting size will be investigated. The efficiency curves of the fan do not suggest that it would significantly change performance.

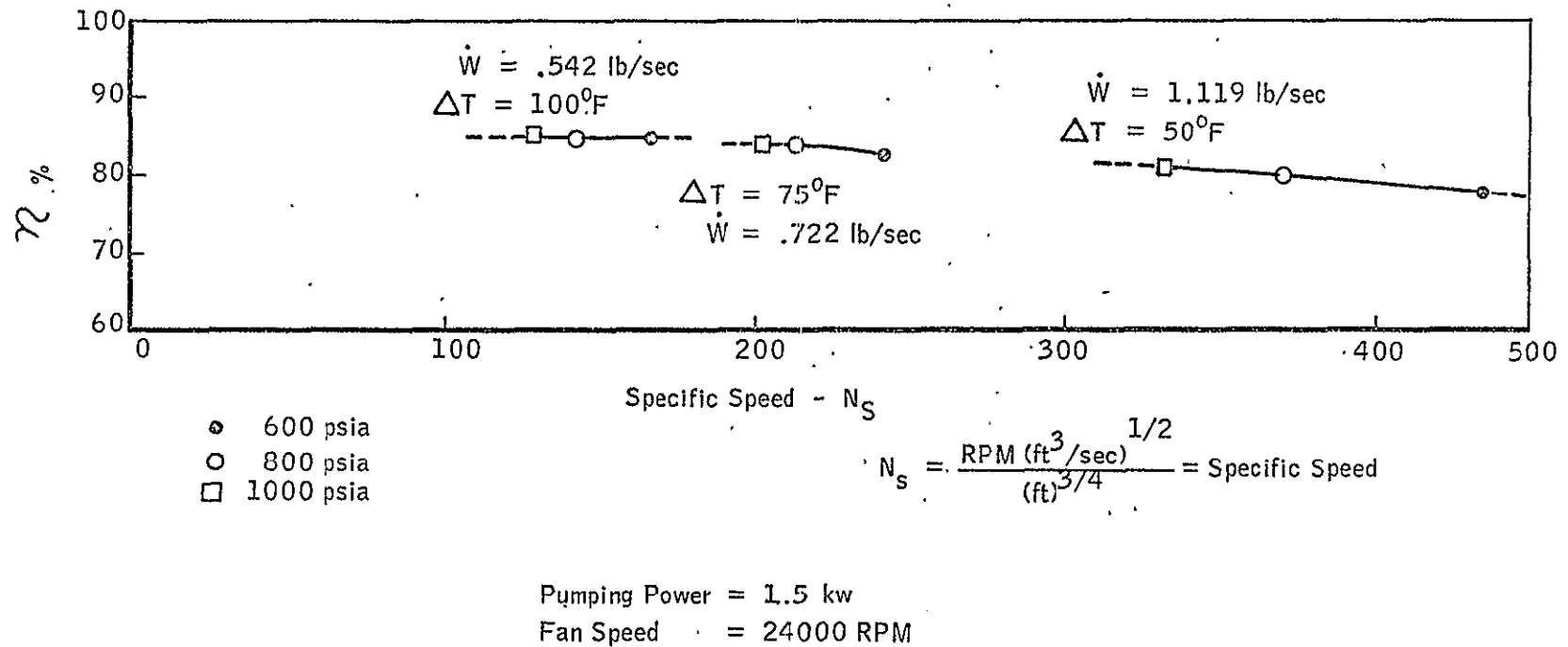
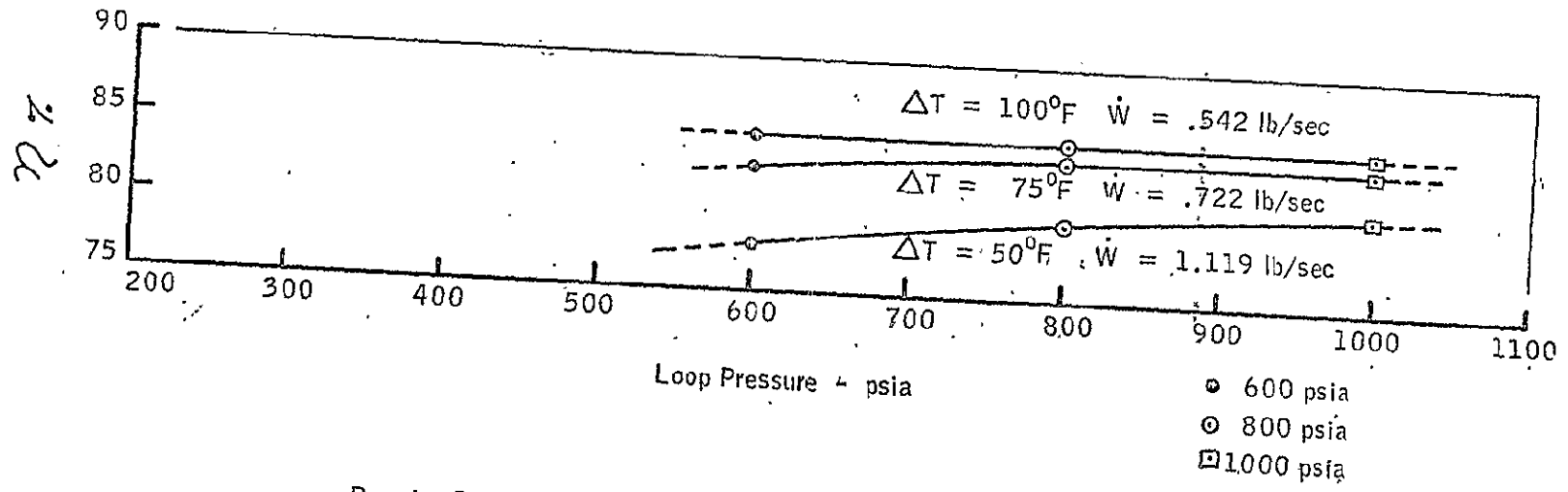


Figure 15 - Specific Speed and Efficiency for Primary Coolant Loop Fan



Pumping Power = 1.5 kw
 Fan Speed = 24000 RPM

Figure 16 - Effect of Primary Coolant Loop Pressure Upon Efficiency of Fan

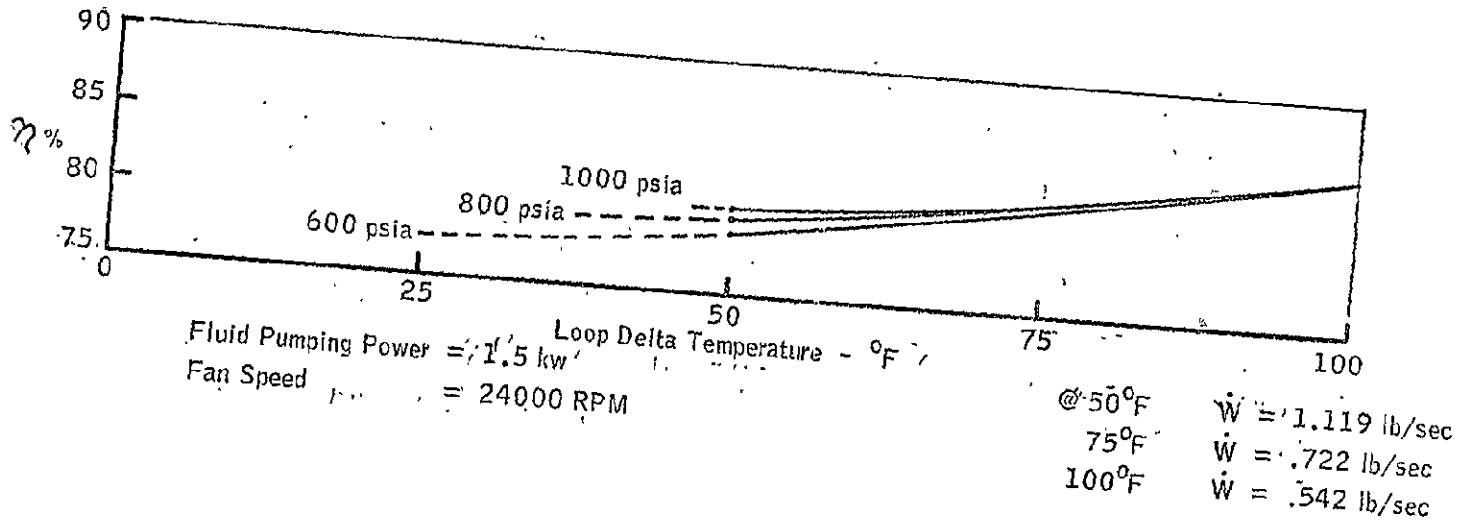


Figure 17 - Effect of Primary Coolant Loop Temperature Difference Upon Efficiency of Fan

B. POWER CONVERSION SYSTEM

Initially, the SNAP power-conversion systems were considered for NERVA application. These included: (1) the SNAP-8 mercury-Rankine cycle; (2) the closed-loop gas turbine or Brayton cycle; and (3) nonrotating systems such as thermoelectric generators. The major problem with the SNAP systems with regard to NERVA electrical application is that they are all designed for much higher maximum cycle temperatures and generally higher heat-rejection temperatures. Figure 18 shows the relationship between the temperature limits currently imposed on the electrical system by the engine materials.

It is somewhat surprising that the maximum temperature from the primary loop is only 775°R; whereas, the normal design temperature is more than 4000°R. The relatively low temperature limit occurs because aluminum is used as a material of construction for the pressure vessel, the inner-reflector cylinder, and the core support plate. In the normal operation mode, these aluminum components are cooled by cryogenic hydrogen and, therefore, normally operate at very low temperature. In the electrical mode, these components would be subjected to temperatures at least as great as the return temperature from the primary loop (approximately 700°R).

As a consequence of the limited maximum temperature available to the dual-mode system and a desire to maintain as high a radiator average temperature as practical, the electrical system must operate with a relatively small temperature differential. In the studies performed, an approximate 200°R temperature differential was appropriate. Thus, the ratio of the sink cycle temperature to the maximum temperature is about 550/750, or approximately 0.7. Since Brayton cycle systems require a temperature ratio of less than 0.5 to be self-sustaining, the Brayton cycle can be dismissed from further consideration for NERVA application. In a similar manner, nondynamic systems (e.g., thermoelectric or thermionic units) do not function

09

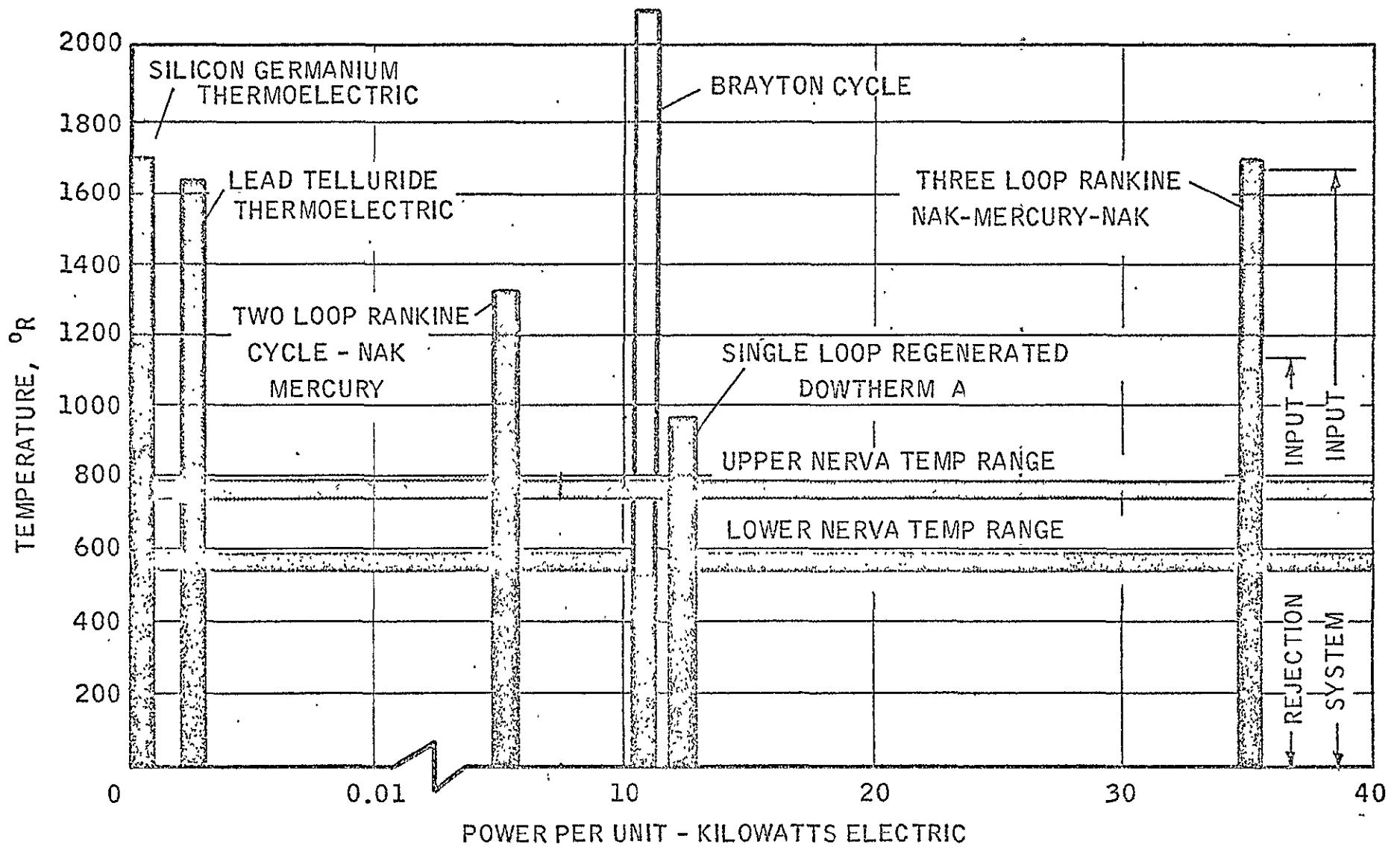


Figure 18 - Temperature Vs Power for Power Conversion Systems

in the temperature range and temperature ratio available to the electrical system. These considerations lead directly to the selection of the Rankine cycle as being the only appropriate thermodynamic cycle that is potentially useful in the NERVA electrical system.

In the Rankine cycle, the majority of the heat input to the cycle occurs during vaporization of the working fluid, a constant temperature process. Most of the heat rejection occurs during the condensation process, also a constant temperature process. As a consequence, the low-temperature Rankine cycle closely approaches the Carnot efficiency for the temperatures available to the cycle. The Carnot efficiency for a maximum upper cycle temperature of 750°R and a sink temperature of 550°R is $750-550/750$, or 26%. Although Carnot efficiency is not obtainable in an actual system, a power-conversion system that attains a reasonable portion of the 26% is potentially useful in the electrical system.

A number of fluids were evaluated for their Rankine cycle performance. Several features of the thermodynamic cycle became apparent. The first was that such fluids as ammonia have high vapor pressures (i.e., approximately 2000 psi) at the maximum temperature of the electrical cycle. Since the boiler feed-pump work is a parasitic load on the cycle, it became apparent that lower maximum pressures were desirable. For example, water with a vapor pressure of approximately 50 psi or organic fluids (e.g., benzene, thiophene, and pyridine) with vapor pressures in the 30 to 45-psi range have boiler feed-pump power requirements that are negligible. Another feature that is desirable for low-power [25 kw(e)] systems is to use a relatively heavy molecular weight working fluid. The higher molecular weight working fluid is important for two reasons: (1) fewer stages are required in the turbine for efficient coupling of the turbine blading to the working fluid (in the case of ammonia, which combines high pressure with low molecular weight, the turbine is impractical as an expansion device); and (2) in the case of water, with low pressure and low molecular weight,

approximately 13 turbine stages are required for efficient coupling to the expanding vapors. Relatively heavy organic fluids such as thiophene and pyridine require from one to three stages for efficient coupling of the blading to the working fluid. Since turbine inefficiency is the major contributor to the losses in the Rankine cycle, it is imperative that this component be selected so it can achieve the highest overall efficiency that is practical.

Another good feature of the higher-molecular-weight organic fluids is that the slope of the saturated-vapor line on the temperature-entropy plot is nearly vertical. Hence, turbine expansion does not become wet and cause turbine-blade erosion because of droplets entrained in the vapor steam. Lower-molecular-weight fluids such as water require reheating to insure a completely dry expansion.

Some very-high-molecular-weight working fluids such as Dowtherm A have a saturated-vapor line with a positive slope on the temperature-entropy diagram. This means that a turbine-expansion characteristic line becomes more superheated as the expansion proceeds. As a consequence, at the turbine outlet the final pressure or condensed pressure is reached at a temperature that is significantly higher than the condenser temperature. To recover the heat that is available between the turbine exit temperature and the condenser temperature, a heat exchanger is provided in the turbine outlet flow, and the heat is transferred to the boiler-feed pump outlet fluid. In the case of such fluids as benzene, thiophene or pyridine, there is relatively small amount of heat available in the turbine outlet flow, and, although the system diagrams show a regenerator, more detailed system studies may eliminate this component.

The variation of the power-conversion system cycle performance with the changing maximum cycle temperature is shown in Figure 19. Also shown in this figure is the effect upon cycle efficiency of the multiple vs single

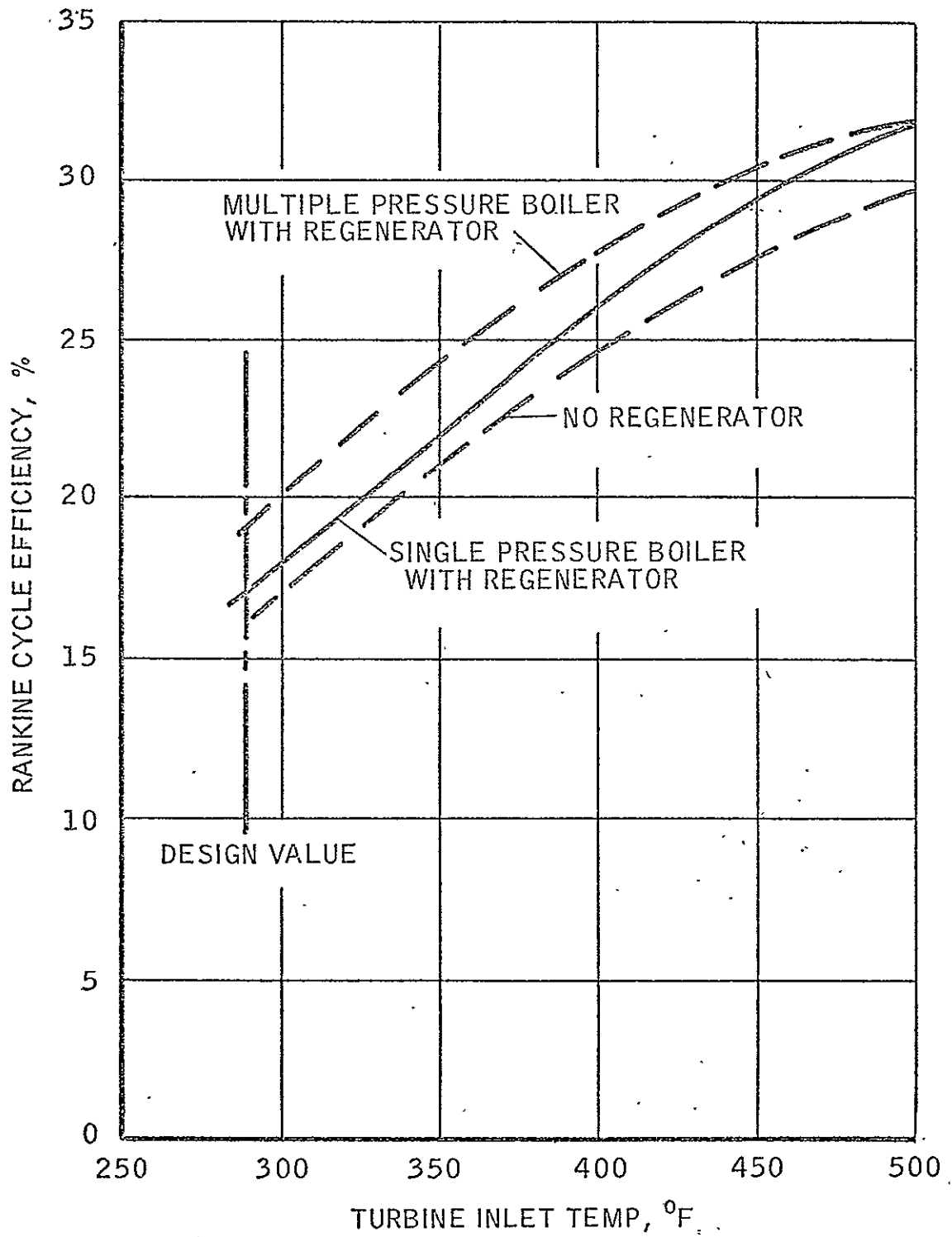


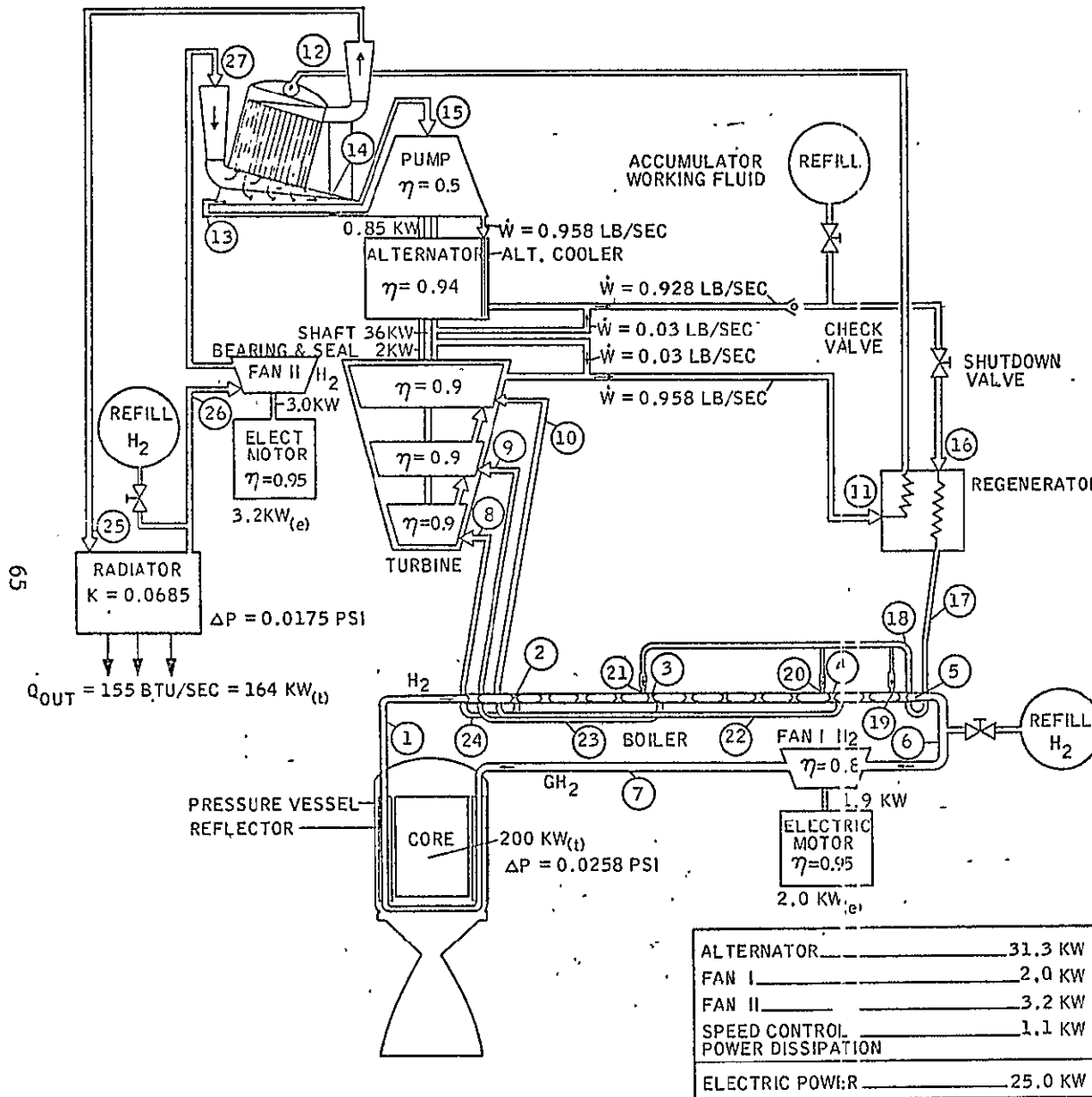
Figure 19 - Variation of Cycle Efficiency as a Function of Maximum Cycle Temperature

pressure level boiler and the regenerator. At the design value of 290°F (750°R), the increased efficiency of the more refined system is approximately 18%.

Another consideration in the selection of a working fluid is its vapor pressure at the condensing pressure. It is desirable to condense at a high pressure. For example, steam systems in power plants often work with condensing pressures of approximately 0.7 psia. At this relatively low pressure, the turbine exhaust flow is a high-volume flow: thus, turbine-leaving losses tend to be higher, as the ducting diameter is large in the regenerator and condenser. A special consideration for space power systems, which must operate in zero-gravity environments, is that a gravity or elevation head is not available in a condensate-liquid column to provide static pressure to cause the liquid to flow out of the condenser and provide NPSH at the boiler feed-pump inlet. This consideration was an important factor in the selection of thiophene rather than benzene and pyridine as the working fluid for the electrical system. The thermodynamic performance of these three fluids was very similar.

An attractive characteristic of thiophene is its relatively low freezing point of -40°F. This value compares favorably with most other Rankine cycle fluids: for example, Dowtherm A has a freezing point of +53°F. The system operation can be tailored to overcome such problems as freezing of the fluid. However, the selection of a fluid which would not be anticipated to freeze in a normal near-earth space environment is preferred.

The power-conversion system state-points for the 25-kw(e) electrical power system are shown in Figure 20. This system schematic includes primary-loop, power-conversion, and heat-rejection state points. The diagram is preliminary because additional study is required to arrive at a more nearly optimum electrical system. For example, the boiler system shown has three pressure levels (and three temperature levels) for maximum utilization of the



NO.	STATION INLET	FLOW LB/SEC	PRESSURE PSIA	TEMP °R
PRIMARY H₂ LOOP				
①	SUPERHEATER	0.722	600	775
②	HIGH PRESS BOILER	0.722	-	770
③	INTERMEDIATE PRESS BOILER	0.722	-	748
④	LOW PRESS BOILER	0.722	-	722
⑤	PREHEATER	0.722	-	713
⑥	FAN I	0.722	599.5	699
⑦	REFLECTOR	0.722	600	700
ORGANIC FLUID LOOP				
⑧	TURBINE	0.464	44.7	750
⑨	TURBINE	0.278	34.7	750
⑩	TURBINE	0.186	28.4	750
⑪	REGENERATOR	0.958	2.6	606
⑫	CONDENSER	0.958	2.48	560
⑬	DRIVE JET	0.928	75	541
⑭	JET PUMP	0.958	2.46	540
⑮	CENTRIFUGAL PUMP	1.968	8.1	540
⑯	REGENERATOR	0.928	75	550
⑰	PREHEATER	0.928	74	582
⑱	BOILER	0.928	73.5	686
⑲	LOW PRESS BOILER	0.186	28.9	686
⑳	INTERMEDIATE PRESS BOILER	0.278	35.2	686
㉑	HIGH PRESS BOILER	0.464	45.2	686
㉒	LOW PRESS SUPERHEATER	0.186	-	686
㉓	INTERMEDIATE PRESS SUPERHEATER	0.278	-	700
㉔	HIGH PRESS SUPERHEATER	0.464	-	720
SECONDARY H₂ LOOP				
⑳	RADIATOR	2.22	599.6	540
㉖	FAN II	2.22	599.5	520
㉗	CONDENSER	2.22	600	521

-Figure 20 - Dual-Mode Electrical Power Generating System

thermal energy levels available from the primary loop. If the flow resistance in the reactor portion of the primary loop is reduced significantly from the values used in this analysis, a more optimum system would be to increase the weight flow rate of hydrogen in the primary loop and, thereby, operate the primary loop with a smaller temperature differential. The temperature differential as shown in Figure 20 is 75° , which is a significant ΔT in comparison with the 200° ΔT available for the electrical system. If the primary loop ΔT were decreased from 75° to 50° , a more nearly optimum electrical power-conversion system would have only two pressure levels in the boiler.

C. HEAT-REJECTION SUBSYSTEM

The function of the heat-rejection system is to remove the heat of condensation from the condenser and transport the heat to the outer skin of the stage where it is radiated to space. The gaseous-hydrogen coolant is only a few degrees cooler than the condensate, and the temperature change of the coolant as it passes through the condenser or radiator is approximately 20°R . The circulating-fan power requirement increases rapidly with the reduction in coolant temperature rise. The heat-rejection loop temperature rise is less than half the temperature rise of the primary coolant loop because the condenser design has been selected to permit a high flow rate of coolant (i.e., low temperature rise) without excessive pumping power. This degree of flexibility has not been permitted in the reactor heat-exchanger design.

A significant feature assumed for the heat-rejection loop is the use of gaseous hydrogen as the coolant. As reported earlier, the radiator represents more than half of the weight chargeable to the electrical system. Gaseous hydrogen has been selected as the candidate radiator coolant on the basis of its ready availability on the nuclear stage and the fact that it will not freeze in the deep-space environment. This is important for the electrical concept because it is anticipated that the system will be shutdown

at intervals to accommodate rocket engine burn. During engine firing the radiator may not be operating and some fluids could freeze in the radiator passages, thus potentially preventing resumption of normal electrical mode operation.

A major design factor in the heat-rejection system has been redundancy and operational flexibility. The design concept for the manifolding of the gaseous hydrogen is to use many individual flow circuits, each with an enclosed electric-motor-driven fan for circulating the coolant. In addition, a means for charging each circuit would permit maintaining pressure, which could be affected by temperature changes or diffusion losses. The charging system(s) would not be effective in the case of a significant leak. In this event, the leaking circuit would be shut down. The concept is to provide manifolding to the entire meteoroid skin (approximately 10,000 sq-ft) which is, in effect, over-designing the radiator.

The design of the fan for the heat-rejection loop is significantly affected by the requirement for 24 separate and independent loops. As shown in Figure 21, high single-stage fan efficiency is achieved only with the high weight flow rate, low ΔT (5°F) coolant circuit. In a constant fluid power circuit a reduction of flow rate implies an increase in head, thus the fan specific speed decreases rapidly with increased coolant temperature different or reduction of weight flow rate. This feature is shown in Figure 22. The specific speed of the fans at low flow rates are in a region where efficiency changes with system pressure level. In Figure 23 the fan efficiency is plotted as a function of system pressure: increasing pressure reduces fan specific speed and causes a reduction of fan efficiency.

These results show the desirability of having a low temperature difference (5°F) in the heat-rejection loop from the standpoint of the fan. If this is undesirable in the design of the condenser or radiator, it may be desirable to use multiple-stage fans to increase overall fan efficiency and thereby have a reasonable parasitic load.

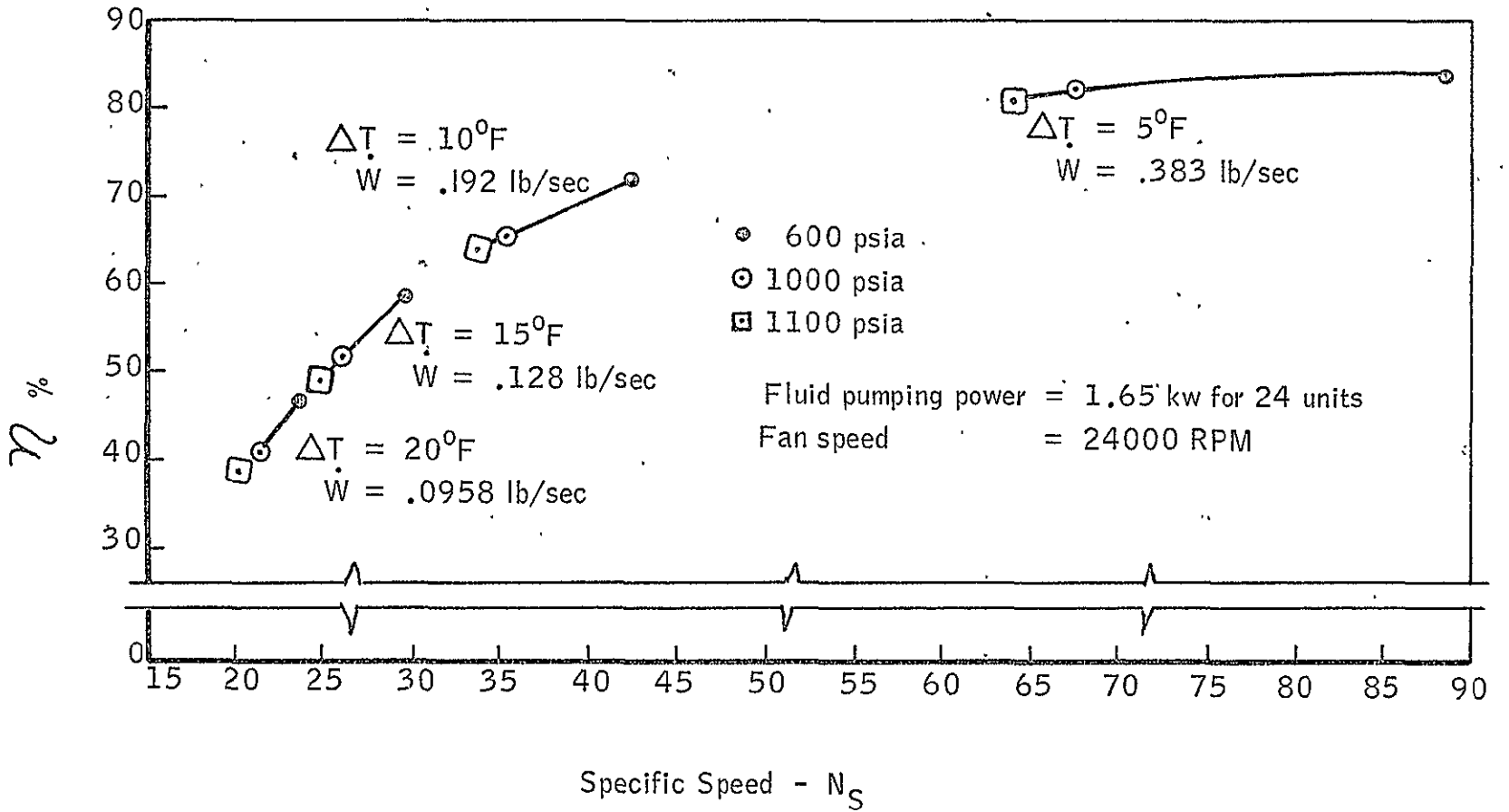
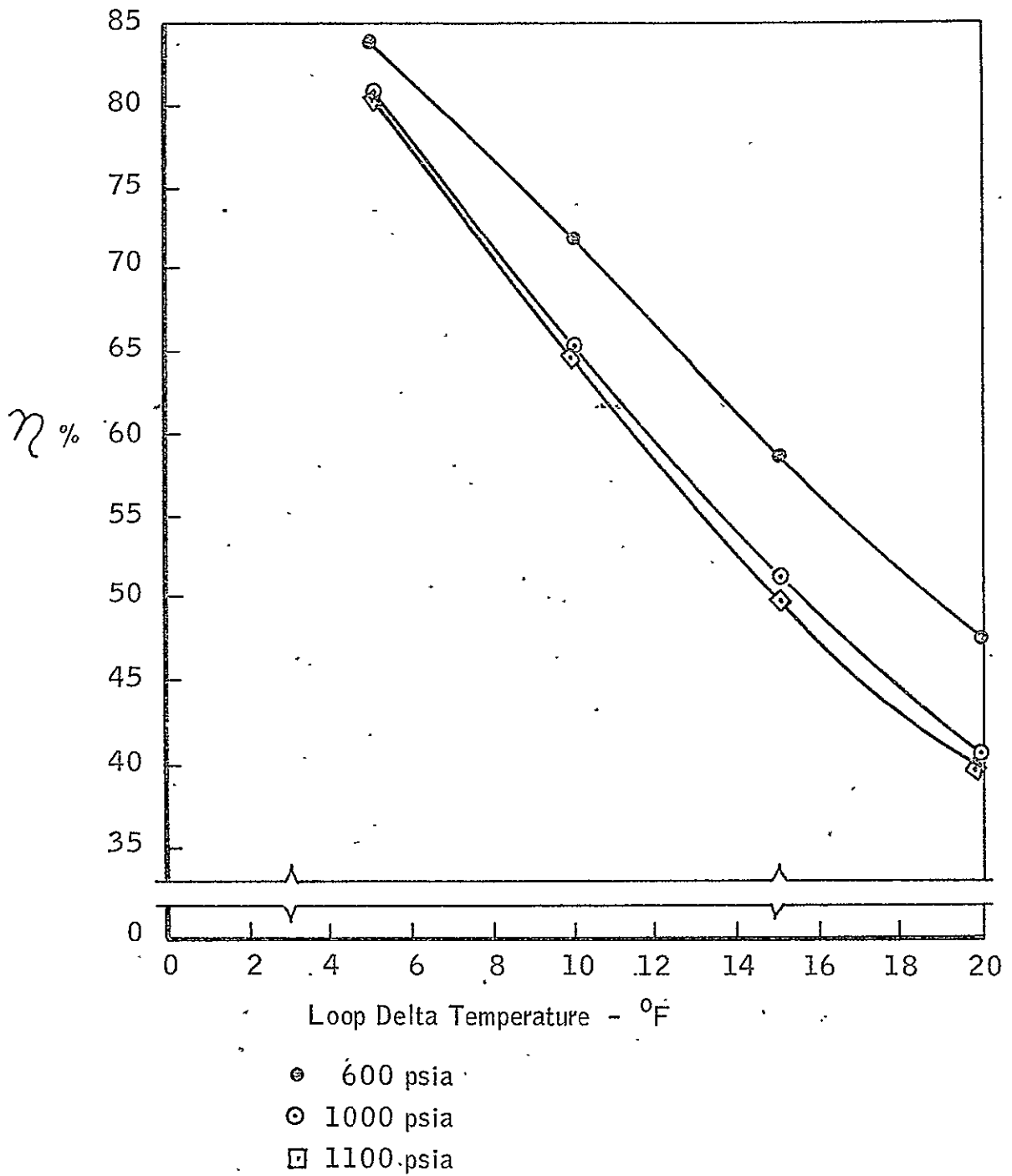


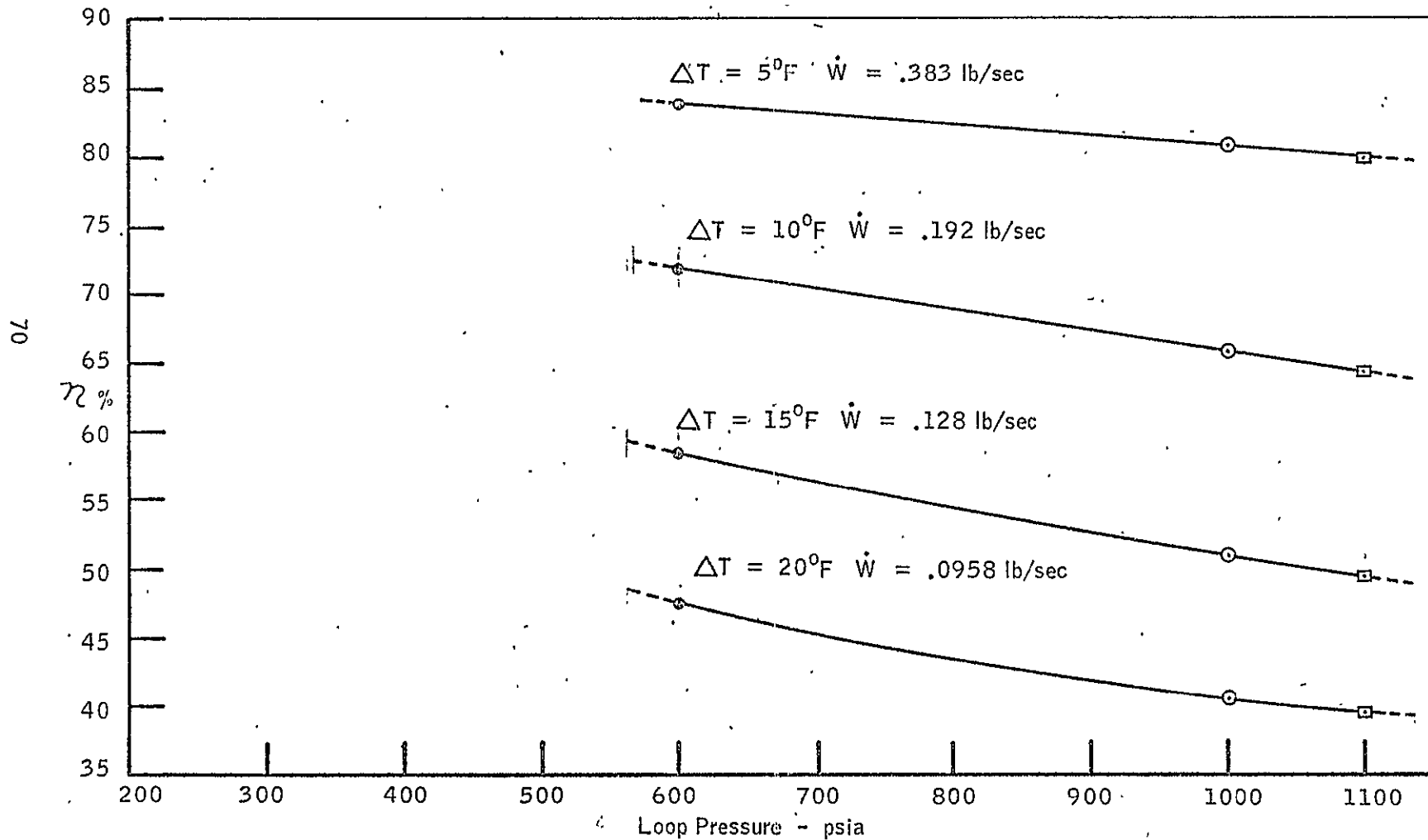
Figure 21 - Specific Speed and Efficiency for Heat-Rejection Loop Fans



Pumping Power = 1.65 kw per 24 units

Fan Speed = 24000 RPM

Figure 22 - Effect of Temperature Difference in Heat-Rejection Loop Upon Fan Efficiency



Pumping Power = 1.65 kW per 24 units

Fan Speed = 24000 RPM

Figure 23 - Effect of Pressure in the Heat-Rejection Loop
Upon Fan Efficiency

D. CONTROL SYSTEM

The control-system block diagram is shown in Figure 24. Included in the electrical control system are the following components:

1. Line voltage compensator
2. Speed control
3. Parasitic load resistor
4. Power-factor correction assembly
5. Vehicle load breaker
6. Motor transfer contactor
7. Start inverter
8. Condenser temperature control
9. System programmer
10. Electrical protective system

The purpose of the control system is to regulate the alternator output voltage and frequency and to provide power to the electrically driven engine auxiliaries. A design objective is to provide a reliable, long-life, maintenance-free control system that will deliver electrical power to the vehicle load at a minimum penalty in system power loss. The control components are designed to be independent of environmental effects and to use the condensed turbine working fluid as a coolant.

1. Line Voltage Compensator

The output voltage of the permanent-magnet alternator is a function of operating speed, load, and power factor. By proper design of the alternator and precise speed regulation, the alternator output voltage may be held within limits of $\pm 5\%$ of rated voltage from no load to rated load. If the effects of speed changes are neglected, voltage regulation is determined by three factors:

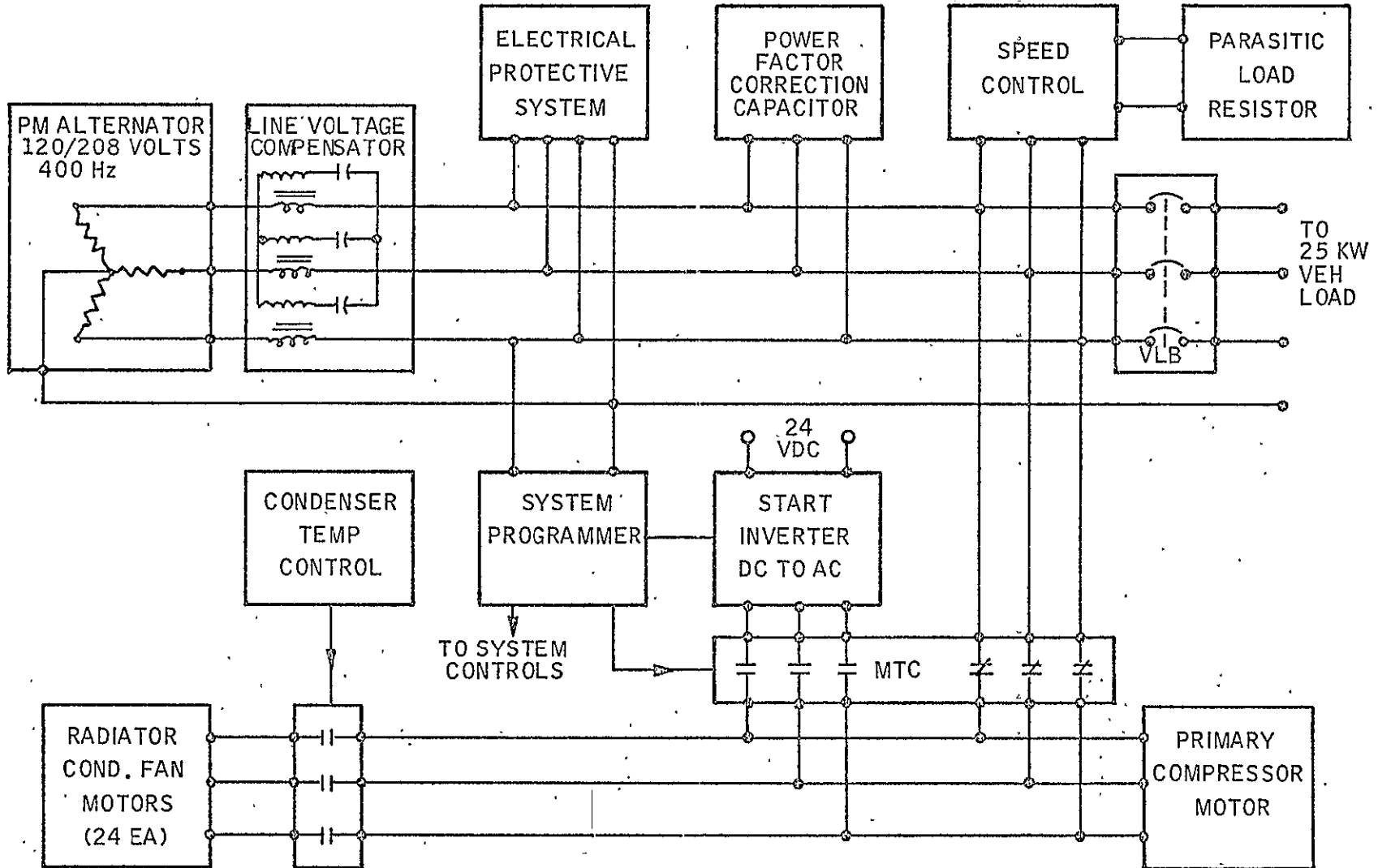


Figure 24 - Control System Block Diagram

1. Load-current armature reaction demagnetizing effect upon field magnets.
2. Alternator stator-winding resistance.
3. Alternator stator-winding reactance.

By proper alternator design and control of the load power factor the demagnetizing effect of load current may be limited to a less-than-5% drop from no load to rated load. The stator-winding resistance is normally low and insignificant in determining voltage regulation. The stator-winding reactance is significant and may result in a considerable voltage change from no load to full load.

The line voltage compensator is a simple open-loop device that nullifies the effect of the winding reactance by adding a series capacitor across which voltage drop is equal and opposite to that of the winding reactance. The line voltage compensator used in conjunction with a well-designed permanent-magnet alternator is capable of providing output voltage regulation within limits of $\pm 3\%$ of rated voltage from no load to rated load.

The design of the line voltage compensator incorporates the use of an impedance-matching transformer to increase the voltage applied to the capacitor terminals for good component utilization.

The use of high-reliability, long-life Kapton film capacitors of the type developed for the SNAP-8 power-factor correction assembly will result in a highly reliable unit.

2. Speed Control

The speed of the turbine-alternator is controlled by regulating the load applied to the alternator. The total load applied to the alternator consists of the vehicle load, the electrically driven auxiliaries, and the

parasitic load resistor power. The speed control regulates the power to the parasitic load resistor to maintain the total load on the alternator at exactly that required for constant speed. If alternator speed decreases for any reason (e.g., increased vehicle load or decreased turbine power), the speed control reduces the parasitic load power in the exact amount required to reach a new equilibrium point and maintain rated operating speed. The speed control is capable of regulating the power to the parasitic load resistor from zero to full rated power.

The speed controller is a solid-state device utilizing silicon-controlled rectifiers to control the power to the parasitic load resistor. The alternator output frequency is sensed by means of a tuned resonant circuit that supplies an error signal whenever the frequency deviates from the design value of 400 Hz. The error signal is amplified and then used to adjust the firing angle of the rectifiers, which control the power flow to the parasitic load resistor. This method of speed control has been used to control the speed of the Aerojet organic Rankine power systems (rated at 6 and 12 kw) with very good results.

The advantages of the solid-state speed control system include accurate speed regulation, fast response, light weight, and the ability to turn off the parasitic load resistor power to zero. The 100%-turnoff feature permits full utilization of the system power capability for the vehicle load with no residual power allowance for the parasitic load resistor. The speed control is capable of maintaining turbine-alternator speed within $\pm 1\%$ of rated speed under all operating conditions.

3. Parasitic Load Resistor

The parasitic load resistor is used to absorb power from the speed control system as necessary to regulate the speed of the turbine-alternator. The resistor is a sealed unit that is cooled by the working fluid. The parasitic load power may either be used to heat the boiler-feed working fluid or may be dissipated to the radiator.

4. Power-Factor Correction Assembly

The power-factor correction assembly is used to compensate for the reactive kva of the motor loads and speed control system. By maintaining the alternator power factor near unity, the alternator will operate at maximum efficiency and provide the best voltage regulation. High reliability, long life, low-loss power-factor correction capacitors have been developed as part of the SNAP-8 program. These capacitors have been operated for over 12,000 hr in a power-factor correction assembly. The capacitors used are made with high-temperature, radiation-resistant Kapton (polyimide) film having a very-low loss characteristic desirable for power-factor correction service. Power loss in the power-factor correction assembly is less than 3 w per kva.

5. Vehicle Load Breaker

The vehicle load breaker (VLB) is used to connect the vehicle load to the electrical power system as soon as rated power is available. The vehicle load breaker will remain open during startup and while the system is coming up to power to prevent substandard power from being applied to the load. The breaker is closed by the programmer when ample power is available. The VLB is a latching unit that requires no input power for steady-state operation in either position, and it may be used to disconnect the power generator from the load in the event of a load fault.

6. Motor Transfer Contactor

The motor transfer contactor is used to transfer the primary compressor and radiator-condenser fan motors from the inverter power source during startup to the alternator system for steady-state operation. The unit is sealed and has welded connections for high reliability. It is designed to latch in the operating position for reliable operation and minimum power loss under steady-state operation.

7. Start Inverter

The start inverter is used to convert battery dc power to ac power to drive the primary compressor motor and radiator-condenser fan motors during system startup before power is available from the turbine-alternator. It may also be used for system shutdown after the turbine-alternator has stopped operating. The inverter converts 28-vdc power available from the battery to three-phase 400-Hz ac power for driving the system motors. The inverter may be either a solid-state device using semiconductors as switching elements or a rotating unit comprising a dc motor and an ac generator. For limited operating times, such as required for system startup and shutdown, the rotating unit offers the advantages of greater reliability due to its simplicity and higher radiation tolerance. Brushes for dc motors have been tested in sealed environments in the SNAP-8 development program and have demonstrated an operating life of hundreds of hours. The ac power is generated by an alternator with a permanent-magnet rotor mounted on a common shaft with the dc-motor armature.

As an alternative, the solid-state inverter can convert dc power to quasi-square-wave ac power by means of semiconductor switches. The inverter performs two functions: (1) increases dc voltage from 28 to approximately 270 vdc; and (2) converts dc power to three-phase, 400 Hz, 120/208-vac power. The first function is accomplished with a high-frequency, single-phase inverter with an output step-up transformer and rectifier used to increase the dc voltage level. The second function is accomplished with an inverter bridge circuit. At the power level, the use of silicon transistors for the switching elements results in the most efficient design. This technique has been used successfully for previously developed motor drive inverters. Parallel switching transistors with fuses that remove any failed devices from the circuit provide a high degree of reliability.

8. Condenser Temperature Control

Condenser cooling is provided by circulating the coolant from the radiator through the condenser by means of 24 electric motors. The coolant circulating motors are switched on and off by the condenser temperature control as required to maintain the condenser temperature within specified limits. The temperature controller must perform two functions: (1) switch on the coolant circulating motors whenever the condenser temperature exceeds the lower design limit; and (2) switch off the motor in the radiator sections where direct exposure to the sun has raised temperatures above the limit where effective cooling is available. To perform these functions, the temperature controller senses the condenser and the coolant-inlet temperatures and operates a power control relay in the motor power circuit. A total of 24 temperature control modules are required, one for each motor.

9. System Programmer

The system programmer provides the necessary logic to control the power-conversion system with a minimum of external controls. Its function is to start up, operate, and shut down the power-conversion system as required from an externally generated signal. The programmer receives its input from sensors that detect conditions in various parts of the power-conversion system (such as boiler temperature, condenser pressure, and output power) and provides the power to operate relays, valves, and power contractors. Some functions are time-sequenced, and others rely on the output of instrumentation. The degree of automation built into the programmer is a function of total system requirements.

10. Electrical Protective System

The electrical protective system senses the quality of electrical power and disconnects the vehicle load if quality is not within

specified limits. The electrical protective system detects the following fault conditions by sensing the voltage output of the alternator:

1. Overspeed - overvoltage
2. Line-to-line fault - undervoltage
3. Line-to-neutral fault - undervoltage
4. Three-phase fault - undervoltage

Upon receipt of a fault signal, the vehicle load breaker is opened to isolate any fault in the vehicle load. If the fault remains, it is assumed to be internal to the power-conversion system and a signal is transmitted to the programmer to shut down the system. If the fault is in the load, a reclosing feature may be added to reapply the power to open protective circuits in the vehicle load.

VIII. DESCRIPTION OF MAJOR COMPONENTS

A. PRIMARY HEAT EXCHANGER

1. Introduction

The primary loop is comprised of a heat exchanger within the NERVA engine, a boiler, tubes connecting the exchanger and the boiler (extending forward across the gimbal axis, and along the outside of the propellant tank to the forward across the gimbal axis, and along the outside of the propellant tank to the forward end of the stage); an electric motor-driven fan (to circulate high-pressure gaseous hydrogen within the closed loop), and a charging unit (to maintain system operating pressure).

The major item of concern relative to the feasibility of the dual-mode system is the heat exchanger within the engine. Initially, studies by the Westinghouse Astronuclear Laboratory were directed toward a system using the core support system for the heat exchanger. This system (reported in Westinghouse Report WANL-TME-2714, August 1970) could provide the required heat flow with a reasonable fan power: however, this concept was found to be unsatisfactory because of excessive leakage. Design alternatives investigated to overcome the sealing problem resulted in significant design changes to the reactor. Another requirement inherent in the use of the core support system as the heat exchanger was the valving used to switch from normal NERVA operation to the closed-loop operation required by the dual-mode electrical system.

The basic design of the NERVA propellant feed system was changed, however, and the reactor altered slightly to include an aluminum inner-reflector cylinder which supports the differential pressure loading of the reflector region relative to the core region. This component is in sufficient thermal contact with the core region to provide thermal energy for the 25 kw(e)

dual-mode system. The cylinder is also of sufficient cross-section to provide space for the closed-loop heat exchanger in addition to the coolant holes required for normal NERVA operation. The separate closed-loop in the inner reflector cylinder provides an independent system relative to the NERVA flow path, eliminating the need for valves between the two systems. This feature improves the reliability potential of both systems.

As described in detail in Westinghouse Report WANL-TME-2714, other flow systems were investigated and found not to be suitable. One Westinghouse ground rule was that the electrical system would operate after engine operation and that no further propulsion mode would be required. This assumption is probably valid for some unmanned interplanetary flights but is not appropriate for lunar missions. The basic problems with reuse of the propulsion mode after electrical operation centers on the potential damage to core components because of excessive temperature. Probably the most sensitive component is the centerline core support stem which is to be made from super alloy A-286. Figure 25 shows the variation of maximum core temperature as a function of thermal power: i.e., at 200 kw(t) the maximum temperature is approximately 1600°R. The core centerline temperature has considerable uncertainty because of the many thermal impedances separating it from the aluminum barrel. A major uncertainty also exists at the insulated region of the core periphery. As shown in Figure 26, the variation in core edge temperature at 200 kw(t) is $\pm 300^{\circ}\text{R}$ from the nominal value of 1500°R. The relatively wide range of uncertainty in temperature profile can be reduced significantly by more detailed calculations.

In the final design, dual-mode coolant channels in the aluminum barrel are completely independent of the channels used for cooling during the propulsion mode. The inner circle of holes in the barrel is assigned to the propulsion-mode coolant function. Each pair of adjacent channels in the outer row forms a two-pass system, with fluid flowing aft in one channel and then returning by the adjacent channel to the forward

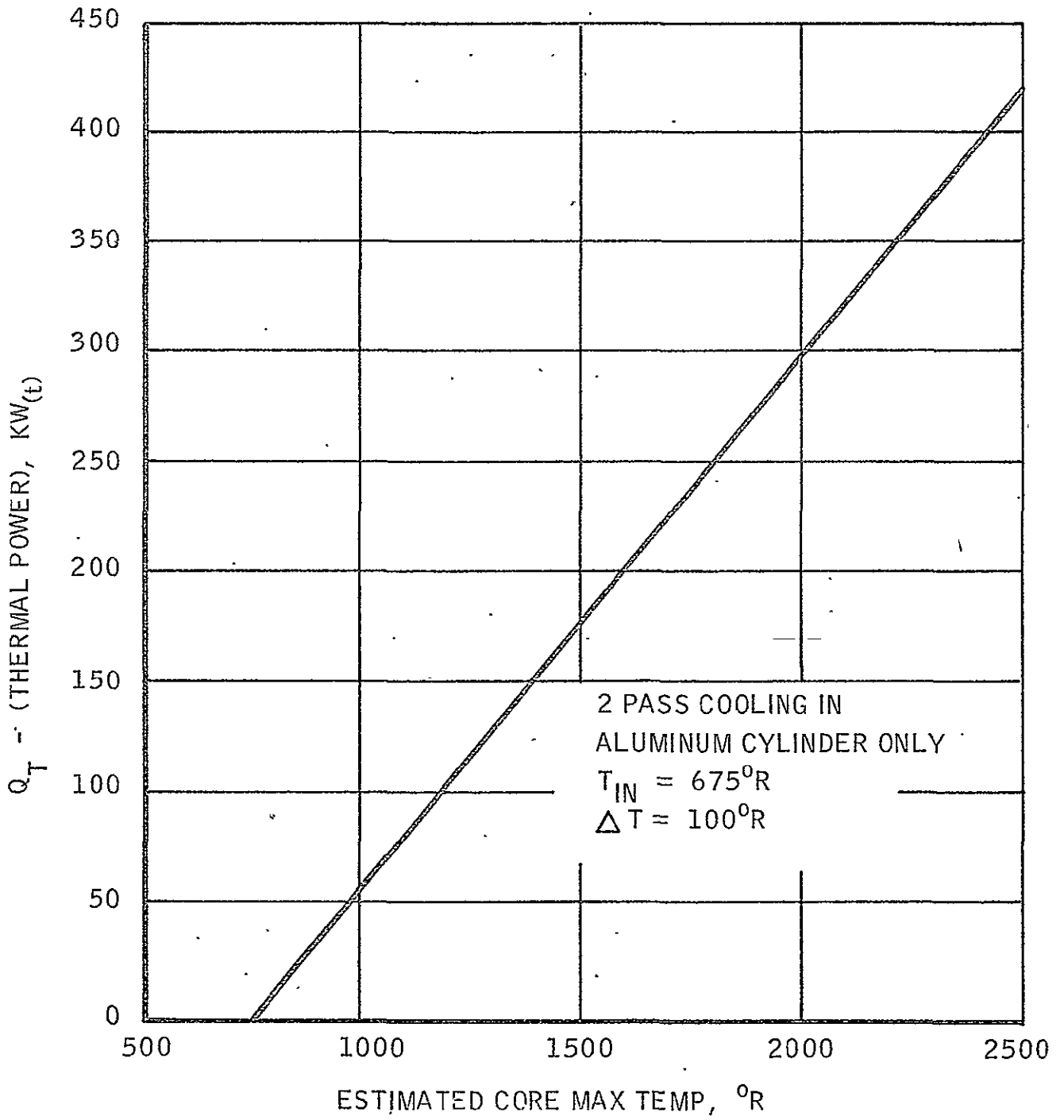


Figure 25 - Estimated Core Centerline Temperature with NERVA R-1
Dual-Mode Heat Removal at Aluminum Cylinder ID

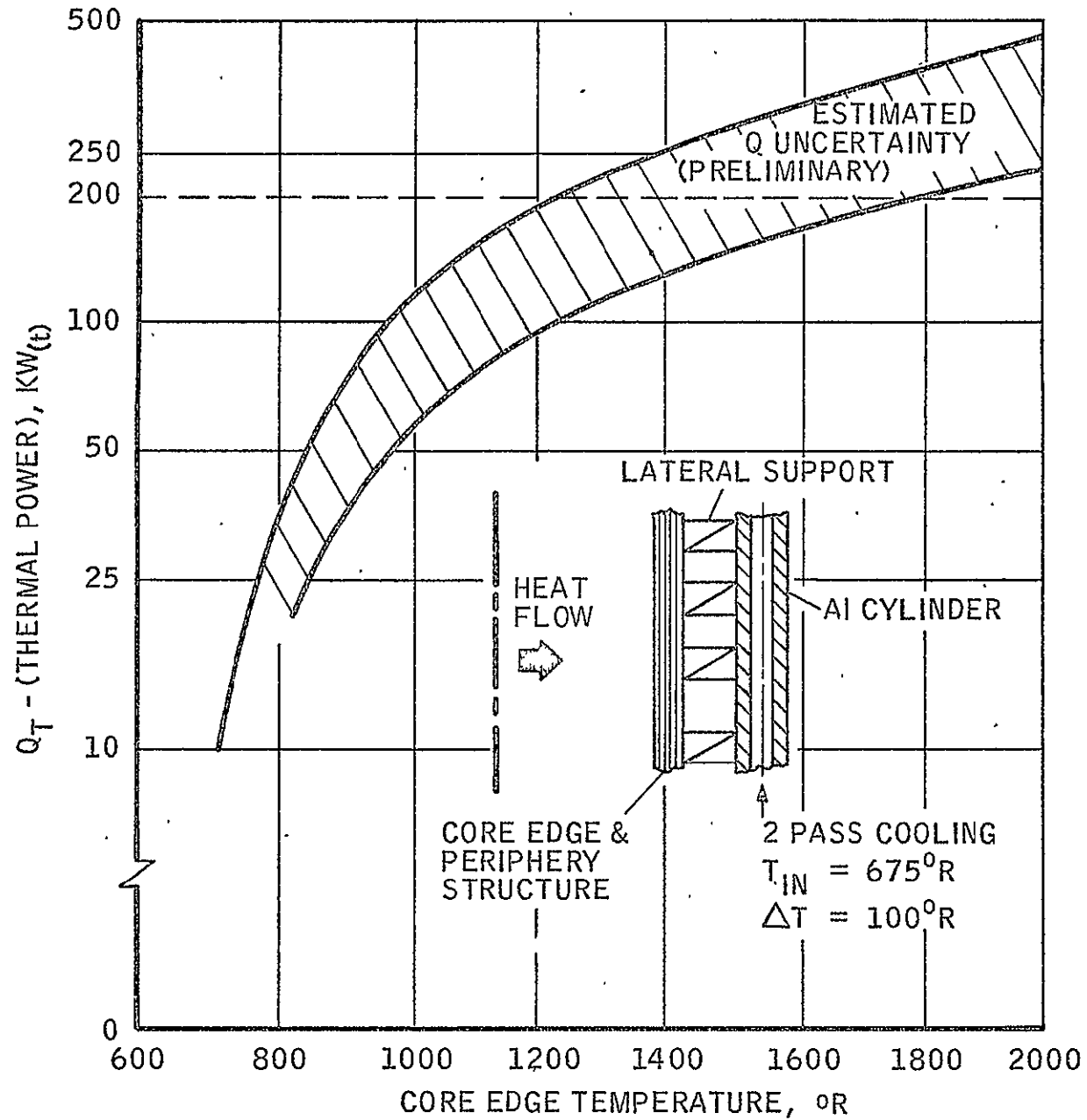


Figure 26 - Estimated Core Thermal-Power Removal by Aluminum Cylinder Coolant Flow Only, NERVA R-1

end (see Figure 27). The electrical-mode working fluid enters the nuclear subsystem at the forward end, traverses the internal shield region in a conical duct, traverses the barrel, and then exits through a concentric conical duct at the forward end. All joints in the system would be welded to obtain a zero-leakage system.

2. Structural and Weight

The effect of incorporating the additional coolant flow passages of the dual-mode system in the aluminum reflector barrel was evaluated in terms of its structural capability and the resulting changes in barrel dimension to retain the present design margin.

The current R-1 aluminum structure reflector was used as the basis for assessing the weight differential. This design consists of a 0.82-in. barrel stiffened by circumferential webs on the barrel outer diameter for an envelope thickness of 1.86 in. Trade studies now in progress will, in all likelihood, result in some modification of this design, but it is expected that the dual mode-propulsion mode weight differential developed will be fairly representative of the final NERVA design as well. This, of course, assumes that extensive further modification to the barrel will not arise as a result of dual-mode systems analysis.

In the recommended dual-mode barrel design developed in this study, the inner row of coolant holes in the barrel was retained with their present dimension, but the function of these holes was expanded to fulfill the total requirement for cooling in the propulsion mode. The outer row of cooling holes was reserved for cooling in the electrical mode only and was increased in number and in diameter from 0.200 to 0.250 in. Within the scope of the feasibility study, no penalty was charged to the dual-mode system to account for the re-allocation of the outer cooling holes to a different function. To compensate for the material removed by the additional holes,

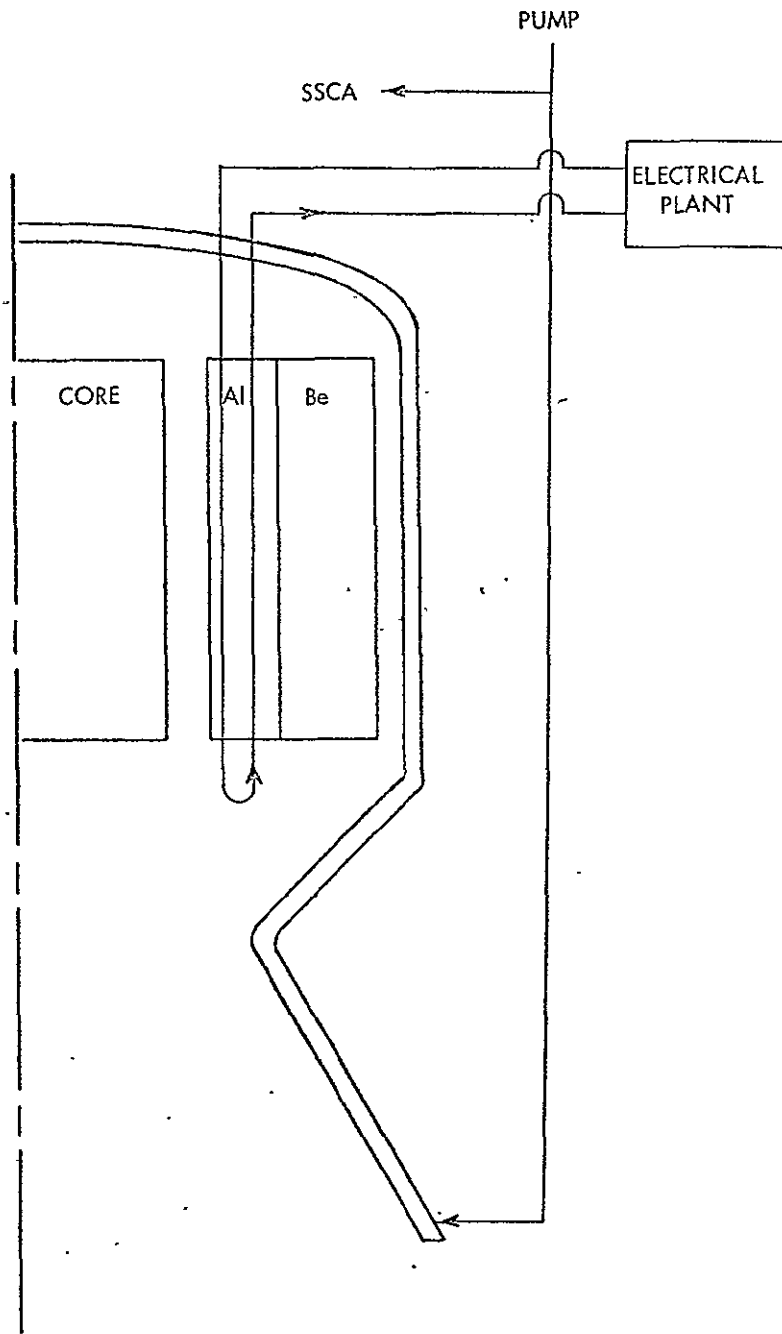


Figure 27 - Flow Schematic, Aluminum Barrel Heat-Removal Concept, Separated Flow System

an increase of 0.10 in. in barrel thickness was made to preserve the effective material section carrying the compressive pressure load on the barrel. The critical section in the dual-mode design exists near the plunger hole, where 0.25-in. holes on the inner and outer circles lie on the same radial line.

Analysis of the propulsion-mode reference design indicated that a barrel thickness of 0.82 in. (exclusive of webs) is required to carry the 864-psia design maximum pressure differential. In that analysis, aluminum 6061-T61 material is used, and only one row of 0.25-in. diameter cooling holes is assumed, giving an effective material section of 0.57 in. In the case of the dual-mode arrangement, where the thickness is 1.10 in. and two rows of 0.25-in. diameter holes are required, the effective material section thickness is 0.60 in., slightly more than the 0.57 in. minimum value shown to be required by the analysis.

The calculations indicate that the present web outer radius of 23.08 in. is sufficient to maintain buckling stability in the aluminum barrel.

The modified aluminum structure employed in the recommended dual-mode design is adequate in compressive hoop strength and buckling stability.

With the changes described above, the barrel weight is increased by about 40 lb in the dual-mode configuration. Compensation for the increase in thickness is partly achieved by the material removed as a result of increasing hole size.

The thickness increase of 0.10 in. in the cylindrical portion of the aluminum structure requires a similar increase in the reflector outer diameter to maintain the fixed beryllium thickness dictated by reactivity considerations. A weight increase of approximately 80 lb results.

The provision of the conical shield support structure and supply piping forward of the reflector is not expected to increase weight of the nuclear subsystem since it replaces a cylindrical shield support structure performing a similar function.

The total weight increase in the nuclear subsystem is, therefore, estimated to be approximately 120 lb. If greater flow area were required for the electrical-mode fluid, the barrel thickness and the beryllium sector outside diameter would increase, increasing the weight penalty charged to the dual-mode system. Although layout designs providing increased flow area could not be generated and evaluated structurally in this study, an approximation of the lower-limit weight increase can be derived. As an example, if it is assumed that a 50% flow area increase or a 50 sq-in. added area were required (and the work performed by drilling holes in the barrel), approximately 260 lb of aluminum would be removed. If it is further assumed that the barrel can be restored to its original compressive strength and rigidity by merely increasing the barrel outside diameter sufficiently to replace the 50 sq-in. of barrel cross-sectional area, the barrel weight under this admittedly optimistic assumption would then be essentially unchanged. However, the outer radius of the barrel would be increased by about 0.36 in. To provide a constant beryllium thickness on a 0.36 in. greater mean radius, the beryllium mass would increase about 300 lb. It should be emphasized that the weight increase derived is considered a lower limit. If the barrel minimum radial section were preserved instead of its cross-sectional (plan view) area, the increase in the outer radius of the barrel might be considerably greater. It is believed, however, that relative to total vehicle weight the increase in nuclear subsystem weight will not severely penalize the performance of the NERVA engine in the dual-mode mission.

3. Thermal and Fluid Flow

Estimates of the aluminum reflector-barrel heat-transfer potential show that core thermal impedance appears to limit heat removal to 200 to 250 kw for any non-core-flow heat removal system. While the power potential of a system utilizing the aluminum barrel is much lower than that of a system using support stems, the power removal capability is sufficient for a 25-kw electrical generation system.

A separated-flow system with flow entering through the pressure vessel dome was the subject of a parametric study to determine the fluid conditions during the electrical-generation mode subject to constraints of 1 kw pumping power, small bulk temperature rise of the fluid, and the aluminum barrel temperature limit. The analysis considered a power level of 200 kw, inlet conditions of 675°R and 600 psia, and a flow range of 0.7 to 1.5 lb/sec. The barrel system's pressure drop is less than 1% of inlet pressure (pumping power depends mainly upon average fluid temperature and flow rate). To maintain pumping power below 1 kw (0.5% of thermal power removal) the coolant channel diameter was varied over a range of 0.25 to 0.625 in. Figure 28 shows power may be maintained below 1 kw for suitable choices of flow rate and channel diameter. Barrel temperatures do not exceed 750°R for flow rates greater than 1 lb/sec, and fluid bulk temperature rises are less than 60°R.

While channel diameters above 0.5 in. give the most efficient heat-transfer characteristics, it is probably unreasonable to consider placing holes of such size in the aluminum barrel. The parametric study showed that total flow area is more important than individual channel diameter: thus, the logical conclusion is to employ a large number of small channels to gain the necessary flow area without creating large voids in the barrel cross-section. Pump power vs flow area is shown in Figure 29. While an optimization of channel size and their placement in the barrel is beyond the

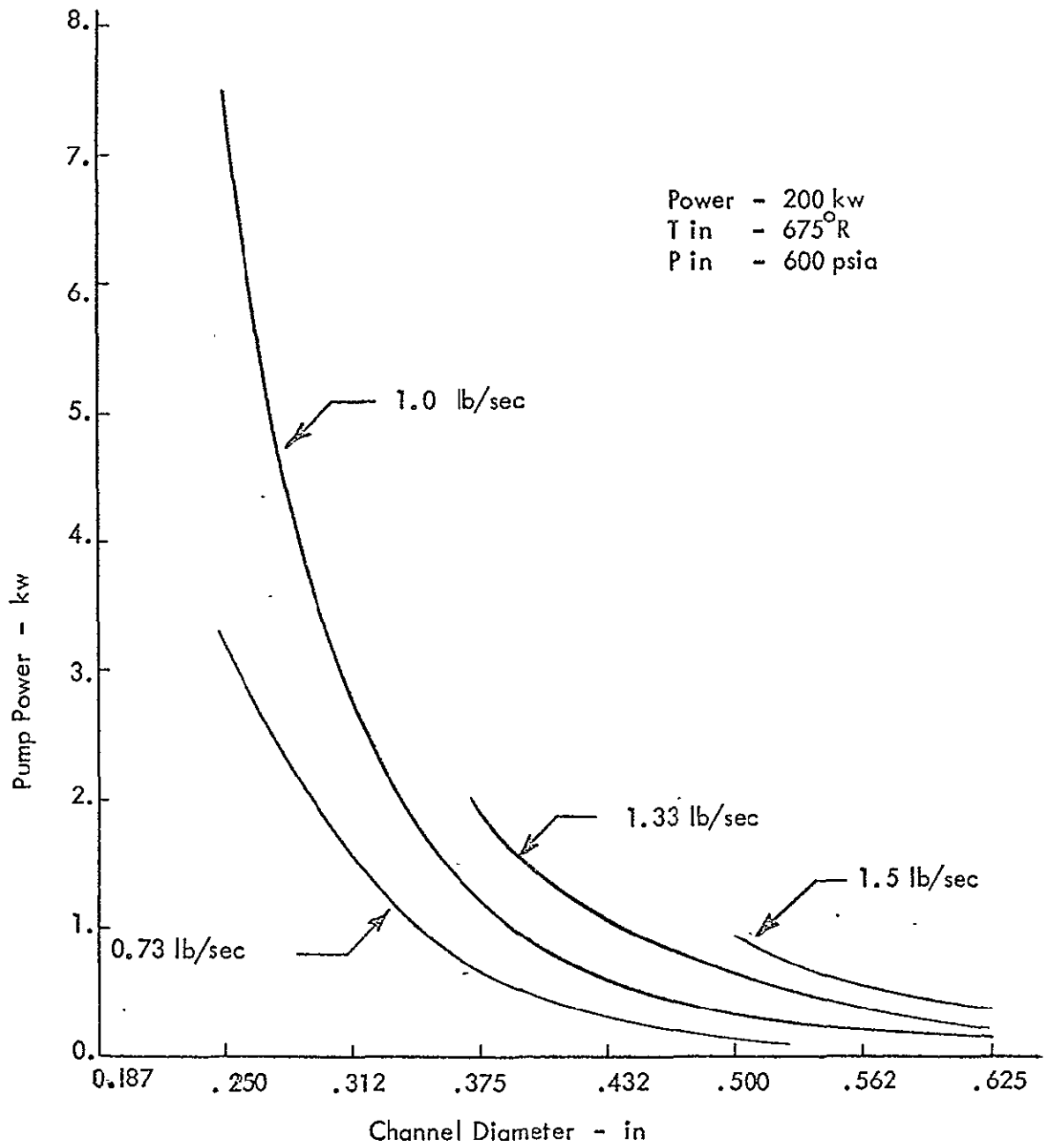


Figure 28 - Pump Power Vs Channel Diameter

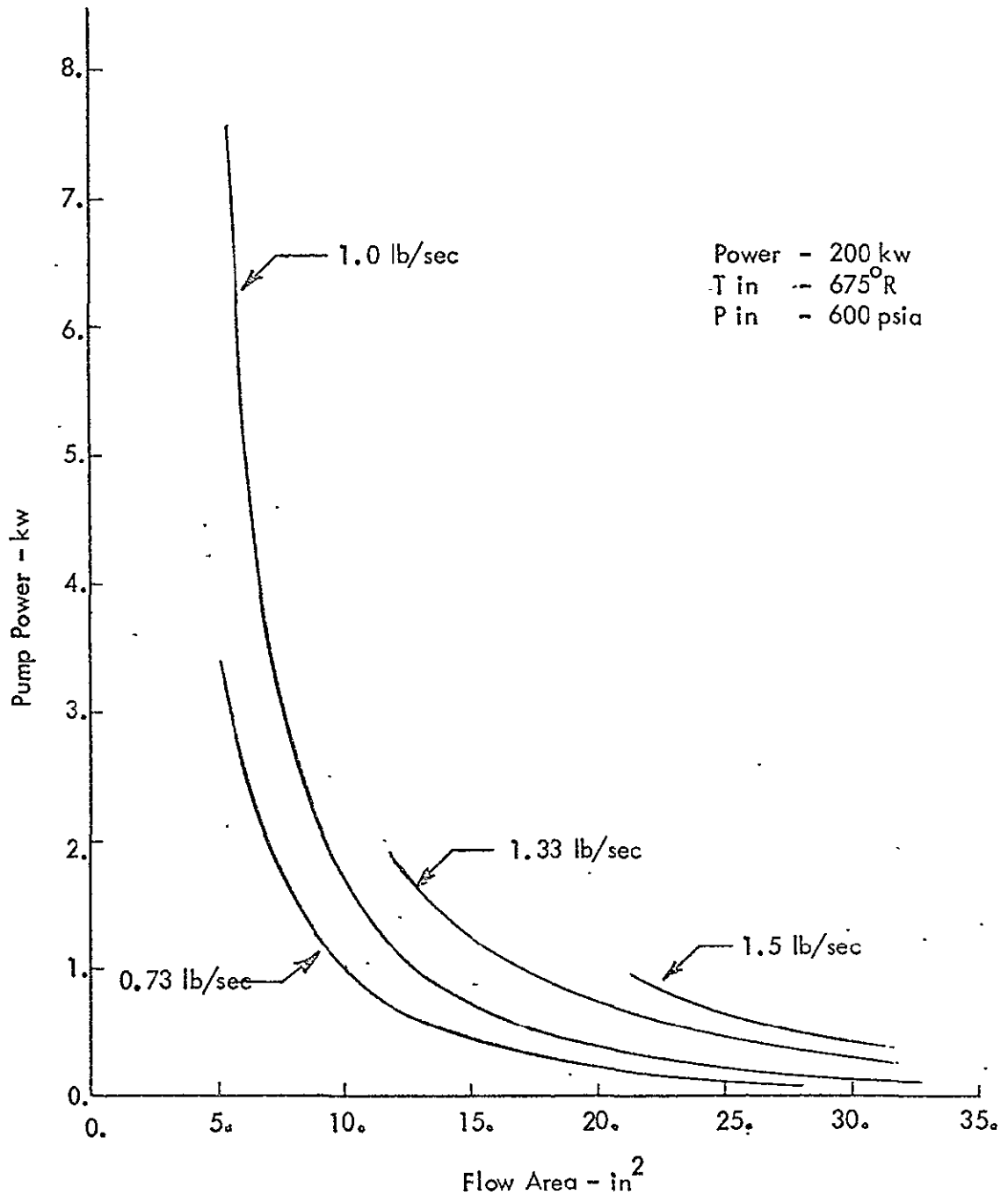


Figure 29 - Pump Power Vs Flow Area

scope of this study (it should be conducted as a detailed study in the future) this study did show that effective thermal and fluid flow characteristics may be obtained with the aluminum barrel although a weight penalty is incurred from its increased size.

Components not in the flow path during the electrical-generation mode must be cooled by radiation. Calculations were performed to determine whether radiation is an acceptable means of cooling the support stems and control drums. The data, shown in Figures 30 and 31, indicate that radiation cooling is adequate. However, more detailed studies of components not in the flow path should be conducted in the preliminary design phase.

Sealing the electrical-mode flow system is considered to be relatively straightforward in the reflector heat-removal concepts using a dome-end access arrangement. Seal welds may be made between the supply and exit ducts and the aluminum reflector ring during assembly to eliminate leakage with the NSS.

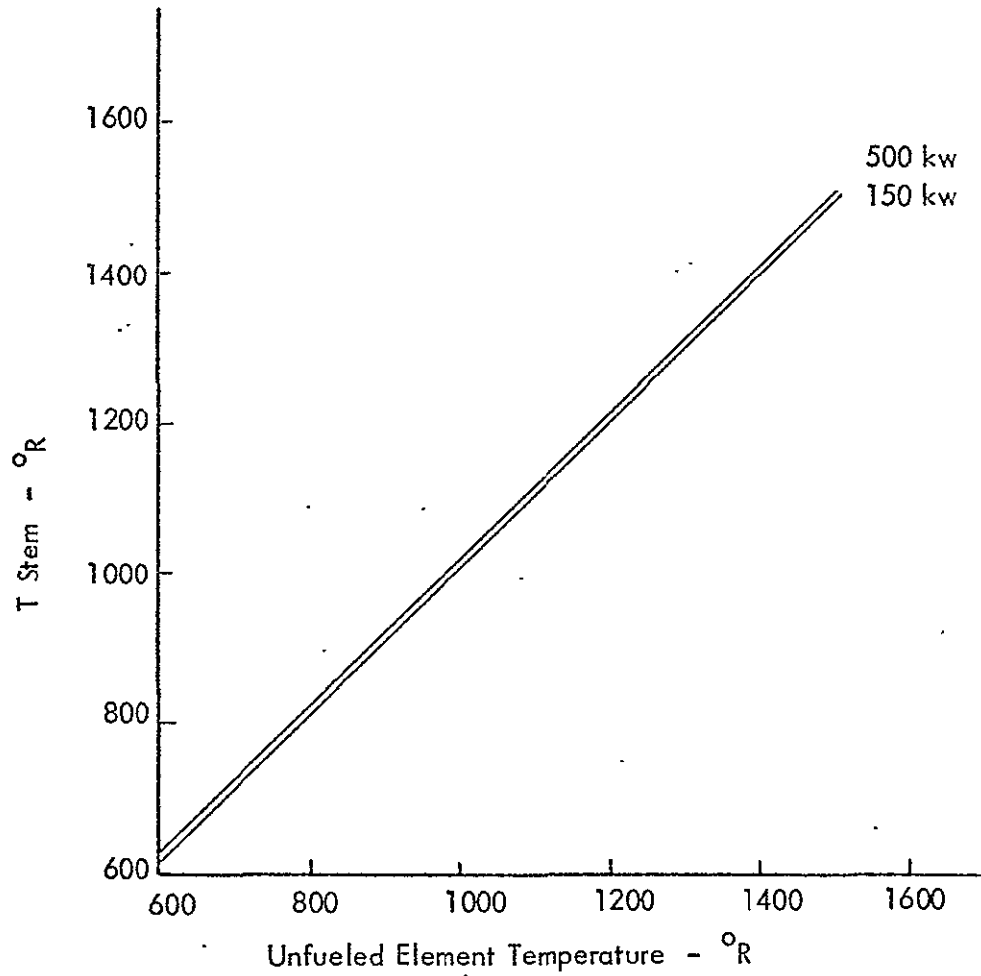


Figure 30 - Stem Temperature Vs Unfueled Element Temperature for Radiation Cooling

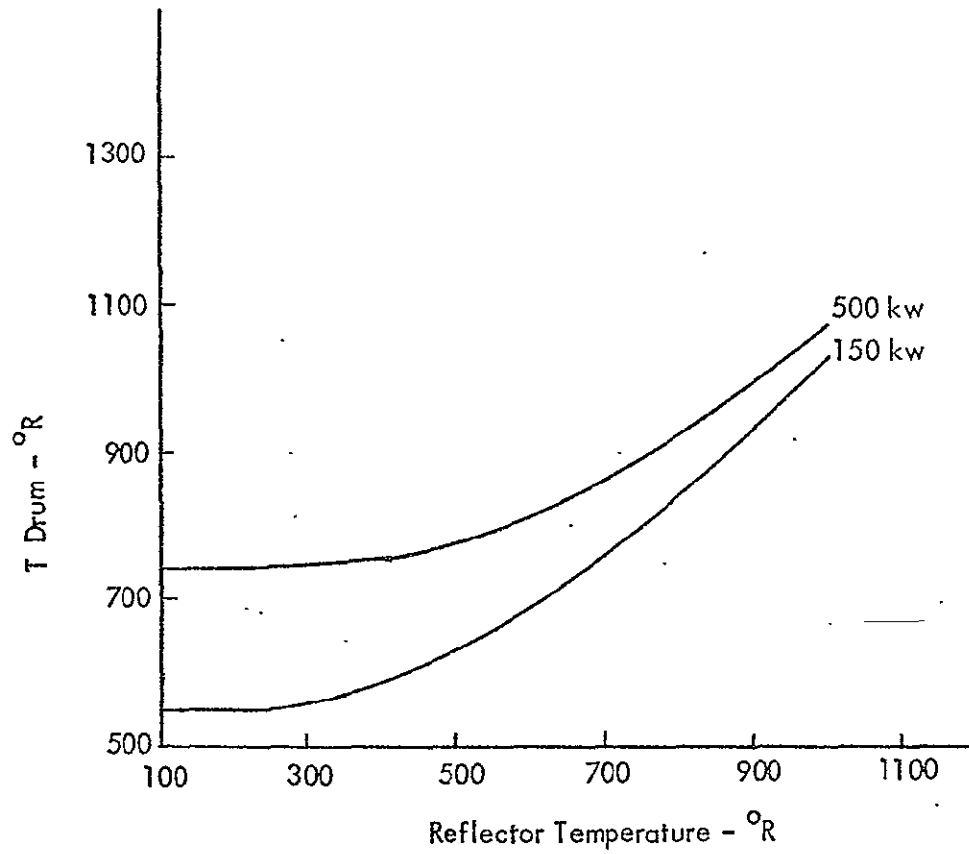


Figure 31 - Control Drum Temperature Vs Unfueled Element Temperature for Radiation Cooling

4. Materials

Materials considerations for the core heat-removal concept applies to the reflector heat-removal concepts as well. The one significant difference from a materials standpoint is the higher maximum temperature attained in the core (approximately 1800°R) using the reflector heat-removal concept as compared to 800°R in the support stem heat-removal concept. The reflector temperature tends to be about the same, while other noncore reactor components, (e.g., the support plate and internal shield) reach somewhat higher temperatures using the reflector heat-removal concept. In these concepts the reactor must develop a higher power to offset the increased heat losses associated with the higher core temperature, increasing nuclear heating of noncore components, and forcing even higher component equilibrium temperatures.

The reflector heat-removal concepts do not require the core to be active, except as a fission heat source: i.e., mechanical or fluid loads are not imposed upon core structural members and thermal stresses should be minimal because of the near-isothermal condition of the core. This fact, together with the assumption that use of the core in the propulsion mode will not be made following electrical-mode operation*, tend to substantially relax the temperature limitations placed upon core components. As an approximate indication, the core temperature should be maintained several hundred degrees below the melting point of the metallic components. Thus for the A-286 support stems, whose melting point in contact with carbon is approximately 2500°R, operating temperatures in the range of 2200°R may be considered. Although core centerline temperatures in the reflector heat-removal concepts are typically 500°R greater than in the stem concepts by virtue of the centerline-to-edge gradient required to conduct heat from the core, the centerline temperature does not exceed 1800°R at a 250 kw(t) power level and is judged acceptable.

* For unmanned deep space missions only.

The 6061-Al reflector ring is currently limited to 800°R where restart in the propulsion mode is anticipated. If this is not assumed, the operating temperature limit would be about 1000° \pm 50°R for the 1000-psi working stress. This number is extrapolated from allowable stresses quoted for Al 6061-T6 forgings, for which a 4000 psi allowable stress is specified at 860°R*. At welded connections, the allowable stress would be reduced typically about 20%.

No significant material problems are identified with the above or other nuclear subsystem components at the operating temperatures presently calculated.

The core components are not subjected to primary loads in the reflector heat-removal concept and, therefore, do not pose significant problems in the context of this feasibility evaluation.

Radiation damage to the fuel elements is not expected to be a significant problem. An average of approximately 0.3% of the uranium inventory is fissioned in the propulsion mode to develop 15,000 Mw-hr of thermal energy. Near the core edge, this value approaches 1%. Assuming operation at 250 kw(t) for eight years, the thermal energy production in the electrical mode is 17,500 Mw-hr. Thus, burnup of uranium-235 will be approximately doubled in dual-mode operation at 250 kw(t), or tripled at 500 kw(t), but will still be very low relative to the fuel capability. Fuel burnups of over 20% are required to produce failure of the fuel particles at 3000°R.

Diffusion of fission products from the fuel elements will be enhanced by the very long operating time. This, however, is more than compensated by the decrease in operating temperature relative to the propulsion mode.

* ASME Unfired Pressure Vessel Code, Section VIII, Appendix VII, Table UNF-23.

The dominant mode of fission product release will probably be, therefore, from those fuel particles whose pyrocarbon shells were damaged in fabrication. If the irradiation were carried to a sufficiently high level, the percentage of particles rupturing would become substantial. However, in the dual-mode application, essentially no increase in the number of failed particles should occur. Moreover, the reactor coolant in the electrical-generation mode does not come into contact with the fuel, so that no contamination of the loop would occur. Activation of hydrogen is negligible also. Together, these facts indicate that no shielding will be required for components in the reactor coolant loop, either in a Brayton-cycle design in which the reactor outlet gas drives the turbo-alternator directly or in the Rankine cycle.

The total fission-product loss through the nozzle during electrical-mode operation, will be only a small percentage of the release during the propulsion mode since the very high temperature in the propulsion mode permits nearly complete diffusion of fission products from all fuel particles, intact and ruptured.

In the case of the beryllium reflector, the primary damage mechanisms are related to the formation of voids and of helium from the (n, α) reaction in beryllium. In high, fast-flux irradiations (e.g., 10^{21} nvt), beryllium exhibits swelling, the amount depending upon temperature. Although data are currently lacking for annealing times of 70,000 hr, extrapolation of data obtained for shorter annealing times, shown in Figure 32, indicates that at 10^{21} nvt a service temperature in the range 1600°R to 1750°R would result in about 1% swelling. The total fast neutron fluence accumulated in dual-mode operation would be about 5.3×10^{20} nvt at the maximum flux location in the core, assuming 500 kw(t) were required of the reactor in the electrical-mode operation. In view of this order-of-magnitude reduction in required fluence and the expected operating temperature of only 700°R , it is concluded that no significant dimension change will occur in the beryllium reflector.

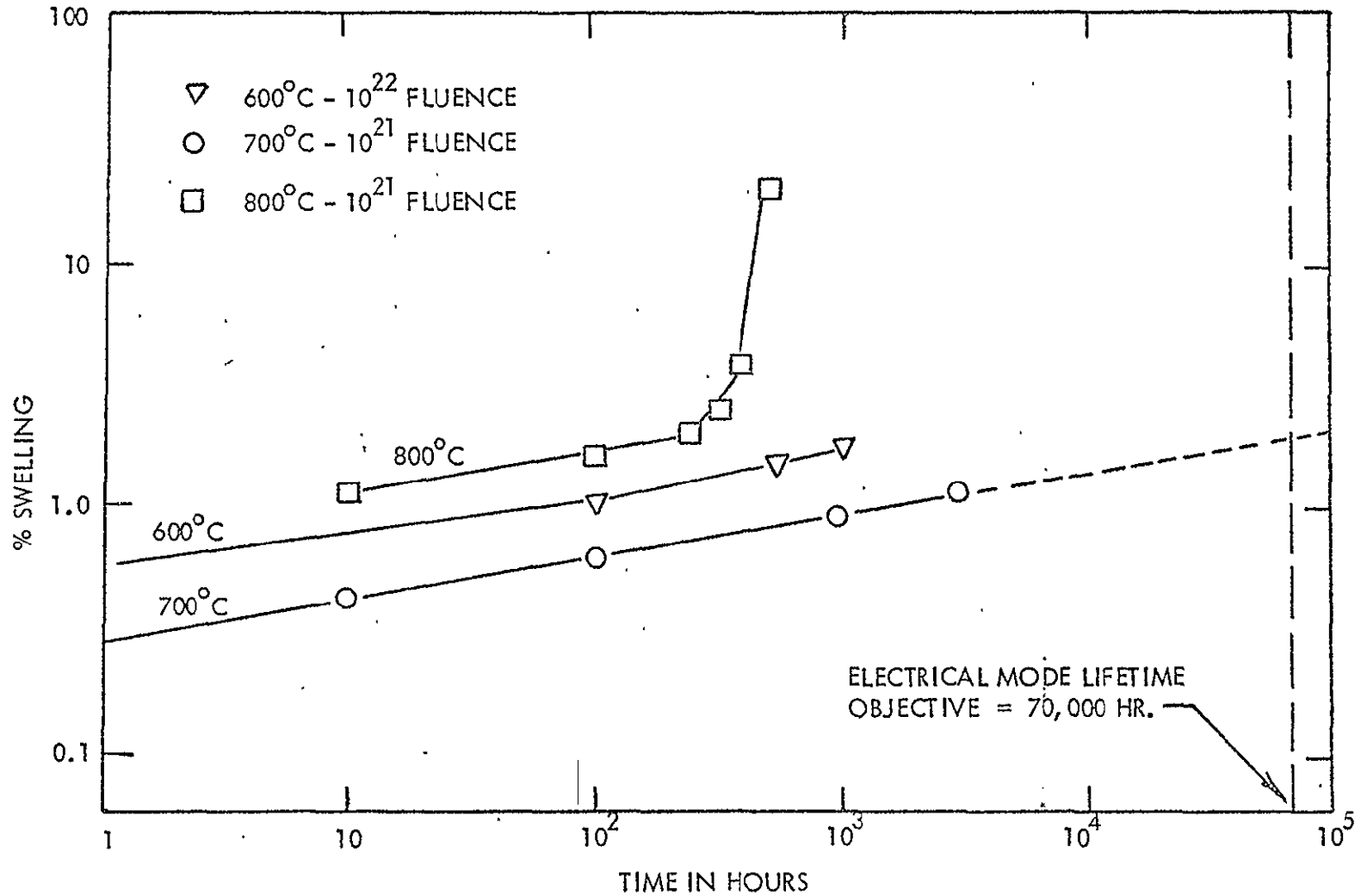


Figure 32 - Radiation Changes in Beryllium

Radiation damage problems are qualitatively similar in the dual mode and propulsion missions. It may therefore be assumed that performance of the nuclear subsystem will not be restricted seriously by radiation effects in the dual mode application.

Most of the vacuum-related problems noted in the discussion of the stem heat-removal concepts apply, at a reduced extent, to the reflector heat-removal concepts as well, where somewhat greater local fracture or other mechanical deterioration of the core may be accepted without jeopardizing an electrical-mode system located in the rather massive aluminum reflector ring. Obviously, re-use in the propulsion mode would place more stringent requirements in this area, but the information available at this time does not indicate that vacuum effects in the dual-mode application will be significantly more difficult to design for than in the propulsion mission alone.

In one respect, the reflector heat-removal potential may be adversely affected by exposure to vacuum to a greater extent than the core heat-extraction concepts. Since the heat-transfer path in this case includes the interfaces between fuel elements, the core periphery/fuel interface, the periphery/lateral support interface, and the seal segment/plunger/reflector interfaces, the concept is dependent upon the existence of reasonably good conduction across gaps. The phenomenon of increased thermal impedance, caused by the removal of adsorbed gases, therefore deserves consideration. However, experimental data concerning this effect in graphite are nonexistent, in particular for surfaces previously "scrubbed" by high-temperature hydrogen.

If the thermal contact resistance is larger than assumed, design changes may be required to increase conduction, or to permit higher core temperatures, depending upon the power requirement. Conceivably an intermittent gas flow could be used to replenish the surface-absorbed gas layer. Further study is required to specify the limiting amount of heat which can be extracted from the reflector, but it does appear that 250 kw(t) is available without refining the design to improve heat transfer.

In the separated-flow reflector heat-removal concept, there are no valves or other moving parts except for the control drum actuators. These are activated only periodically to make small reactivity adjustments as required by electrical load changes, changes in solar heating of the engine, and fuel burnup. Since the drum actuator must be designed for a three-year space storage, redesign for the electrical mode is not anticipated.

5. Nuclear Design

The nuclear impact of dual-mode operation can be assessed under two categories, electrical-mode nuclear requirements and by-product effects. Electrical-mode nuclear requirements are changes necessary to the propulsion system initial nuclear design to accommodate the electrical mode operation, including burnup and operating reactivity effects. By-product effects are incidental nuclear changes in the propulsion system as a result of changes to accommodate dual-mode operation. None of those identified to date warrant further consideration in a feasibility study.

The NERVA reactor is designed for a total of 10 hr operation at about 1500 Mw thermal power, or a total energy production of 15,000 Mw-hr. During the electrical-power generation mode, an additional 17,500 Mw-hr would be produced if the reactor operated at a thermal power of 250 kw, assuming an eight-year life. Thus, the total energy production in the dual-mode case would be 32,500 Mw-hr, about twice that of NERVA. The cumulative number of fissions and other neutron-induced reactions in U^{235} , B^{10} , and other materials will accordingly also be approximately doubled. At 0.50 Mw thermal power in the electrical mode, the combined effect is more nearly a factor-of-three increase over NERVA.

As shown in Table 6, the reactivity loss during electrical-mode operation is estimated to be about 22¢, assuming a reactor power level of 250 kw(t), or 44¢ if 500 kw(t) is required. Because of the 10^4 reduction in power, the rate of production of Xe^{135} is reduced by 10^4 , and the amount of

TABLE 6
 SUMMARY OF BURNUP ANALYSIS FOR
 DUAL-MODE REACTOR

	NERVA Propulsion Mode	Electrical Propulsion Mode	
	Thermal Power, Mw	1500 Mw	0.25 Mw
Total Operating Time	10 hr	70,000 hr	70,000 hr
Thermal Energy Production, Mw-hr	15,000	17,500	35,000
No. fissions $\times 10^{-24}$	1.73	2.02	4.04
Mass U ²³⁵ fissioned, kg	0.67	0.78	1.56
Mass U ²³⁵ consumed, kg	1.00	1.17	2.33
Reactivity Loss during operation, β			
U ²³⁵ depletion	12.8	15	30
Xe ¹³⁵ poisoning	5.2	0.2	0.4
Sm ¹⁴⁹ + long-lived fission products	6	7	14
U ²³⁶ buildup	0.7	0.8	1.6
Total Reactivity Loss	24.7	23.0	46.0
Additional reactivity loss at peak Xe ¹³⁵ concentration, β			
		0.2	0.4

Xe¹³⁵ (which exists when equilibrium is reached) is greatly reduced. Sm¹⁴⁹, a stable fission product which is not appreciably burned out, is accumulated in each mode at a rate approximately proportional to the fission rate: i.e. the total Sm¹⁴⁹ inventory is proportional to the energy produced. This is true also of the remaining fission products which typically have low cross-sections. The reactivity loss because of fission products other than xenon has been shown experimentally to increase linearly with time for integrated energies comparable to those expected with the NERVA or dual-mode mission.

The problem of Xe¹³⁵ poisoning following reactor shutdown is greatly reduced in the electrical mode, the equilibrium xenon level essentially depending only upon the generation rate by I¹³⁵ decay and the loss rate by Xe¹³⁵ decay: i.e., burnout of either nuclide is negligible at electrical-mode power levels. Consequently, the equilibrium is not affected by shutting the reactor down: thus, no postshutdown Xe¹³⁵ override problem exists.

Burnout during propulsion-mode operation holds the equilibrium concentration of Xe¹³⁵ to a much lower value than is reached after shutdown. As a result, shutdown and restart of the reactor during electrical mode operation create no additional reactivity requirement above that for continuous operation.

The reactivity change from a dry, ambient (assumed to be 524^oR) condition to the design point during electrical-power generation is shown in Table 7 for both the support stem and reflector barrel heat-removal concepts. The data were computed for 350 and 250 kw(t) power levels respectively, but are representative of power levels in the range of 150 to 500 kw(t), providing core and reflector material temperatures are maintained near the assumed values. Reactivities at other temperatures may be computed using the core and reflector temperature coefficients of reactivity (-0.09¢/°R and -0.05¢/°R respectively).*

The electrical-mode operating condition is substantially more reactive in the stem heat-removal concept because of the lower core moderator

* The latter value includes the effect of the increase in drum worth as reflector temperature increases, using a typical value for inserted negative reactivity.

TABLE 7

CALCULATION OF COLD-TO-HOT REACTIVITY
IN ELECTRICAL MODE

	Propulsion Mode (Typical)	Electrical Generation Mode Stem Heat Removal Concept	Reflector Heat Removal
<u>Core Reactivity Effects</u>			
$\Delta \rho$ due to Core Temperature	\$-2.28 (3100°R)	\$-0.24 (800°R)	\$-0.95 (1600°R)
Fuel Channel H ₂ worth	+1.14	0	0
Stem H ₂ worth	<u>+1.81</u>	<u>0.47</u>	<u>0</u>
Total	+ .67	+0.23	-0.95
<u>Reflector Reactivity Effects</u>			
$\Delta \rho$ due to Be Temperature (Temp.)	\$+0.15 (225°R)	\$+0.05 (700°R)	\$+0.05 (700°R)
Lateral Support H ₂ worth (Mass)	+0.09 (0.15 lb.)	0	0
Al Barrel H ₂ worth (Mass)	+0.24 (0.42 lb.)	0	+0.10 (.14 lb)
Be Web and Sector (Mass)	<u>+0.11 (2.34 lb.)</u>	<u>0</u>	<u>0</u>
Total	+0.59	+0.05	+0.15
Total Cold-to-Hot Reactivity Change	+1.26	\$+0.28	\$-0.80

temperature and the stem hydrogen content. As noted below, however, the reactivity and control requirements of both systems are satisfied by the NERVA reactor at the end of propulsion-mode operation.

The current NERVA reactor design provides more than \$2 excess reactivity at end-of-life in the dry, ambient condition. This value depends upon design factors undergoing continuous re-evaluation at the present time, but it is conservative to expect that at least \$1 to \$1.25 excess reactivity will be available without imposing new requirements upon the reactor to permit dual-mode operation. The initial excess reactivity requirement in the dry, ambient-temperature reactor prior to electrical-mode operation is shown in Table 8, giving \$-0.1 for the stem heat-removal concept and \$1 for the reflector barrel heat-removal concept. These values apply for a 250 kw(t) power level in the electrical mode. An additional \$0.2 reactivity would be required in either design if a 500 kw(t) power level were specified. By comparison with the \$1 to \$1.25 excess reactivity expected, the present NERVA nuclear design is adequate for dual-mode operation also.

The NERVA reactor has proved remarkably stable. Its stability to changes in power and propellant flow rate has been demonstrated in many reactor tests, most notably the NRX/EST and XE-Prime tests. In these tests, for example, it has been demonstrated that the reactor can be brought to power without control drum motion by merely injecting hydrogen, which has a positive reactivity coefficient. The reactor rises in power and then levels off at a point at which the positive reactivity provided by the full-power hydrogen inventory is just compensated by the reactor's inherent negative reactivity coefficient per unit increase in core material temperature.

In addition to its negative temperature coefficient of reactivity, the reactor exhibits a negative power coefficient of reactivity, since a raise in power decreases the density of the hydrogen coolant, in effect expelling this moderator from the reactor. This effect acts in conjunction with the

TABLE 8

REACTIVITY REQUIREMENT FOR
ELECTRICAL-MODE OPERATIONS

NERVA Electrical-Generation Mode
70,000 hr at 250 kwth
Steam Heat Removal Heat Removal

Operating Reactivity Requirement, \$

Moderator loss due to corrosion	0	0
Fuel burnup & fission product poisoning	-0.2	-0.2
Xe ¹³⁵ override (10.5 hr after 1 hr burn)	0	0
Cold-to-Hot Reactivity Change	+0.3	-0.8
TOTAL	+0.1	-1.0

more-immediate negative reactivity effect associated with core moderator temperature coefficient to make the NERVA reactor self-regulating with respect to an external reactivity perturbation. This provides the control system designer considerable latitude in designing the high-reliability system required for long-term applications. For example, reactivity control during electrical-mode operation might be effected with a relatively slow-acting, reactivity-shim type control device instead of the present control drum system. No requirement is actually envisioned at the present time for an auxiliary reactivity control device during the electrical-generation mode, because the control drum drive actuator subsystem appears adequate for use in the electrical-generation mode with only minor modifications to accommodate the relatively high temperature and 70,000-hr design objectives. The hard-vacuum problem must be assessed but is essentially no different than the NERVA requirement.

It is assumed for this study that the electrical plant will demand a constant thermal power from the reactor, with any excess electrical power either dissipated through resistors or otherwise utilized on board the spacecraft. Under this assumption, the operating reactivity change with time will be extremely slow, perhaps -0.2c/month . This could be compensated by an adjustment of the control drum position once each month. In the intervening time, the control drums would remain stationary and the reactor material temperatures would slowly decline about 3°R as the reactor responded with its negative temperature coefficient of reactivity to the reactivity loss.

6. Reliability

The reliability of the present NERVA reactor in the electrical-mode configuration is developed in Table 9. The basis for this table is current estimated failure-rate data for NERVA components, multiplied by subjective factors to account for the less-stringent stress/temperature environment during the electrical-mode operation. Specifically, the failure rates for the support plate and plenum, internal shield, cluster hardware, and core periphery were assessed at the NERVA "coast" condition with failure rates reduced by three orders of magnitude from the run condition. The fuel and reflector were assigned

TABLE 9

INITIAL REACTOR RELIABILITY ESTIMATE FOR
THE DUAL-MODE SYSTEM

Component	Failure Rate, failures per million hours.	
	Propulsion Mode	Electrical Mode
Fuel	110	1.1
Cluster Hardware	40	0.04
Core periphery	200	0.2
Support Plate and Plenum	6	0.006
Internal Shield	0.1	0.0001
Reflector Assembly	16	0.16
Control Drum Drive Assembly	19	0.019 *
Control Instrumentation	20	20
Total	<u>412</u>	<u>22</u>

* Assumes control drum actuators are active only 0.1% of the time during electrical mode operation, or 44 minutes/month.

a reduction factor of 100: i.e., more stressed than the "coast" condition, but much less than propulsion mode. The instrumentation was assigned its full propulsion-mode failure rate. The drum actuators were similarly assigned the ordinary failure rate per hour of actuator operation. However, the actuators were assumed to operate only 0.1% of the time, giving a 10^3 reduction in failure rate per hour of reactor operation. Multiplying the total failure rate of $22 \times 10^{-6} \text{ hr}^{-1}$ from the table by the endurance objective of 70,000 hr required in the electrical-generation mode yields 1.5 failures per mission, an unacceptable value.

This assessment indicates that the present NERVA instrumentation is inadequate for use in the dual-mode application, if the estimated failure rate is valid. Fortunately, the rate of reactivity change with time is very small if constant power demand is assumed, as shown in the previous section. Under this assumption, then both the neutronic instrumentation and actuator systems need operate a small part of the time. Actuation of these systems could be signalled by a very reliable transducer, such as a thermocouple or possibly even a bimetallic strip type of thermostat. Under the assumption of a 0.1% duty cycle, the contribution of the instrumentation to the reactor failure rate decreases to $0.2 \times 10^{-6} \text{ hr}^{-1}$ and the total of Table 9 becomes $1.7 \times 10^{-6} \text{ hr}^{-1}$. The mean number of failures per mission would then be $(1.7 \times 10^{-6}) (7.0 \times 10^4) = 0.12$. While this is much too high, the result must be evaluated in context. With the exception of the intermittent duty cycle assigned to the instrumentation, the reliability estimate has been based upon generally pessimistic assumptions in that no design modification to increase reliability has been assumed. The following need further study:

1. Reactor component failure rates at electrical-mode operating conditions. The fuel and reflector warrant special attention.
2. Design of a high-reliability control system for both reactor and electrical plant. It may be noted that the assumption

of an intermittent duty cycle for the reactor essentially transfers the reliability problem to the electrical control system.

It is tentatively concluded on the basis of the present review that with suitable design effort, the achievement of satisfactory reliability in the nuclear subsystem (e.g. 95 to 99%) should be feasible. For manned applications, with their more stringent reliability requirements, the need for a detailed reliability explanation is clear. The problems of developing control devices for long operation in space are, of course, common to all space power systems.

B. BOILER

The boiler (preheater; low-, intermediate-, and high-pressure boilers; and low, intermediate superheaters) has the same design influences as the engine reflector heat-exchanger in addition to the problem of a second fluid, thiophene, that must have numerous piping interfaces to and from the heat-transfer interface. The possibility of using a single chambered boiler that combines the preheating, boiling, and superheating cannot be considered for the three pressure level cycle used as the basis for this study. If the potential cycle efficiency gain of a multiple pressure-level system is later determined to not be worth the complexity, the single chambered boiler can be considered.

The primary influence upon design is that both fluids must have low pumping losses. This dictates relatively large frontal areas and a minimizing of turbulence generators in the heat-transfer passages. In addition, the requirement for low pumping losses (hence, low velocity) makes the hydrogen side limiting for the heat-transfer rate, even in the superheater portion. The film driving temperature-pumping power product, $T_f \times \dot{H}_p$, for the hydrogen side is slightly greater than that of thiophene vapor, in spite of the lower viscosity, higher thermal conductivity, and higher specific heat of the hydrogen. The high specific weight (15 times that of hydrogen) is the controlling property as pumping power

is a function of the specific-weight rates squared. As a result, the boilers must be designed to have a relatively large hydrogen-side frontal area. In addition, the large number of thiophene side ports precludes the use of a larger bundle of tubes for the hydrogen flow (i.e., the inner reflector-cylinder heater design).

The designs would suffer from flow-distribution problems caused by their short length or would be required to be crossflow configurations, which are undesirable from an effectiveness standpoint. The configuration selected as most efficient and reliable is a simple 2-in.-diameter tube to carry the 600-psia hydrogen (see Figure 33). Around this tube will be an annulus area to carry the lower-pressure (28 to 45 psia) thiophene. The annulus would be bridged by high-pitch fins, as required, to transfer heat to the outside wall of the annulus and centrifuge the thiophene to ensure liquid contact with a heating surface and thus avoid slugging of liquid through the boiler section.

Typical mean driving temperatures for the superheater are: hydrogen side, 22.5°F ; wall, 3°F ; and thiophene, 18.5°F . The relatively high hydrogen-side resistance is the result of the low velocities used to maintain pumping power at a low level. In the boiling sections, the typical driving temperatures are: 8.7°F for hydrogen film; 0.4°F for the wall; and 23°F for the thiophene side (reflecting the conservative heat-transfer coefficient assumed for thiophene).

C. TURBINE-ALTERNATOR PUMP ASSEMBLY

The turbine-alternator pump assembly (TAPA) shown in Figure 34 is representative of a rotating unit which would be used with a thiophene-Rankine cycle as described in the flow schematic. The central element on the rotor shaft is the alternator rotor. A permanent magnet rotor-alternator operating at approximately 24,000 rpm was selected as being a low-weight and highly reliable unit. This rotor assembly is supported by two thiophene-lubricated, tilting-pad, hydrodynamic bearings. Bearings and the alternator housing are vented directly back to the condenser to furnish the lowest density gaseous environment to the

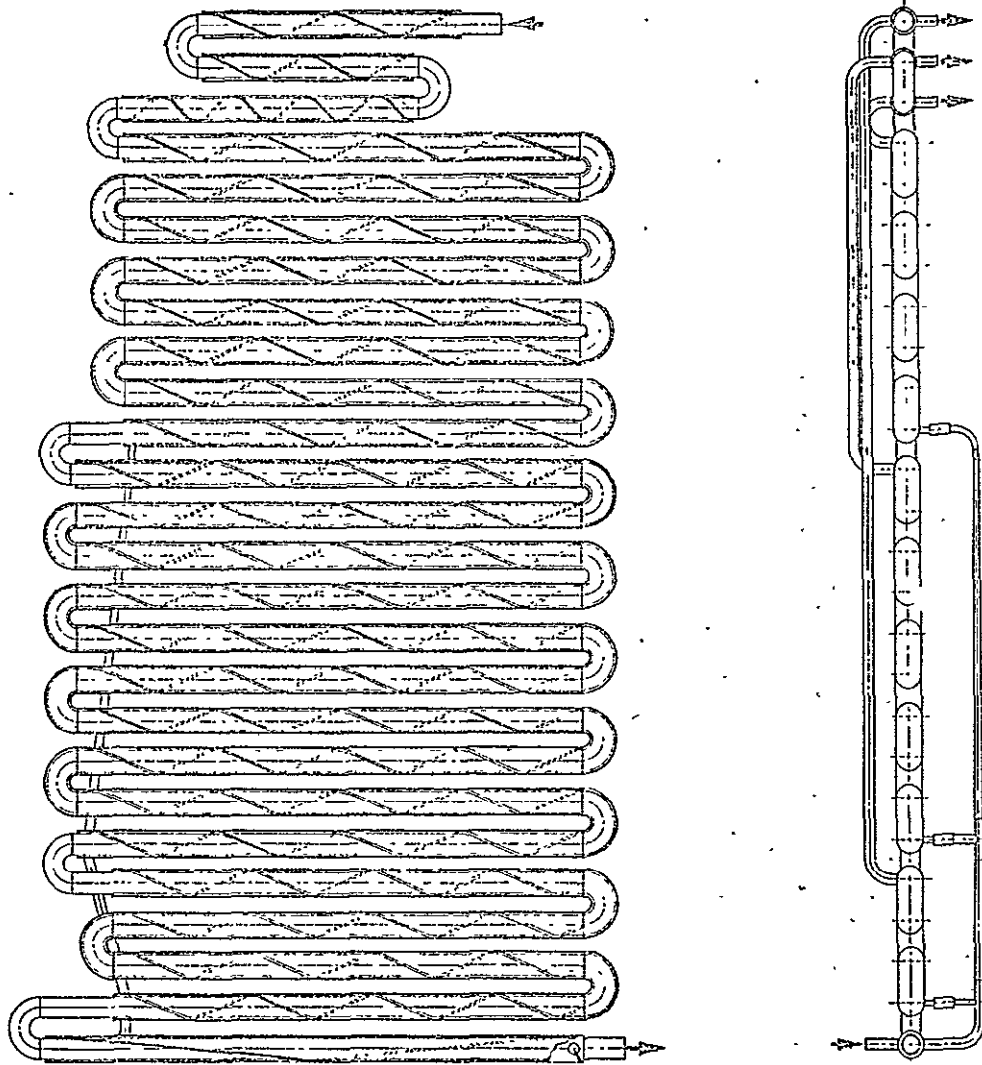


Figure 33 - Boiler, Dual-Mode System, 25 kw(e)

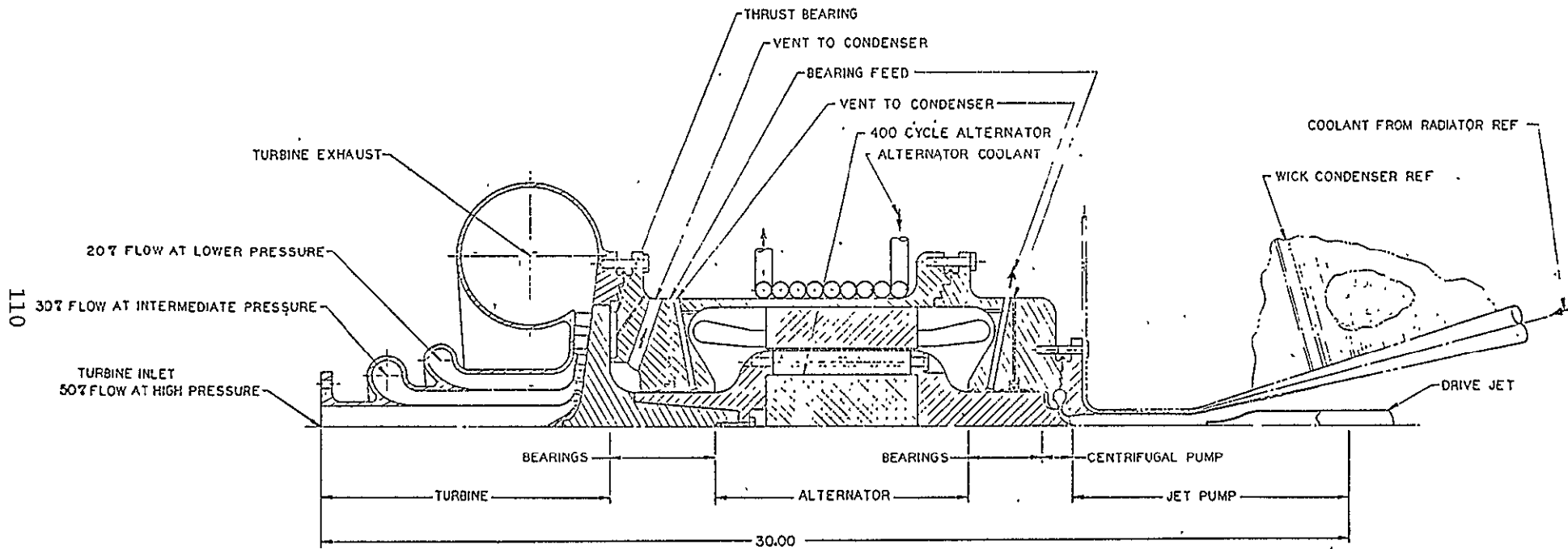


Figure 34 - Turbine-Alternator-Pump Assembly

alternator rotor. The alternator housing is cooled by liquid thiophene coming directly from the condensate pump. This fluid passes through independent passages cooling the stationary windings and then continues to the boiler. As there is only one fluid (thiophene) used throughout the TAPA, there is no need for any rubbing contact seals. The requirement for isolating liquid from gaseous cavities can be accomplished by labyrinth, control gap, or hydrostatic seals, all of which have no rubbing contact during full-speed operation. The entire TAPA is hermetically sealed, having all welded joints.

The turbine rotor is overhung at one end of the unit, and the boiler feed pump is integral at the opposite end of the unit. The turbine assembly is unique in that it was specifically designed for the three pressure levels generated in the boiler loops. Only a portion of the flow (approximately 50%) passes through the first-stage blading, which is near the hub. This flow is joined by an additional 30 and 20% in the second and third stages, respectively. The primary portion of the turbine work is performed in the final turbine stages. This is because of the high-pressure ratio available to the third stage (see Table 9) in addition to the fact that all of the flow passes through this last stage. To achieve high efficiencies for the first two stages, the blade velocity of these stages must be maintained considerably lower than that of the third stage. Thus, the need for extremely large change in blading diameter, stage to stage, resulted in the selection of the radial flow configuration (see Figure 34). The ability to control axial movement of the TAPA rotating assembly to several thousandths of an inch by the use of hydrostatic thrust bearings will permit the minimizing of turbine-blade-tip clearance losses. The back face of the turbine rotor carries the major thrust load. The rotating assembly will require an additional bearing (not shown in Figure 34) to resist any reverse thrust.

The boiler feed pump is comparatively small because of the low-pressure system. The pump impeller handles approximately two times the boiler feed pump flow-rate requirement. Approximately half of the flow is recirculated through a jet pump to supercharge the boiler feed pump, and thereby provide sufficient net NPSP and preclude cavitation in the impeller.

A 75-psia discharge pressure was assumed for the boiler feed pump to ensure the necessary throttling stiffness for the boiler. The power cost of the additional pressure above boiling pressure is small for a pump of less than 1-in. diameter. The larger diameter required for additional pressure produces a pump with a higher efficiency, thus offsetting some of the increased power. Configuration of the impeller is that of a typical Francis centrifugal pump but without a suction side shroud.

Long life for the centrifugal pump impeller blading is insured by designing to a suction specific speed of 12,250. To achieve this low suction specific speed by subcooling the thiophene is not practical because of the low absolute condensing pressure of the cycle. The condensing pressure at 90°F is 1.71 psia. Even if the vapor pressure were reduced to zero, an NPSH of less than half of that required for the 12,000 suction specific speed range would be achieved (see Table 10). A jet pump was, therefore, selected to boost the approximate 1-ft NPSH (that can be achieved by 10°F subcooling of the 2.46-psia condensate) to the 13.5 ft needed.

The jet pump is, of course, also limited by NPSH. It, however, can be designed to require much less suppression than a centrifugal pump. The jet pump was designed to have twice the NPSH required to produce head drop-off. The parameter

$$\omega = \frac{P_2 - P_v}{\frac{\gamma V_n^2}{2g}} = \frac{V_3^2}{V_n} (1 + K_s) ,$$

where:

- | | | |
|-------|--|---------------------|
| g | = acceleration due to gravity | ft/sec ² |
| K_s | = driven fluid inlet friction loss coefficient | -- |
| P_v | = vapor pressure | lb/ft ² |

TABLE 10

TYPICAL OPERATING PERFORMANCE

Description - Turbine-Alternator-Pump-25 kw (e)

<u>Pumps</u>	<u>Dimensions</u>	<u>Jet</u>	<u>Centrifugal</u>
Propellant		Thiophene	Thiophene
Propellant Temperature	°F	80	80
Propellant Density	lb/ft ³	65	65
Shaft Speed	rpm	-	24,000
Total Discharge Pressure	psia	8.08	75
Total Suction Pressure	psia	2.46	8.08
Total Pressure Rise	psi	5.62	66.9
Total Head Rise (cavitating)	ft	12.45	148
Weight Flow (Driven/Driving)	lb/sec	0.958/0.928	1.89
Capacity (Driven/Driving)	gpm	6.6/6.4	13
Specific Speed (Based on Cavitating Head)	$\frac{\text{rpm} \times \text{gpm}^{-1/2}}{\text{ft}^{-3/4}}$	-	2030
Efficiency	%	25.5	44.7
Fluid Horsepower	h.p./kw		0.51/0.38
Shaft Horsepower	h.p./kw		1.14/0.85
Net Positive Suction Head	ft	1.11	13.5
Suction Specific Speed	$\frac{\text{rpm} \times \text{gpm}^{-1/2}}{\text{ft}^{-3/4}}$	-	12,250
 <u>Turbine</u>			
Gas			Thiophene
Shaft Power	h.p./kw		38/28.4
Gas Weight Flow (Stage 1/2/3)	lb/sec (0.464/0.742/0.928)		0.928 (total)
Gas Inlet Total Temperature	°F		290
Pressure Ratio (Stage 1/2/3)			1.29/1.22/10.9
Static Back Pressure	psia		2.6
Shaft Speed	rpm		24,000
Efficiency (Stage 1/2/3)	%		83/70/85
Gas Inlet Total Pressure (Stage 1/2/3)	psia		44.7/34.7/28.4

Reference

Gas Properties Monsanto Company, CP-34 Data, 20 June 1967

P_2	= driven fluid total pressure	lb/ft ²
V_n	= nozzle velocity	ft/sec
V_3	= driven fluid velocity	ft/sec
γ	= specific weight	lb/ft ³

was assumed as design criteria*. The cavitation parameter, ω , was determined from Sanger's empirical data in Figure 13 of NASA Report TN D-4592 on the basis of the driven-to-driving velocity ratio required to satisfy the impeller eye diameter and jet-pump pressure. Taking twice the ω parameter means the jet pump NPSH can be reduced to one-half of the operating value of 1.11 ft before the jet pump will start to lose its capacity to pump.

There will be cavitations in the mixing zone where the drive jet interacts with the suction flow from the condenser. No component damage is expected to occur, however, when this cavitation occurs in the free stream away from the metal walls.

* Sanger, Nelson L., Cavitation Performance of Two Low-Area-Ratio Water Jet Pumps Having Throat Lengths of 7.25 Diameters, NASA Report TN D-4592, May 1968.

Sanger, Nelson L., Noncavitating and Cavitating Performance of Two Low Area Ratio Water Jet Pumps with Throat Lengths of 5.66 Diameters, NASA Report TN D-4759, August 1968.

Sanger, Nelson L., Noncavitating and Cavitating Performance of Several Low Area Ratio Water Jet Pumps Having Throat Lengths of 3.54 Diameters, NASA Report TN D-5095, March 1969.

D. CONDENSER

The design of the condenser is probably the most difficult problem associated with the Rankine cycle for space application. The basic problem is in moving the condensed fluid from the condensing zone into the condensate pump or boiler feed pump. The characteristics of the fluid play an important part in the selection of the condenser design. In the case of the mercury-Rankine or SNAP-8 system, the condensate has very high thermal conductivity and relatively high vapor pressure. In addition, the mercury-condensate droplets do not wet the surface of metal tubes in the condenser. These properties are unique to liquid-metal working fluids and are substantially different from the corresponding characteristics of organic working fluids (e.g., thiophene or pyridine).

The jet condenser has been utilized for such organic working fluids as Dowtherm A. The jet condenser provides condensation surfaces on subcooled jets of liquid, which spray into a small-diameter throat and are then diffused for pressure recovery. The subsequent static pressure rise is used to provide pressure for circulating the drive fluid and the condensate through the radiator and to provide sufficient NPSP for the boiler feed pump. The jet condenser requires the recirculation ratio in a range of 15 times as much liquid as condensate and requires a subcooling of about 25° to operate. Increasing the subcooling permits reduction of recirculated flow and vice versa. To minimize the parasitic power losses associated with the large recirculated flow, additional design consideration was given to the condenser for the dual-mode electrical system.

The condenser selected for further study is of the wick type. The condenser is comprised of an array of 24 radial surfaces each consisting of 86 one-eighth-inch diameter tubes with cold-hydrogen cooling flowing in the tubes (see Figure 35). The outer surface of adjacent tubes is bridged with three layers of metal screen thermally attached to the tubes. Layers are of three different mesh sizes. The first layer adjacent the tubing is coarse. A second layer covers approximately two-thirds of the surface and is of intermediate mesh.

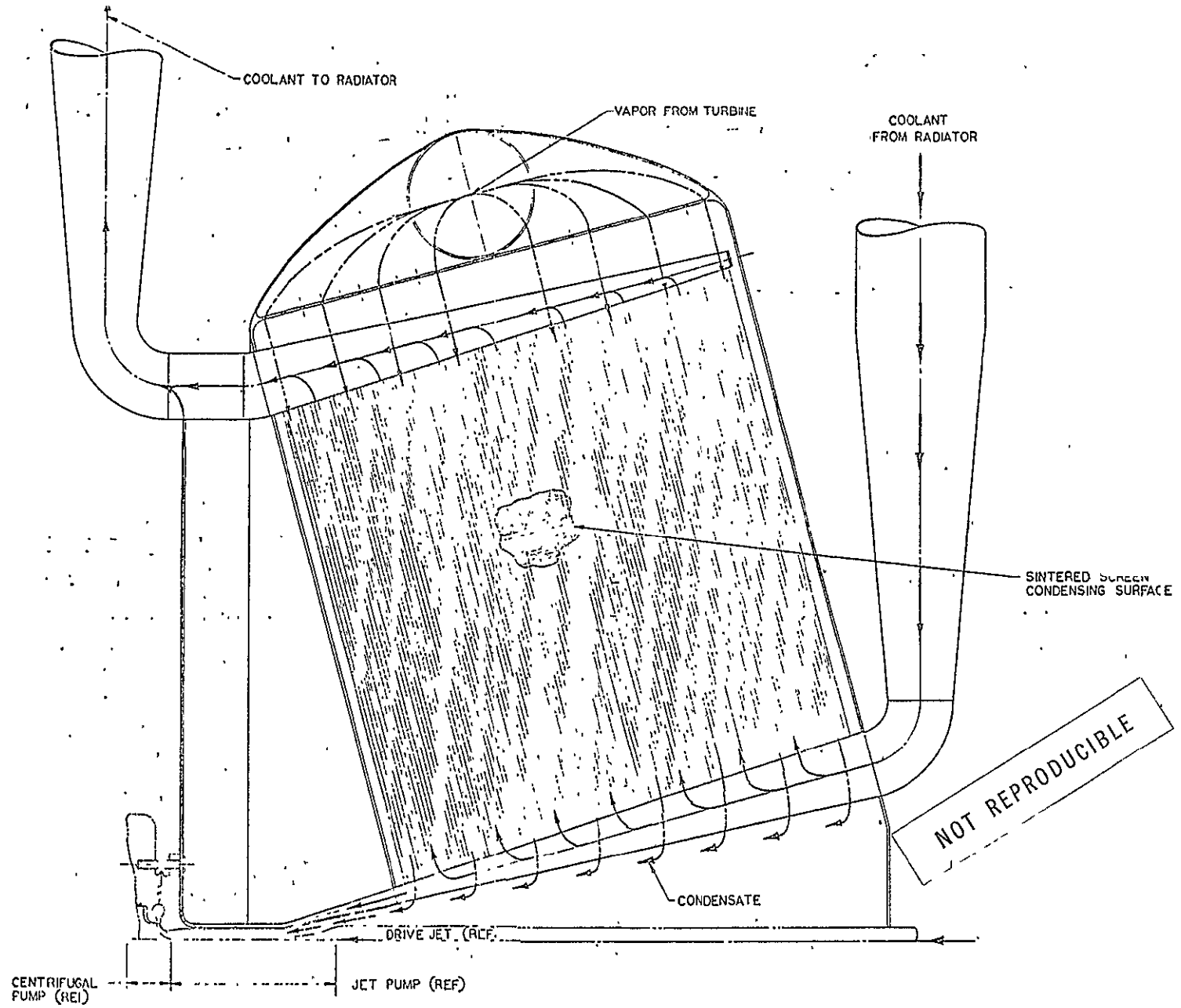


Figure 35 - Wick Condenser

Overlaying the first two screens is the finest mesh surface which covers the third of the surface closest to the hydrogen-coolant inlet header. All screens are continued around the inlet header to bridge the gap between the 24 headers. The screens thus act as a capillary barrier between the vapor and liquid, thereby keeping vapor from reaching the pump suction. The screens are sintered to the one-eighth-inch tubing to provide a metal path and thus insure good conduction to the outermost screen.

The condensate fills the small ducts below the screening between the tubes which lead to a common plenum, terminating at the suction nozzle of the jet pump. The ample flow area provided by the multitude of small ducts minimizes the pressure drop between the condensing surface and the jet-pump suction nozzle. Thus, only a small amount of subcooling is required, as the velocity head necessary to move the condensate is very small.

The condenser design is very flexible in that either gaseous or liquid coolants could be used in the coolant flow circuit. In the case of the electrical system using hydrogen as the coolant fluid to minimize the parasitic pumping power associated with the coolant, a Reynolds number of approximately 10,000 was selected in the design of the coolant tubes. At this relatively low Reynolds number, the heat-transfer coefficient between the hydrogen and the metal walls is about twice that of thiophene. With the differences in surface areas, the thiophene film temperature drop is 14°F and the hydrogen film drop is 13°F .

The conical inlet headers are continued past the condensing surface tubing to maintain subcooling of the jet pump and centrifugal pump housing. This hydrogen coolant bypasses the condenser to rejoin the coolant returning to the radiator.

Each of the 24 condensing surfaces is cooled by a separate coolant loop. Thus, the loss of a loop to meteoroid damage will only partially diminish cooling capacity. Metal-screen contact between cooling loop headers will provide sufficient heat conduction to insure that only condensate enters the jet pump suction.

The condenser area was determined by using empirical data for benzene condensing at one "g" on a horizontal tube. The similarity of benzene and thiophene, and the use of a porous condensing surface, makes this assumption conservative.

E. RADIATOR

1. Constraining Influences Upon the Selection of Radiator Loop Pressure

A review of the first preliminary design studies of the reactor, power conversion system, and the radiator has revealed which design parameters are significantly sensitive. The radiator, a relatively simply mechanical part, demonstrates that the simplest machines are frequently the most complex and difficult to design. Although many parameters were varied to illustrate their effect upon weight and reliability, it is believed that the radiator configuration, loop pressure, and fin effectiveness are major influences upon the weight of the radiator, the heaviest single component of the electrical power generating system. Of secondary interest is the gas-to-wall film driving temperature drop and the temperature change of the hydrogen as it passes through the radiator. To illustrate these influences the following study was made.

2. Status and Constraints

Initiation point of this study started with a review of the ANSC preliminary design of an electrical power conversion system using the NERVA rocket engine as a heat source. The North American Rockwell Space Division made a parametric design study of radiators that are integrated into the meteoroid bumper of the reusable nuclear shuttle on earth and lunar orbital missions.

The North American Rockwell study pointed out that radiator configuration, radiation temperatures, radiator loop pressure, fluid stream temperature change while flowing through the radiator, and tubing size all have a significant effect upon radiator weight. As the radiator consists of approximately half of the weight that is chargeable to the dual-mode system

and is an order of magnitude larger than any other single component, it was believed pertinent to review the studies in order to narrow the range of system design parameters.

To clarify the commonalities and differences between the prestudy baseline reusable nuclear shuttle, the North American Rockwell radiator study, and the review reported in this section, the following summary is made:

	<u>North American Study</u>	<u>ANSC Review</u>
Electrical Power-kw(e)	25	25
Reactor Power-kw(t)	200 & 290	200
Radiator Inlet Temperature - °R	540 & 600	540
Radiator Loop Pressure - psia	600 & 1000	600 & 2000
Radiator Configuration - Tiers x Circuits	3 x 8	1 x 24
Radiator Fin Thickness - in.	0.020 & 0.030	0.020
Number of Penetrations Allowed	3	3
Probability of Penetration	0.995	0.995
Structural Safety Factor	2	2
Life - years	3	3
Missions	10	10
Environmental Heat Rate-BTU/ft ² hr	60	60

The baseline shuttle currently has three oxygen-hydrogen fuel cells which develop a total of 7.5 kw(e).

In reviewing the North American Rockwell study, the complexity of defining the design parameters of the radiator became evident. It may be generalized by saying the desire to have a lightweight tubing network to spread the heat to be rejected over the meteoroid bumper surface results in requiring either high pumping powers or low-weight flow rates. High pumping

power robs the system of electrical power that has been generated, an undesirable option. Reducing the flow around the radiator loop is also undesirable because that requires an increase in the loop "delta" temperature for a given power to be radiated. Every degree increase in loop "delta" temperature is a degree that must be taken from the temperature difference available for work extracted from the cycle. Efficiency of the cycle and, therefore, electrical power generated is directly reduced. The parameters influencing pumping power and the radiator loop "delta" temperature were further examined to better understand the potential tradeoffs between these parameters.

3. Weight Study

The weight of radiator tubing and its required meteoroid shielding for a longitudinal loop radiator configuration was determined using most of the design constraints used in the North American Rockwell radiator study (see Figure 36). Figure 37 is a plot of the combined weight of tubing and shielding as a function of the number of tubes and their diameter. The exceptions to the North American Rockwell study are that all tubes are stress-limited, are of a minimum wall thickness of 0.020 in. as required by fabrication consideration, and that pumping power is limited to 0.825 kw. A stress-limited design results in the tube diameter and pressure scales being related. In addition the average fin length and the loop "delta" temperature is cross-plotted to illustrate the interrelation between the various parameters of design. The numbers of tubes are multiples of the 24 independent condenser sections used in previous studies.

Examination of Figure 37 readily defines an area of interest confined by: (1) weight; (2) pressure; (3) minimum number of tubes; (4) maximum fin length; and (5) loop "delta" temperature. Achieving minimum weight is an obvious goal (3,000 lb was the original weight goal). Low tube pressure is always desirable as high pressure is generally synonymous with

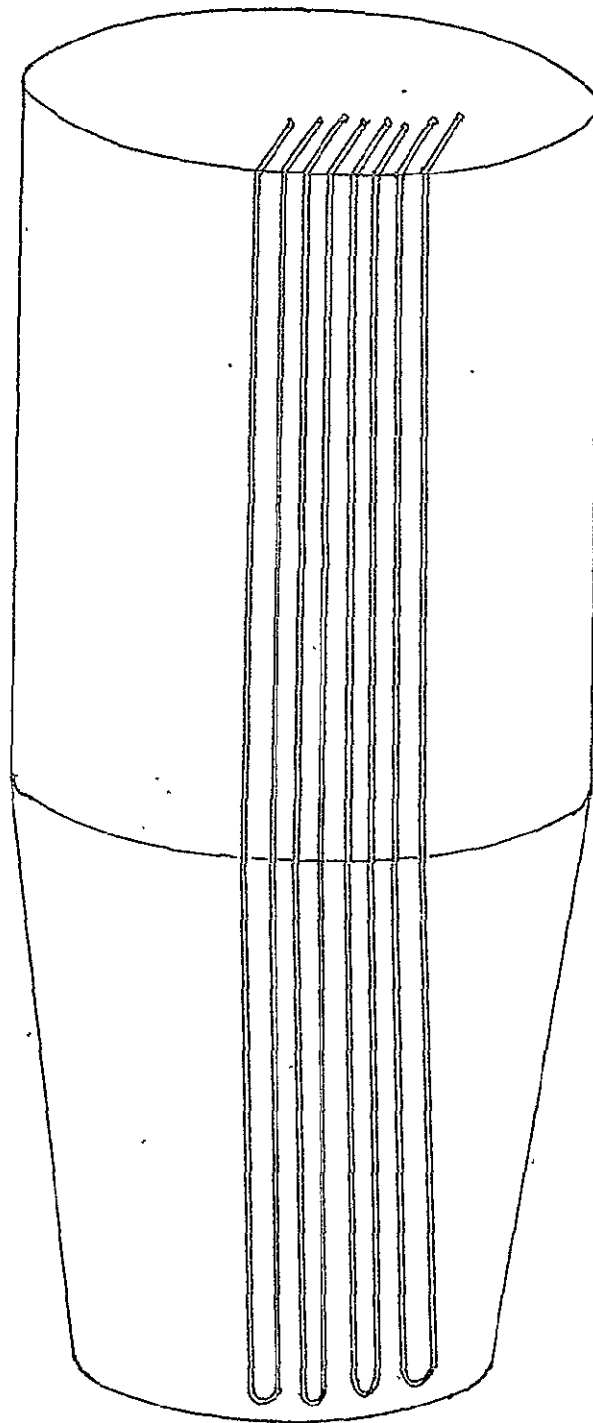


Figure 36 - Tubing Layout, No Interposition

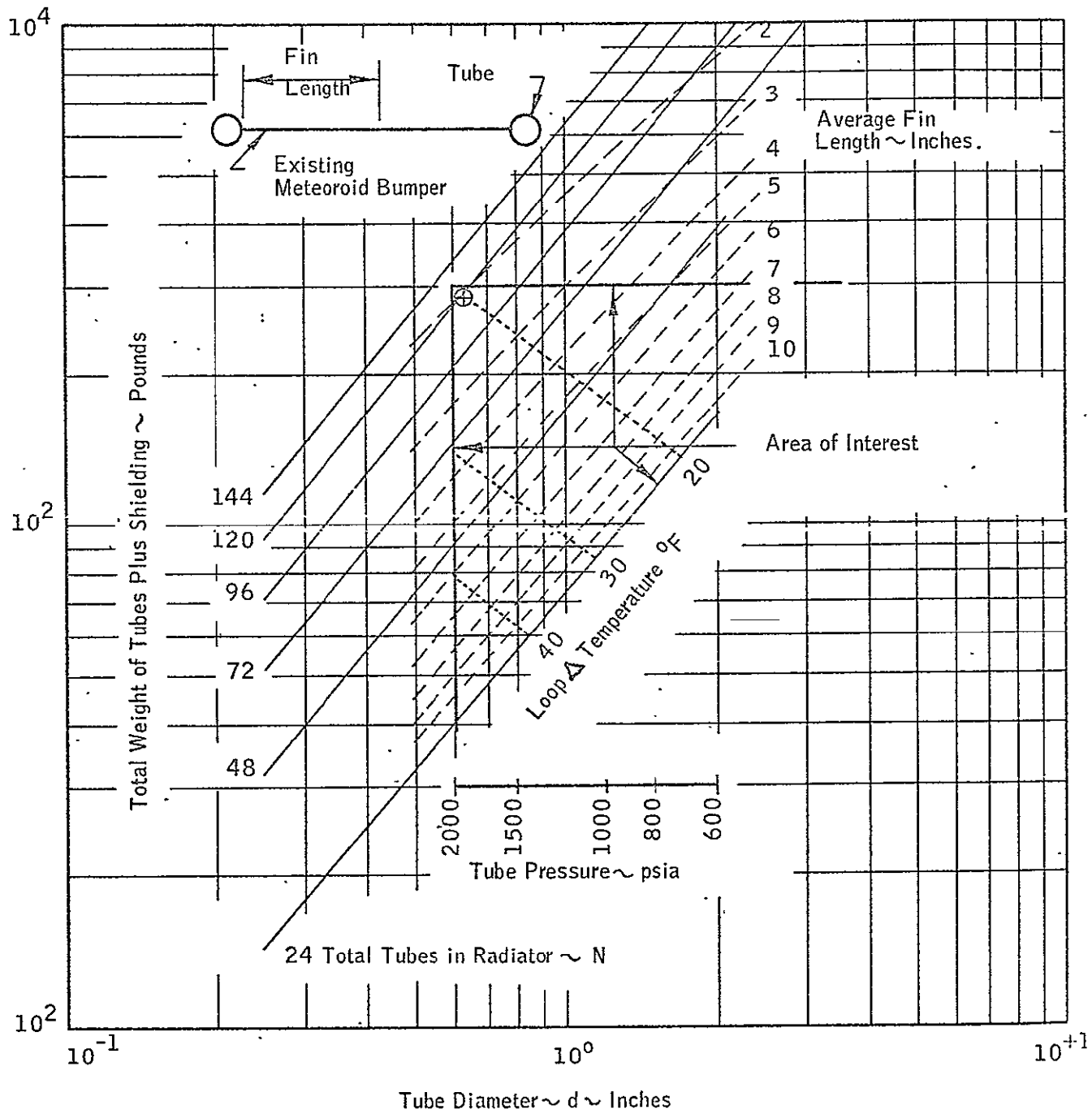


Figure 37 - Total Weight of Tubes and Additional Meteoroid Shield Vs Tube Diameter

requirements for a high-pressure source, hence either weight or much energy. Pressure bottles were originally thought of as the charging source for the various loops. NERVA engine turbopumps could produce pressures in the 1000-psia range as an intermittent pressurizing source. However, the need for pressurization after launch does not appear to be needed if the system is designed to exclude mechanical fittings. Permeability of hydrogen through an aluminum wall is negligible at the temperatures encountered by the radiator loop even for an eight-year life. At this point of assessment, there is no firm upper limit on the selection of the radiator loop pressure.

The determination of the minimum number of tubes in the radiator depends upon the number of separate condenser loops and the relative effectiveness of the meteoroid skin that acts as the radiator fin. Final determination of the number of independent condenser loops will be determined by setting the amount of loss in condenser capacity that can be tolerated over the life of the vehicle. The 24 loops used in the studies to date can be changed to accommodate power degradation limits set in the future. The significance of fin effectiveness is great since 80 to 90% of the radiation surface is fin. Figure 38 illustrates the strong influence of fin length and the radiation temperature upon the effectiveness of a fin. It should be pointed out that a review of the spectrum of radiator designs considered in the North American Rockwell radiator study yields the conclusion that an effectiveness of 40% or above will be required to maintain radiator size below 10,000 sq-ft and at an acceptable weight. It may be concluded therefore, that a radiator will have to be limited to fin lengths below 4 in. for solid fin designs. A possible design point is noted in Figure 36 at 120 tubes of 0.64-in. diameter that will weight less than 3000 lb and require an internal pressure of 1900-psia.

Loop "delta" temperature has been cross-plotted in Figure 37 to illustrate its dependency upon the tubing configuration. A loop "delta" temperature of 20°F was originally assumed and appears to be an achievable value. As noted previously, a low loop "delta" temperature is desirable

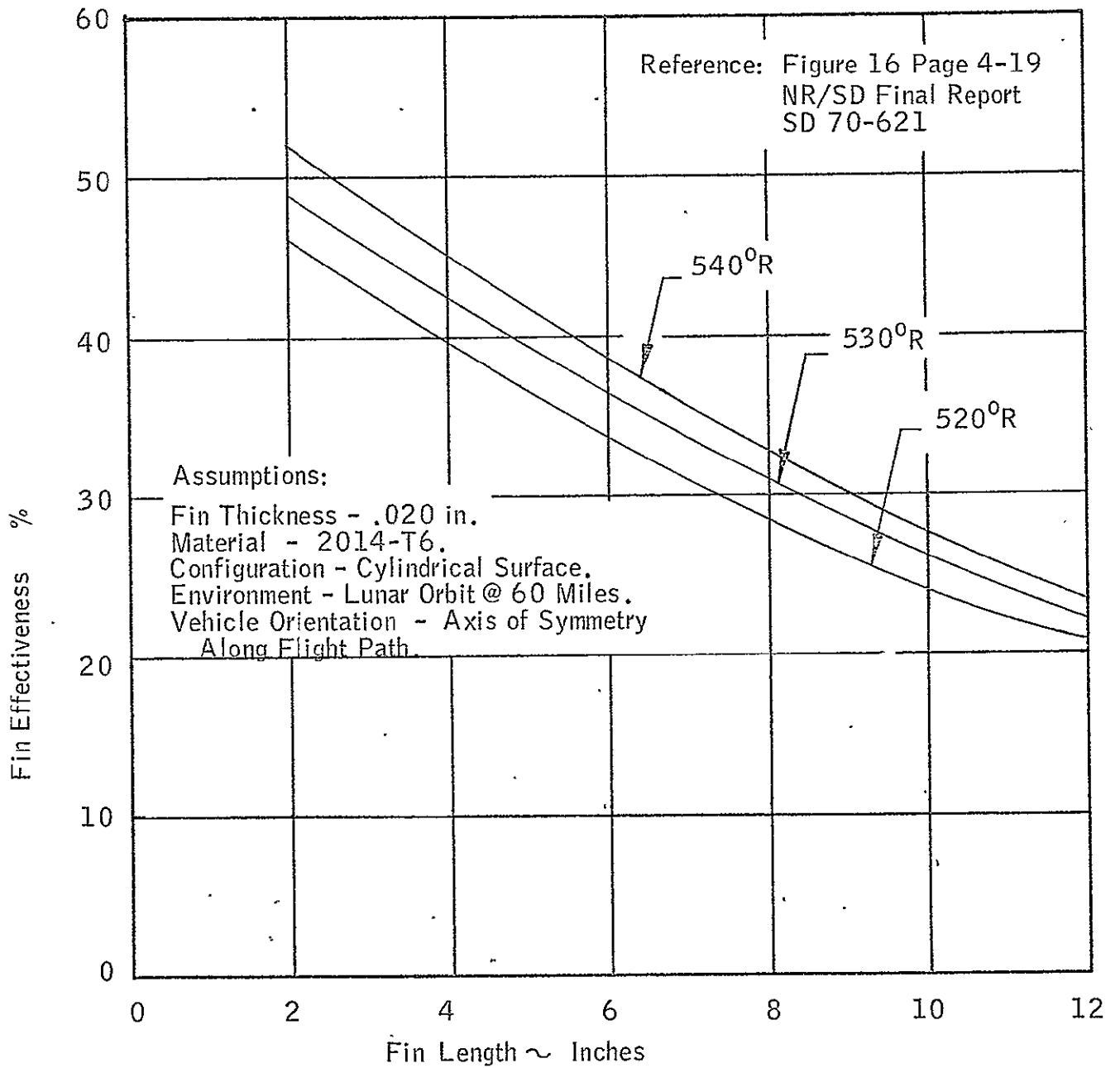


Figure 38 -- Extended Surface Effectiveness Vs Fin Length

in achieving high cycle efficiency. This fifth boundary constraining the radiator design should also be considered.

Meteoroid shield thickness used for the previous calculations is based upon North American Rockwell data to allow three punctures but otherwise no perforation as plotted in Figure 39. Total thickness as required in the plot was reduced by 0.020 in. to account for the meteoroid bumper already there. No credit was taken for the tube wall thickness as there can be spalling on the back side of the shield without being perforated.

Loop "delta" temperatures are shown separately in Figure 40 as a function of tube diameter and the total number of tubes. The area of interest designated illustrates the tendency to prefer large numbers of tubes and large tube diameters in order to maintain a small loop "delta" temperature. A scale for total loop flow rate is also marked: flowrate is a direct inverse function of loop delta temperature. The previously noted design point has a flow rate of 2.4 lb/sec.

The temperature drop because of the gas-to-wall film resistance proved to be an insignificant design parameter. Figure 41 relates this film drop to tube diameters and number of tubes for the radiator spectrum considered. The acceptable design point has a quarter degree drop while most of the designs considered are a degree or less.

It should be noted that Figure 36 depicts a configuration that alternates hot and cold tubes. Two potential penalties can be incurred by this configuration. First, if the temperature gradient in the fin is not sufficient, there tends to be a heat flow from the hot tube (i.e., inlet to radiator) to the cold end of the same and adjacent tubes (i.e., exit of radiators). This obviously lowers fin efficiency. Secondly, should a tube be punctured by micro-meteoroid, the fin length of the remaining serviceable tubes increases threefold. This length increase could be held to two times

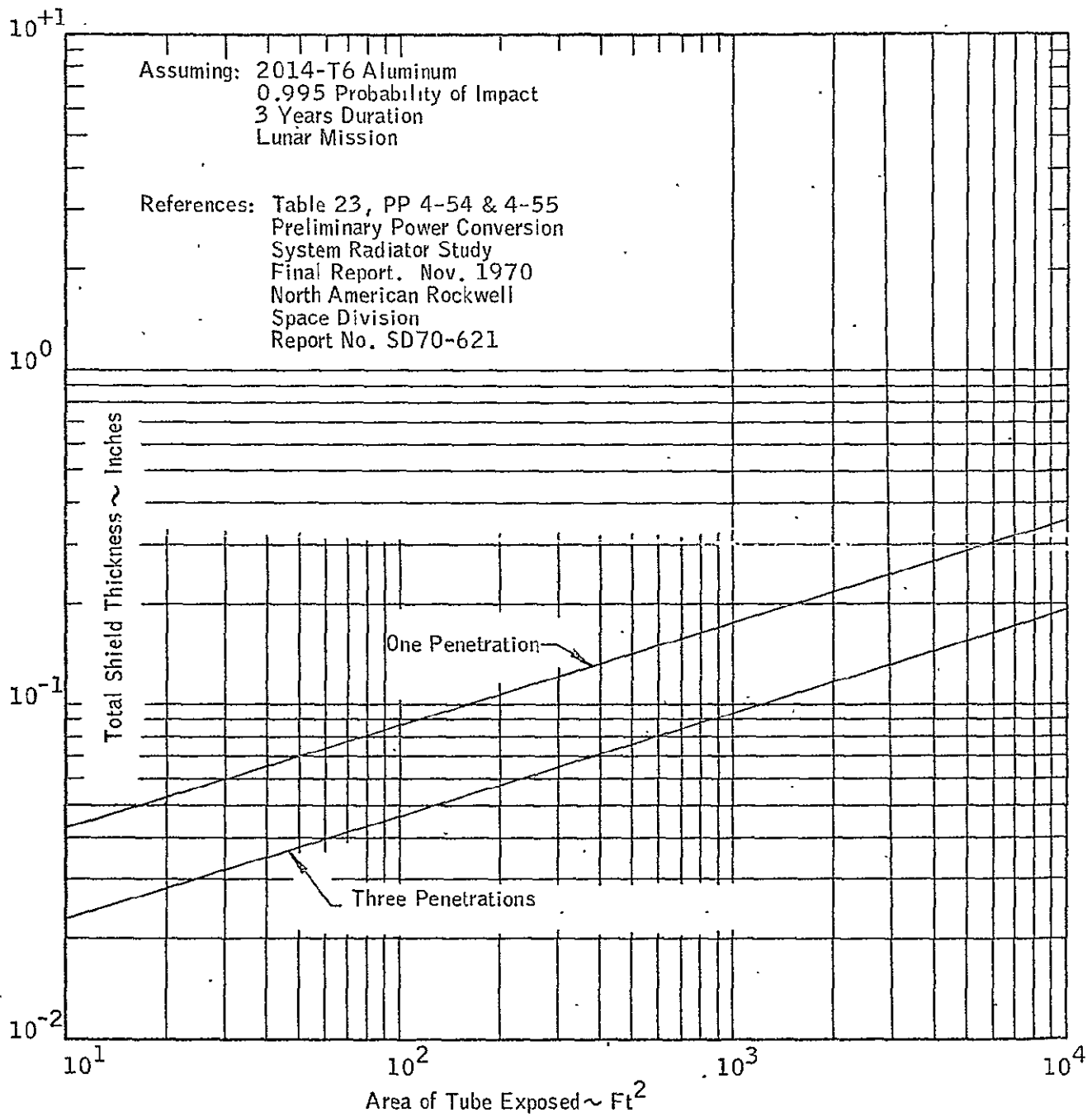


Figure 39 - Meteoroid Shield Thickness Vs Area Exposed

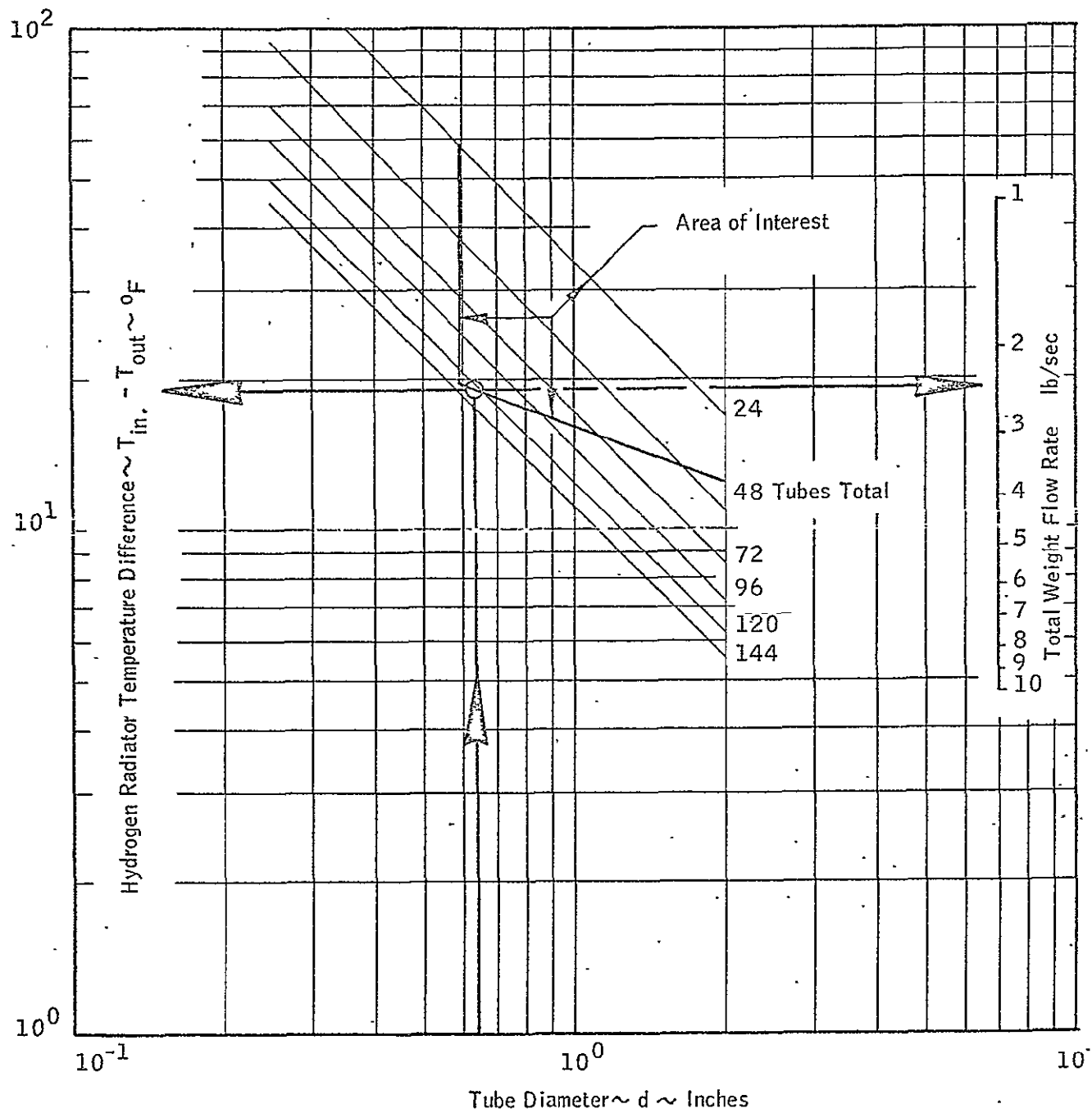


Figure 40 - Hydrogen Radiator Inlet to Exit Temperature Difference Vs Tube Diameter

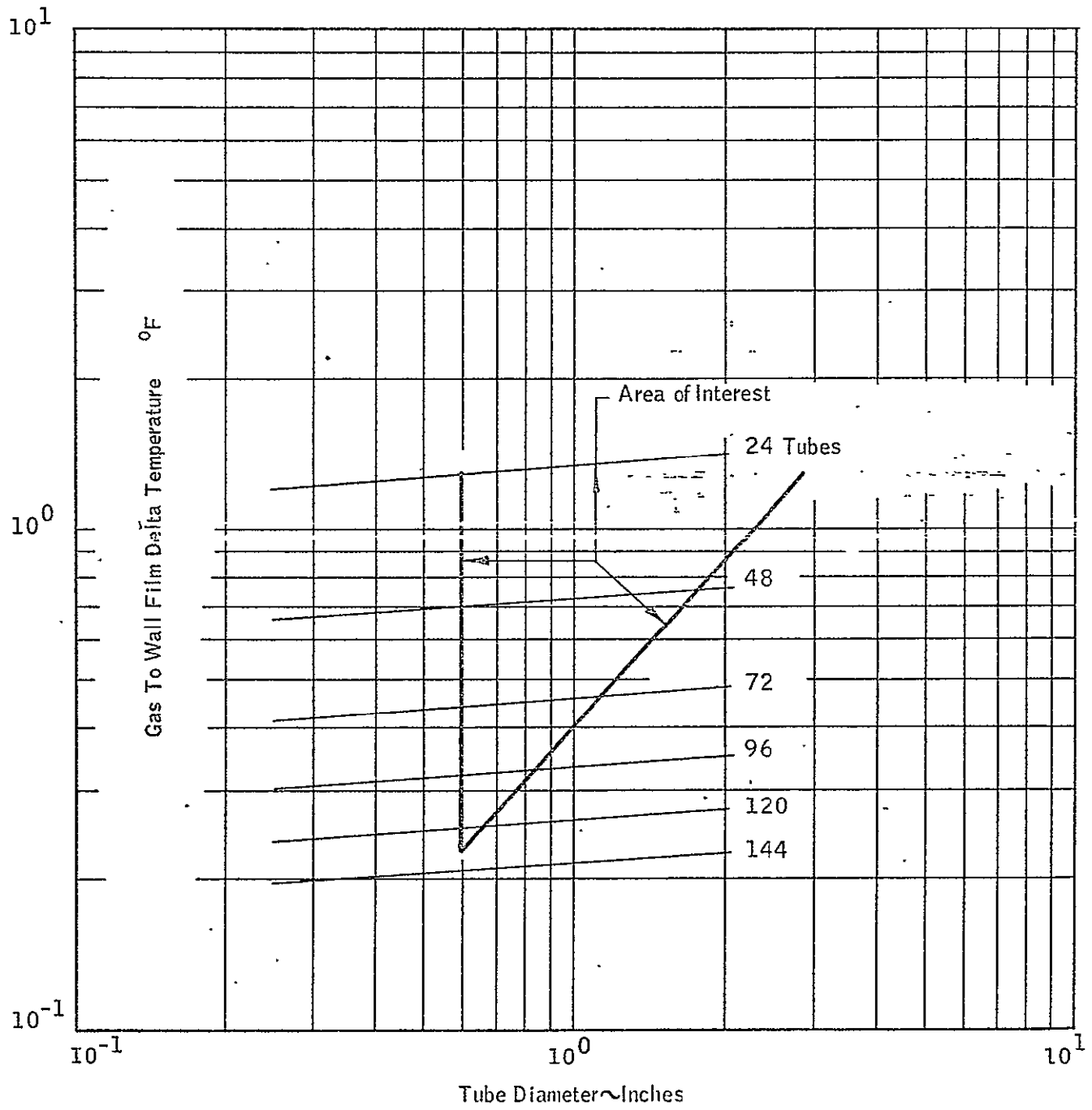


Figure 41 - Gas-to-Wall Film Delta Temperature Vs Tube Diameter

the original length if the individual loops are interposed as illustrated in Figure 42. Interpositioning also reduces the potential loss in fin efficiency by a factor of one over the number of loops overlapped. The degradation of fin efficiency because of the temperature difference between tubes would affect only one loop or 25% of the four interposed loops illustrated in Figure 42. The number interposed could be as high as 6 to 8 without incurring a large difference in the respective loop lengths.

By observing the five significant radiator parameters of weight, pressure, number of tubes, fin length, and radiator loop "delta" temperature, it is clear that weight would be significantly reduced if the fins were better conductors of heat. Changing the material of construction from aluminum to beryllium or magnesium would help somewhat but benefit would be small. The possibility of using heat pipes to increase the thermal conductivity of the fin, however, is not without merit. Preliminary examination indicates that heat-pipe systems could be designed into the 0.020 to 0.030-in.-thick meteoroid bumper with little or no weight penalty. Being able to maintain fin effectiveness at 40 to 50% has the potential of reducing the radiator weight to one-half the current estimate of 3000 lb. Some of the benefit comes from the higher average radiation surface temperature, while the major portion results from reducing the total radiator tubing length by increasing the fin length to 12 in. (see Figure 37).

This review of the design studies performed to date and the weight estimates for the radiator tubing and its protective meteoroid shield have identified the significant design parameters and their magnitudes. The radiator weight estimate of 3000 lb is achievable within the design restrictions so far imposed by the studies. A radiator loop pressure of approximately 2000 psia is required to achieve this design weight. The ability to reduce this weight by one-half would be possible if a heat-pipe system could be integrated into the meteoroid shield without a large weight penalty.

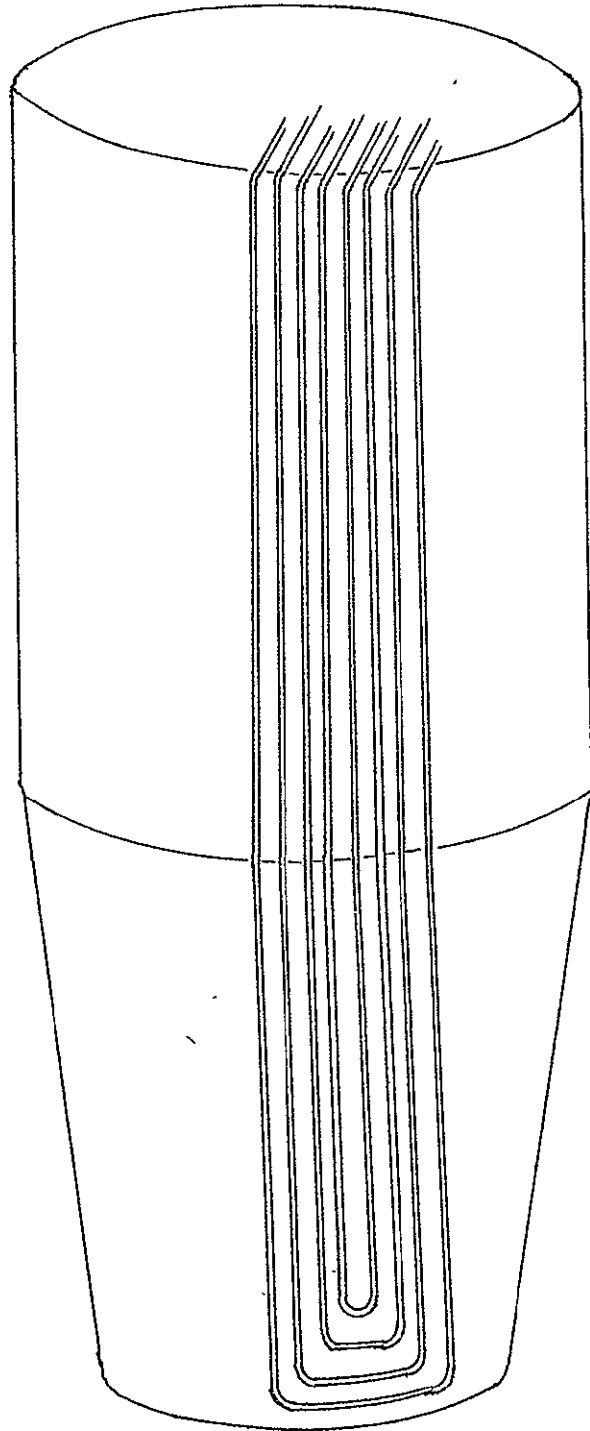


Figure 42 - Tubing Layout, With Inerposition

IX. RECOMMENDATIONS FOR FUTURE WORK

A. 25 KW ELECTRICAL SYSTEM

1. Primary Loop

Selection of size, location, and pressure level of flow channels in the aluminum barrel, consistent with other demands on the design of the barrel, is necessary. This selection includes a stress analysis.

The equilibrium temperature of reactor components not in the flow path during electrical power generation should be calculated. More detailed calculations are required to establish the thermal power limitations for reuse of the reactor for propulsion mode.

If an increase in reflector size is required, the nuclear, control, and weight effects need to be evaluated.

The identification of several organic fluids as candidates for low-temperature-ratio Rankine cycles generates the need for empirical heat-transfer coefficients. Design studies to date have used the coefficients for benzene, a similar composition, to estimate boiler size and weight. Determination of the organic fluid selected for future study or design should be followed by laboratory tests to obtain actual heat-transfer coefficients for liquid, boiling, and gas phases. These tests could also be done using the channel configuration that appears will be utilized in future designs.

2. Power Conversion Loop

The selection of pressure level in the primary loop affects the design of the boiler and fan. In the feasibility study reported herein, the primary loop pressure given most consideration was 600 psia. Reactor heat-exchanger space limitations may make the selection of a high pressure desirable.

The radiator study conducted by North American Rockwell showed that some potential flight environments (e.g., low-altitude lunar orbit) cause wide variations in radiator thermal-rejection capability. In an actual machine the result would be an increase in radiator temperature. Off-design operating characteristics of a power-conversion unit to assess this situation needs to be performed.

The design concept of the space condenser is new, and additional study is required to assess its operating limitations. For example, subcooling of the liquid to provide NPSP for the jet pump is accomplished by counterflowing the gaseous hydrogen coolant and providing a generous "delta" temperature in the coolant. This temperature difference also affects the fan design and the selection of pressure level in the radiator.

Candidate organic working fluids for the Rankine-cycle loop do not have sufficient empirical heat-transfer histories to embark upon final condenser designs. In addition, a condenser employing a screen or other porous interface between the condenser and the condensate pump has not been developed. The determination of the condensing heat-transfer coefficients for one or more of the most promising fluids (e.g., thiophene and pyridine) should be made. These tests could be most valuable if they were conducted in a prototype screen-matrix surface design. Confirmation of the load-sharing between individual loops, the degree of subcooling achievable, and off-design (i.e., flow rate) performance are functions that should be determined before full-scale designs are attempted.

A small but perceptible amount of hydrogen will permeate the boiler tube-walls between the primary loop and the lower pressure organic loop. The amount should be verified to determine its effect upon condenser performance and the condensate pump. If there are deleterious effects from hydrogen accumulation in the organic fluid loop, then efforts should be

initiated to remove the hydrogen from the loop either at the rate at which it enters or greater. This might be accomplished by placing a palladium "window" in the organic loop, heating it if required, and permitting the hydrogen to diffuse through the "window" to space vacuum.

3. Heat-Rejection System

The predominate component from the standpoint of weight is the radiator. The studies have shown that a 600-psia system is feasible but that significant weight reductions in manifolding, tubes, and meteoroid protection result from higher pressure. Higher pressure also permits more desirable arrangements and greater latitude in selection of the "delta" of the coolant (or weight flow rate). For these reasons the pressure level of the heat-rejection system should be studied to provide a more optimum system design.

Another design feature which could have a significant impact upon radiator design is use of heat pipes in the fin material. Space radiators are very sensitive to the temperature gradient inherent in high-length-to-thickness ratio fins. The improved fin effectiveness would allow greater spacing between coolant tubes, thus reducing the weight of tubing and meteoroid protection.

B. IMPACT OF 25 KW ELECTRICAL SYSTEM

The use of the NERVA rocket engine as a heat source for a 25-kw electrical system is the first step toward a space energy system. This feasibility study illustrated many potential applications for the dual-mode system. Most applications involve use of primary-loop heat independently and in conjunction with electric power, or the use of the heat-rejection loop. The effect of the space energy system approach is to enhance the performance and operational flexibility of the rocket mode. The dual mode of operation

greatly extends the usefulness of the energy system. There is a need to continue to investigate other potential applications of the dual-mode system to more fully utilize the inherent potential of nuclear power for space flight.